2020-01

Comparative Techno economic Analysis of Ammonia Electrosynthesis

Wang, Miao

UNIVERSITY OF CALGARY

Comparative Techno economic Analysis of Ammonia Electrosynthesis

by

Miao Wang

A THESIS

SUBMITTED TO THE FACULTY OF GRADUATE STUDIES

IN PARTIAL FULFILMENT OF THE REQUIREMENTS FOR THE

DEGREE OF MASTER OF SCIENCE

GRADUATE PROGRAM IN CHEMICAL ENGINEERING

CALGARY, ALBERTA

JANUARY, 2020

Abstract

Ammonia (NH_3) is a valuable chemical that is used as fertilizer, antimicrobial agent, and household cleaner and is among the largest chemicals produced globally. Currently, the Haber-Bosch (H-B) process, which requires elevated pressure (~100 bar) and temperature (~450°C), is used to produce the majority of NH_3. The H-B generates large quantities (1500 kg-CO_2/ton-NH_3) of greenhouse gases (GHG), especially during the steam methane reforming process to produce hydrogen (H_2) feedstock. There has been growing interest in alternative electrochemical processes for NH_3 synthesis due to their modular design, reduced capital cost, and potential to reduce GHG emissions over that of the H-B process. In this thesis, six alternative NH_3 electrosynthesis routes are analyzed from both economic and environmental aspects. Among the six routes, electrosynthesis of NH_3 from N_2 and H_2O at room temperature is found to be the most economically compelling process (levelized cost ~\$414/ton-NH_3). Compared to a conventional H-B plant, electrosynthesis using electricity from clean sources could reduce CO_2 emissions by 75-90%. Based on this analysis, we have estimated the target performance metrics that need to be achieved at scale to make the electrochemical NH_3 synthesis route economically and environmentally viable. This analysis reveals that electrochemical processes have merit and potential to replace the H-B process if target performance parameters (current density higher than 400 mA/cm^2, selectivity higher than 60%, energy efficiency higher than 50%, and overpotential lower than 1.5 V) are achieved. This analysis gives an early indication for the electrosynthesis route to be economically viable and environmentally sustainable as compared to the century-old H-B process.

Acknowledge

This remarkable journey would have destroyed me if I did not get support from professors, friends, and families. First and most importantly, I would like to express my deepest appreciation to Dr. Md Golam Kibria. Your wisdom, professionalism, and patience influenced and changed me. This thesis would not be finished without your treasurable help. The countless hour we worked together helped me built my sense of research. Your thinking-outside-of-the-box ability reshaped my brain. Thank you for giving me a chance working in this group.

Secondly, I would like to convey my deep thanks to my co-supervisor, Dr. Ian Donald Gates. He is an encouraging, knowledgeable, and imaginative professor who always gives me enlightening insights. I will always remember those dark cold winter mornings, your office lights were already on when I thought I was the first one arrived. Those weekly chats we had really revolutionized my opinions toward research. Thank you for being such a supportive and patient mentor.

Next, I am truly grateful for having Dr. Sean McCoy and Dr. Edward Ted Roberts as my committee members. The suggestions from you in my earlier presentation pointed out a huge mistake, which might be fatal in the following calculation. Thank you for your time and precious suggestions. A particular thanks to Dr. Kazi Sumon, thank you for helping me solving thermodynamic problems.

This work cannot be finished without the help from my colleagues. I would like to thank all the members of this fantastic group: Nidhika Bhoria, Imtinan Mohsin, Nael Yasri, Shariful

Kibria Nabil, Tareq-Al-Attas, Nedal Marei, and Ugochukwu Nwosu. The encouragement from you helped me survived. Especially, I would like to thank Imtinan Mohsin for his support in simulation and calculation.

I am glad to have my friends helped me went through those devastating moments. Sincere thanks goes to Dr. Chongchong Wu and Dr. Ye Xiao, thank you for pulling me out when I struggled and for the countless help you gave. Yusang Ye and Dr. Boning Ma, thank you for the caring when I was lost and heartbroken. Zheyu Zhang, thank you for the help when I knew nothing about electrochemistry. Jiawei Ji, thank you for being a kind friend. Dr. Yuanchao Feng, thank you for your valuable advice and priceless help.

I would like to acknowledge the financial support for this research, including Global Research Initiative in Sustainable Low Carbon Unconventional Resources (GRI) and the Canada First Research Excellence Fund (CFREF). Research funding and support are gratefully received from the Government of Alberta, University of Calgary Department of Chemical and Petroleum Engineering, and Faculty of Graduate Studies (FGS).

Finally, yet importantly, I would like to appreciate my warm family for their unconditional love. I would not go this far without their thoughtful advice and support. Unique thanks to my parents, who always support me.

Dedication

To my mother, who always told me to try my best.

Table of contents

Contents

List of tables

List of figures

Epigraph

“Now this is not the end. It is not even the beginning of the end. But it is, perhaps, the end of the beginning.”

-Winston S. Churchill

Chapter 1 Introduction

1.1 Background

1.1.1 Ammonia usage

Ammonia (NH_3) is an important chemical feedstock mainly used to produce nitrogen-containing fertilizer materials. To date, most of the produced NH_3 is used to produce fertilizer (Figure 1) including urea (CH_4N_2O), ammonium bicarbonate (NH_4HCO_3), etc.[1].

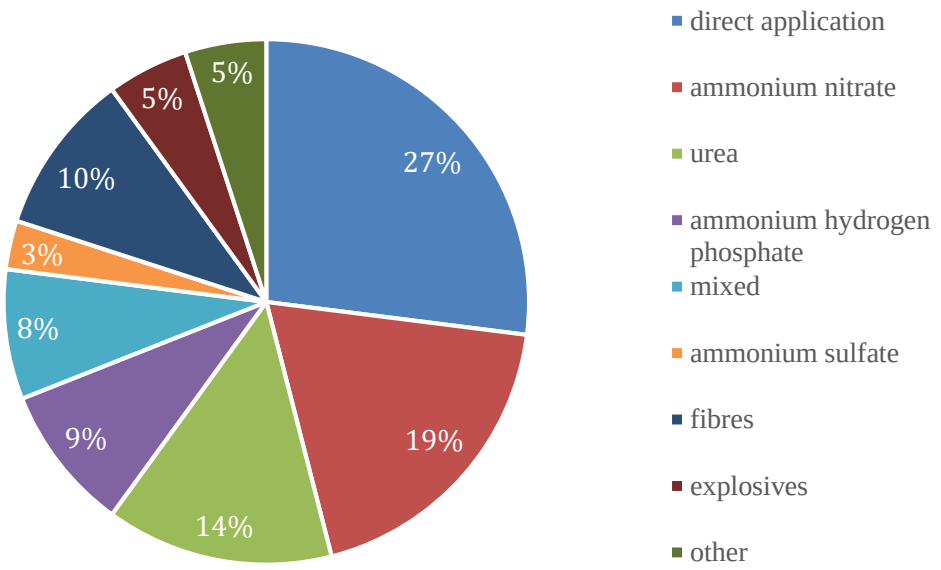

Figure 1 The major uses of ammonia[2].

As shown in Figure 2, it is believed that nitrogen-contained fertilizers have been a key contributor to the rapid growth of the human population, since the middle of the 20th century[3]. Apart from its widespread use in agriculture, it is also an essential chemical feedstock in multiple modern chemical industries, including explosives, refrigeration systems, and household cleaners[3–5].

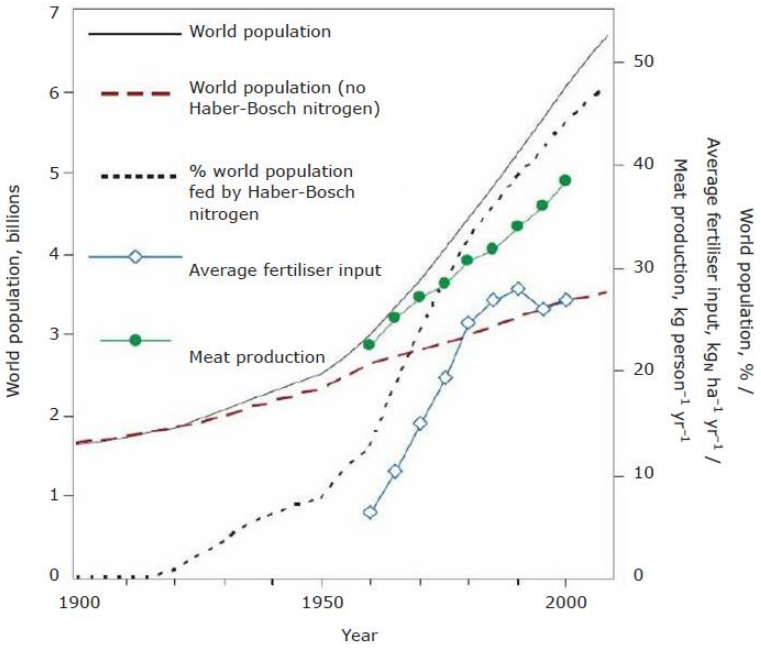

Figure 2 Trends in human population and nitrogen use throughout the twentieth century[3]. Reprinted with permission from Ref. [3].

Apart from these, ammonia can serve as a versatile energy-dense fuel in high-temperature solid oxide fuel cells, cracked for low-temperature fuel cells, and partially cracked for internal combustion engines and to produce electricity in a power plant. But currently, ammonia's highest value is as a rich source of hydrogen, which can be used to power fuel-cell vehicles[6]. Liquid NH_3 also has a higher energy density (11.5 MJ/L) compared to that of liquid H_2 (8.5 MJ/L)[7]. Alternatively, NH_3 can be combusted for power generation or used in fuel cells, due to its high volumetric energy density[8,9]. Combustion or cracking of NH_3 releases carbon-free nitrogen in the atmosphere[10].

1.1.2 History of Ammonia development

In the early 20th century, numerous scientists investigated the reaction between N_2 and hydrogen (H_2), and the possibility of synthesizing ammonia under high temperature[11]. The German scientist Fritz Haber observed that the NH_3 synthesis reaction is preferable under higher pressure [11]. In 1908, Haber approached the BASF (Badische Anilin & Soda Fabrik at that time) company to support his high pressure and recycling idea. Within five years, Carl Bosch, a chemist who worked for BASF, with a team of experienced co-workers successfully demonstrated this process at commercial scale after over 6,500 experiments on over 2,500 different catalysts[11]. In 1919, Fritz Haber was awarded the Nobel Prize in Chemistry and in 1931, Carl Bosch was awarded the Nobel Prize in Chemistry, then NH_3 synthesis approach they developed is then named after them, i.e., Haber-Bosch (H-B) process[12,13]. After World War I, the H-B process was widely applied throughout Europe[11]. After World War II, NH_3 plants using the H-B method had reached a total production rate of hundreds of tons per day[14]. In 2007, Gerhard Ertl, a German Scientist who worked in Fritz Haber Institute of the Max Planck Society was awarded Nobel Prize in chemistry for explaining the NH_3 synthesis mechanism on iron surfaces[15,16]. Till now, the H-B process is used globally for NH_3 synthesis. However, the single-pass conversion of ammonia synthesis through the H-B process is quite low (0-15%, depending on the temperature and pressure). To solve that, ammonia manufacturers use a series of reactors to increase the overall efficiency, which corresponds to the enormous capital investment for a traditional H-B plant[11,17,18]. With recycling, the overall conversion efficiency of the H-B process can be reached to over 95%.

1.2 Ammonia market and prediction

As shown in Figure 3, NH_3 produced by the Haber-Bosch process increased about 57 times by 2012 compared to the amount produced during World War II[19]. In 2017, global NH_3 production was estimated at over 150 million tons and was expected to increase by 3 to 5% every year, and over 99% of NH_3 is produced by the Haber-Bosch process[20]. Figure 4 shows a prediction of future NH_3 production until 2050.

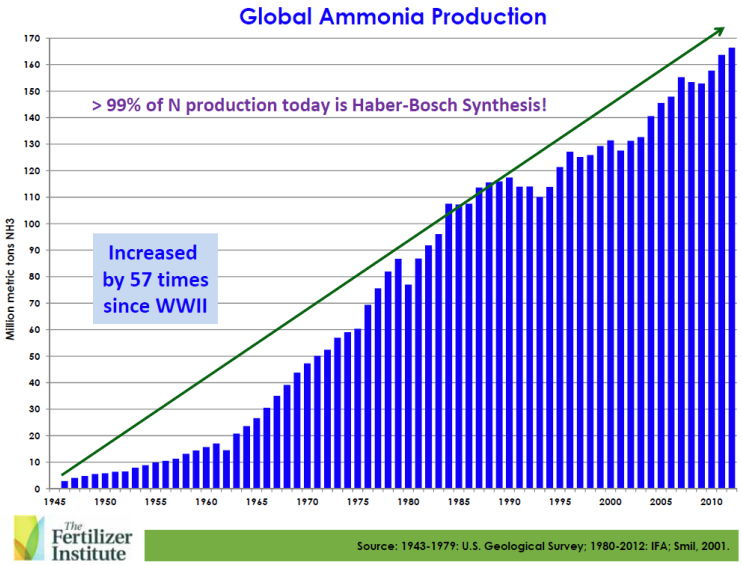

Figure 3 Global Haber-Bosch ammonia production from the mid-20th century to the present[19].

1.3 Ammonia production status and problem

N_2 and H_2 are needed as feedstock chemicals for NH_3 synthesis via the H-B process. Air separation unit (ASU) is typically used for the production of N_2. In 1895, Carl von Linde successfully conducted the first continuous liquefied air separation experiment in his Munich laboratory based on the Joule-Thompson effect[21]. Joule-Thompson effect is that compressed air cooled down after it passes through an expansion valve, about 0.25°C temperature decrease for

every bar of pressure drop[21]. In 1902, Carl von Linde built the first air separation plant for Oxygen (O_2) production using

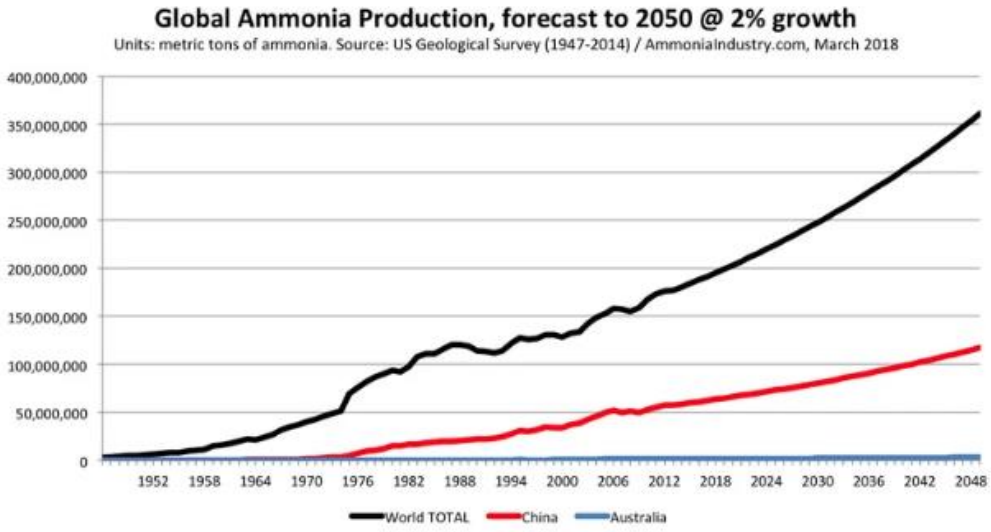

Figure 4 Global Ammonia production, forecast to 2050[20].

a single-column rectification tower[21]. Since then, air separation technology has been commercially deployed. Nowadays, Linde plc, a gas company founded by Carl von Linde, has become the largest industrial gas supplier in the world[22].

For the production of H_2, various methods have been investigated. Typically, H_2 is produced through Steam Methane Reforming (SMR) operated at 3-25 bar and 700-1000°C[23]. Figure 5 gives a process illustration of a typical Haber-Bosch plant[24].

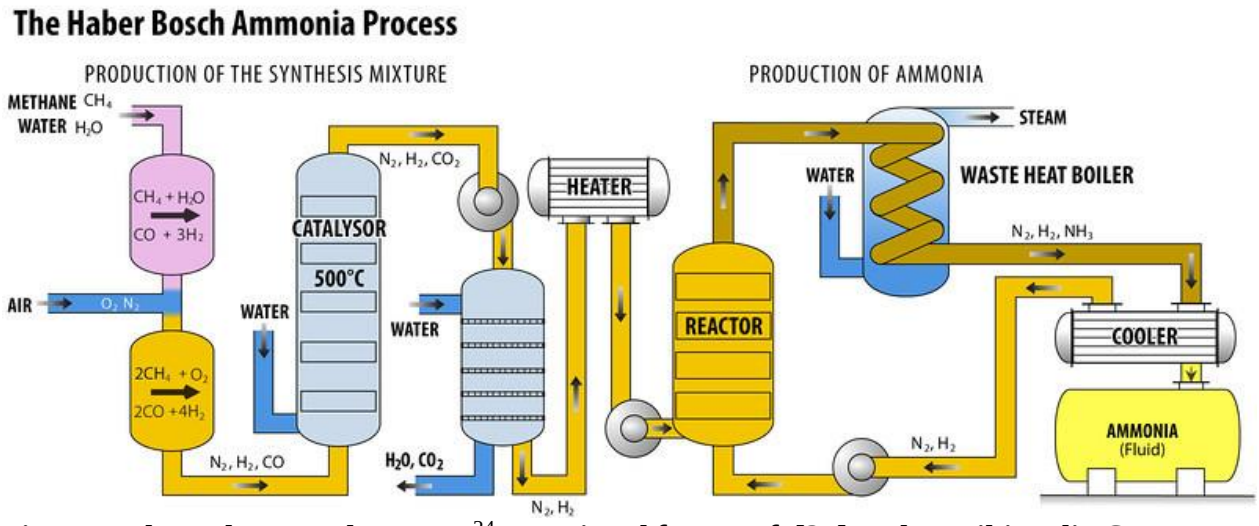

Figure 5 The Haber-Bosch process[24]. Reprinted from Ref. [24] under Wikimedia Commons. The H_2 is produced from SMR.

First, natural gas needs to be desulfurized as the sulfur content in natural gas poisons the catalyst. Methane and water (steam) react to carbon monoxide (CO) and H_2 with the help of catalyst (mostly nickel) to produce a mixture of CO and H_2, which is normally referred to as synthesis gas (syngas):

$$CH_4 + H_2O \xrightarrow{\Delta} CO + 3H_2 \quad (1)$$

In the next step, the syngas is fed to the second water-gas shift reformer along with air to ensure all CO reacts with H_2O to produce more H_2 and, accordingly, produce more CO_2:

$$CO + H_2O \xrightarrow{\Delta} CO_2 + H_2 \quad (2)$$

At the outlet of the SMR unit, the products are N_2, H_2, and CO_2. The CO_2 is removed and the N_2 and H_2 mixture is sent to the Haber-Bosch reactor. Accordingly, SMR and the H-B reactions emit an enormous amount of GHG, with a CO_2 emission of around 1,500 kg/ton NH_3[25,26].

In the Haber-Bosch reactor, the temperature of the N_2 and H_2 mixture is raised by using a heater. Fundamentally, the Haber-Bosch process prefers lower temperature and higher pressure to

shift the NH_3 synthesis reaction in a favorable direction; however, the kinetics of the reaction would decline with decreased temperature[11]. Hence, both high temperature and pressure are required for this reaction to fulfill the requirement for production rate and chemical equilibrium. Even though the single-pass conversion is still low, a series of reactors, as pointed out by Fritz Haber, is required to improve the overall efficiency[11].

Apart from using natural gas, H_2 can also be produced from partial oxidation of heavy oil, gasification of coal, etc.[27]. For example, more than 97% of the hydrogen required for NH_3 production in China is obtained from gasification of coal[28]. However, those approaches are causing elevated CO_2 emission and severe environmental pollution as well as climate change. NH_3 is one of the most energy-intensive (Fig 6A) and GHG emissive (Fig 6B) chemical among all significant industrial feedstock.

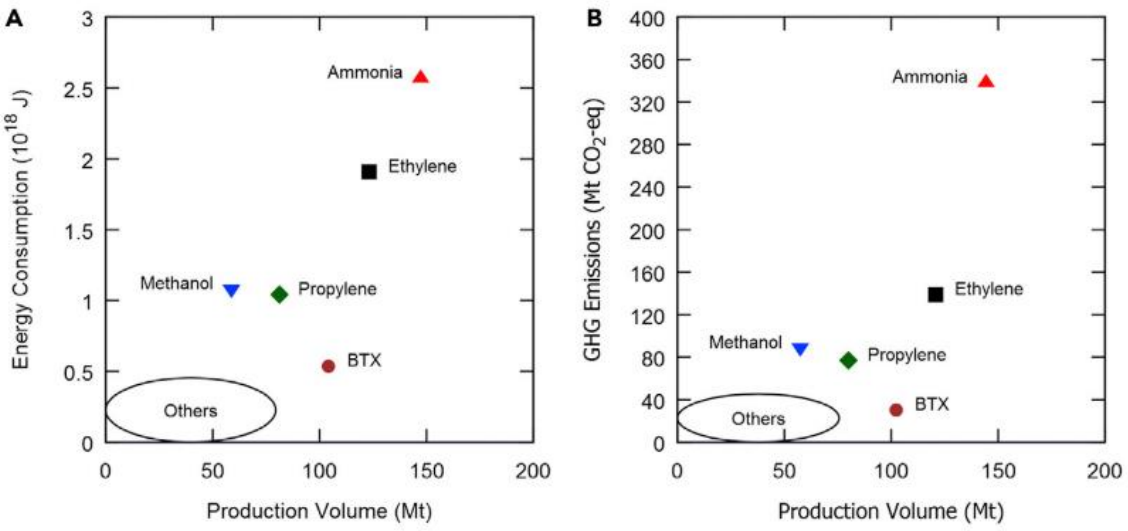

Figure 6 (A) Energy consumption and (B) GHG emission of Ammonia compared to other significant chemicals[29]. Reprinted with permission from Ref. [29].

1.4 Opportunities to replace Haber-Bosch plant

With the rapid cost reduction of renewable electricity (notably wind and solar), nearly carbon-free and low-cost (even harmful in some markets) electricity is becoming abundant in several geographical locations[30,31]. In 2017, the global weighted average cost of renewable electricity fell into the range of fossil fuel-based ones, i.e., between $0.047-0.167 per kilowatt-hour (kWh). Since 2010, the utility-scale solar and onshore wind electricity price dropped 73% and 23% to $0.10/kWh and $0.06/kWh, respectively, in 2017. With recent auctions in Saudi Arabia, Brazil, Canada, Germany, Mexico, and Morocco, onshore wind electricity price declined as low as $0.03/kWh[32]. Figure 7 illustrates US DOE Sunshot Progress and goals for solar electricity price in recent future.

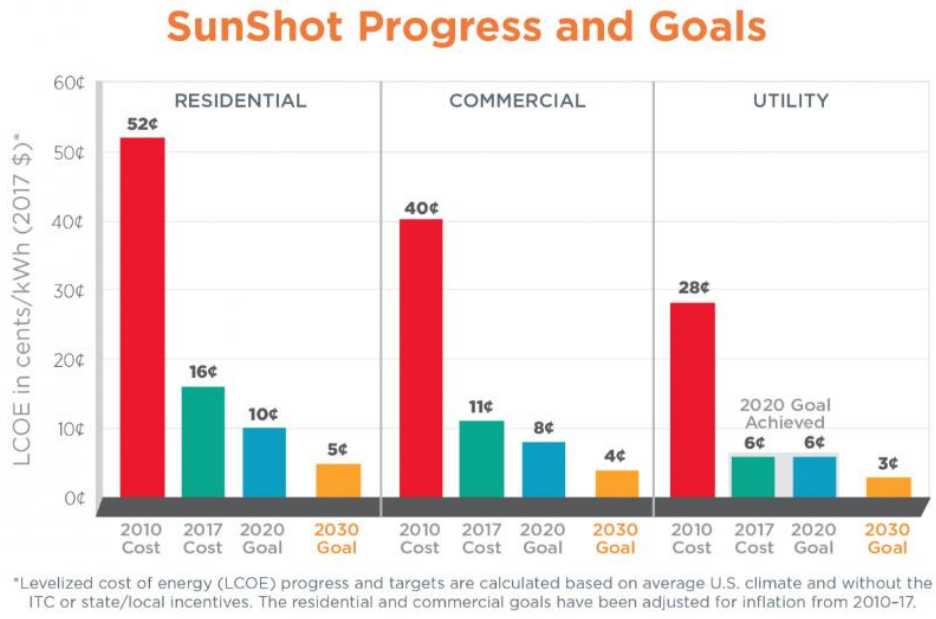

Figure 7 Electricity price landscape[33].

On the other hand, with increased penetration of intermittent renewable energy sources, the development of energy storage technologies is becoming essential to enable even higher

penetration of these renewables[34–36]. As a result, there is growing interest focused on electrochemical processes for the synthesis of fuels and feedstock for long-term energy storage, including water (H_2O) electrolysis to generate H_2, CO_2 electrolysis to produce carbon-based products, etc.[37,38]. For example, commercial H_2O electrolyzers have been successfully commissioned, which can reach 20 MW power capacity with a 4000 Nm^3/h production rate[39]. Furthermore, established companies and start-ups are investing in pilot-scale CO_2 electrolyzers[40]. Likewise, research focus on electrochemical synthesis of NH_3 has been growing in recent years[10,41–48]. As shown in Figure 8, the combination of clean electricity or low-carbon electricity and electrosynthesis processes have a potential that could lead to a near-zero emission chemical and energy industry[29].

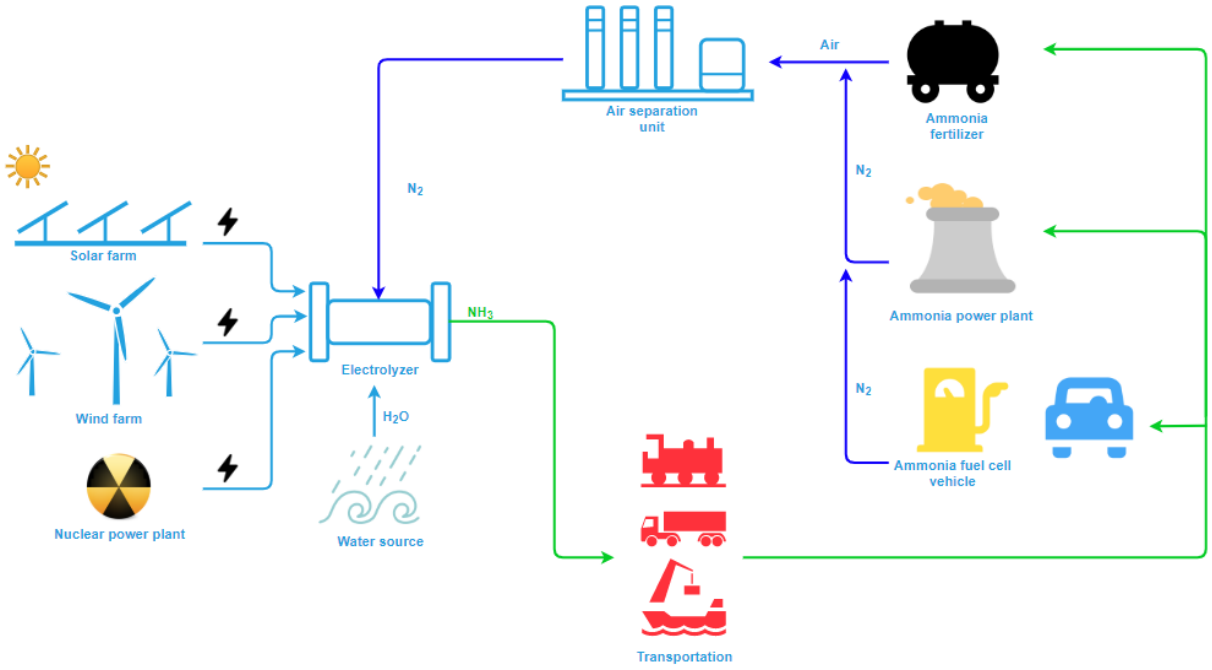

Figure 8 Renewable ammonia production route.

Electrosynthesis could operate reactions under moderate temperature and pressure and, when coupled with a renewable source of electricity, generates nearly zero GHG emission[49]. Additionally, electrosynthesis, compared to the H-B process, offers substantially lower capital expenditure[49]. Unlike the traditional large-scale H-B process, modular scaling of the electrochemical system could potentially enable highly distributed NH_3 production from small to large-scale applications[29,47,50,51].

1.5 Overview of the thesis and keys contributions

This thesis focused on the process design and comparative techno-economic analysis of various electrochemical NH_3 synthesis routes. First, we reviewed recent progress in ammonia electrosynthesis from various aspects, both feedstock and experimental conditions. Based on those reported studies, the electrosynthesis routes can be classified as: 1) one-step NH_3 electrosynthesis using N_2 and H_2O at room and elevated temperature, 2) NH_3 electrosynthesis using N_2 and H_2 at room and elevated temperature, where H_2 is produced through H_2O electrolysis, 3) Using traditional H-B reactor to synthesize NH_3, wherein H_2 is produced from H_2O electrolysis, 4) Using Lithium-related (Li) redox reaction to produce NH_3, wherein Li served as intermediate. In general, five units were considered in the design: Air Separation Unit (ASU), NH_3 synthesis cell, Pressure Swing Adsorption (PSA), distillation, and condensation. For the ASU, distillation, and condensation unit, we used Aspen HYSYS to simulate the process and Aspen Economic Analyzer to perform cost analysis. For the synthesis cell and PSA unit, we calculated the costs based on reported or commercialized parameters. From the assumption we chose, material and mass balance were performed. Next, we calculated the related cost for synthesis (capital and operating cost). From the results of those costs, we compared the synthesis routes from various aspects. We

compared the Net Present Value (NPV), Levelized Cost of Product (LCP) from various aspects, energy consumption and CO_2 emission against those from the conventional H-B process. The results showed that electrosynthesis has the potential to replace traditional H-B plant if crucial performance parameters are achieved in the future, and the CO_2 emission of the H-B plant can be reduced significantly.

The results of the research documented in this thesis indicate the target performance matrices of ammonia electrosynthesis to improve its environmental and economic performance.

Chapter 2 Literature Review

In this chapter, several alternative routes for NH_3 electrosynthesis were reviewed. First, the current stage of H_2O electrolysis was reviewed, which was considered as the clean production route of H_2. After that, the status of NH_3 electrosynthesis was reviewed, including electrosynthesis experiments and hybrid of electrolysis and chemical reactions. From reported studies, the state-of-art parameters from lab-scale experiments were gathered. The reactions were categorized into four major categories: one-step NH_3 electrosynthesis from N_2 and H_2O; NH_3 electrosynthesis from N_2 and H_2, where H_2 is produced from H_2O electrolyzer; NH_3 synthesis from the H-B plant, where H_2 is produced from H_2O reactor; and redox chemical reaction.

2.1 Review of water electrolysis

2.1.1 Introduction

Currently, H_2 production is primarily from fossil fuels, namely methane. In 2017, more than 95% H_2 was produced from methane and caused massive CO_2 emissions[52]. Using a H_2O electrolyzer for H_2 production has the potential to replace current H_2 production methods. Electrolyzers generate less CO_2 emission and could create a new downstream market for renewable power[52]. H_2O electrolysis can be defined as water molecule split to H_2 and O_2 gas under the influence of applied cell voltage, as shown in the equation below:

$$2H_2O \xrightarrow{e^-} 2H_2 + O_2 \;\; E^\circ = 1.23\,V \tag{3}$$

In pure water, a reduction reaction happens at cathode side:

$$2H^+(aq) + 2e^- \xrightarrow{yields} H_2(g) \tag{4}$$

While the oxidation reaction happens at anode side:

$$2H_2O(l) \xrightarrow{yields} O_2(g) + 4H^+(aq) + 4e^- \quad (5)$$

The theoretical reaction voltage is 1.23 V (for the reduction half-equation). However, the cell potential is dependent on the concentration of H^+ and OH^-[53].

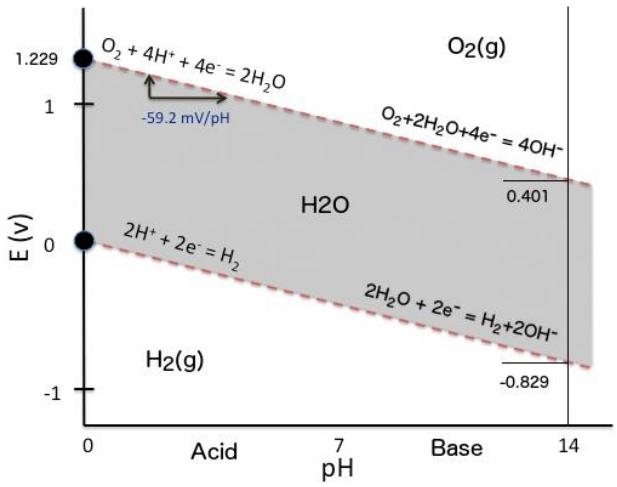

Figure 9 Pourbaix diagram for water[53]. Reprinted from Ref. [53]. under Wikimedia Commons.

In pure water, the reaction is inefficient due to the low conductivity of H_2O, so acid, base, or their salts are added to the electrolyte to increase the conductivity, which causes the difference in reaction voltage[53]. As shown in Figure 9, the reaction voltage is influenced by the pH of the solution. However, the actual applied voltage is normally higher than theoretical voltage, and additional voltage needed is called overpotential. In electrochemistry, overpotential is a term included three parts: charge-transfer overpotential, mass-transfer overpotential, and reaction-related overpotential [54].

2.1.2 Review of major hydrogen electrolysis approaches

Here, we reviewed current practical H_2O electrolysis approaches: Alkaline Electrolysis Cells (AEC), Proton Exchange Membrane Electrolysis Cells (PEMEC), and Solid Oxide Electrolysis Cells (SOEC)[55].

2.1.2.1 Alkaline Electrolysis Cell (AEC)

AECs have been used in industry-scale H_2O electrolysis since the 1920s, the cell configuration is shown in Figure 10[55]. Normally, the KOH solution is used as the electrolyte and O_2 is produced at anode side while H_2 is produced at the cathode; the electrodes are divided by the separator, which also keeps H_2 from mixing with O_2 while remains permeable for OH^-[56].

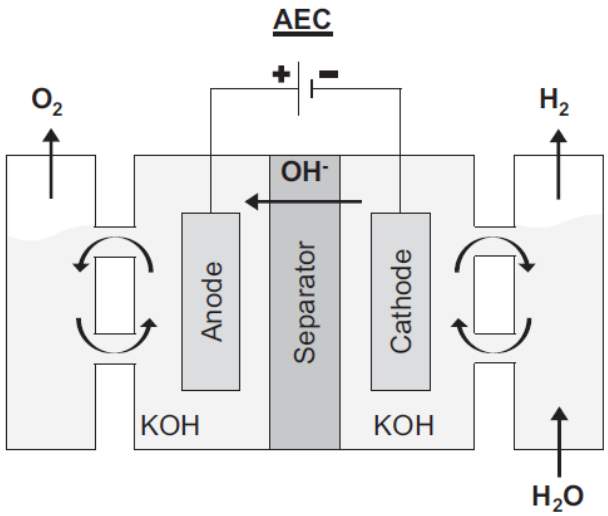

Figure 10 Cell configuration for AEC[55].

AEC has been well investigated for centuries; it is a more mature technology compared to other H_2O electrolysis systems[57]. It has relatively lower capital cost due to the avoidance of noble metals; the electrodes for AEC are commonly Ni or Ni alloy[55]. AEC could operate at a satisfactory

H_2 production rate for its end users with over 99.9% H_2 purity and 99.5% O_2 purity[58]. Currently, over 10 years of service time has been achieved for existing commercial AECs[58].

However, AECs operate at relatively lower current density and their pressure requirements harmfully influence the cost and the size of the system, therefore the overall efficiency of the AECs is relatively less competative[55].

2.1.2.2 Proton Exchange Membrane Electrolysis Cell (PEMEC)

PEMEC, displayed in Figure 11, is a technology that was first introduced by General Electric in the 1960s[59]. It uses a solid polymer electrolyte, which conducts H^+ from anode to cathode side, separates produced O_2 and H_2 gas, and insulates electrodes, as illustrated in figure 11[32]. The electrodes are pressed against the membrane to form a membrane electrode assembly (MEA)[58].

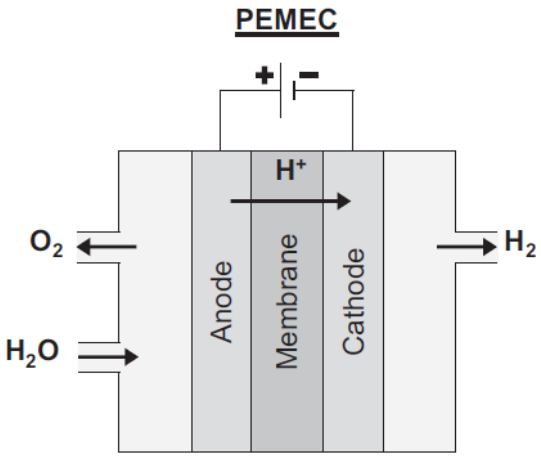

Figure 11 Cell configuration for PEMEC[55].

PEMEC can be operated at high current density (up to 2.0 A/cm^2), higher energy efficiency (up to 82%), with a requirement for high purity H_2 (over 99.99 % H_2)[58,59]. It can also be produced in a modular set-up, which provides potentials for more flexible applications[58]. However, the catalysts used in this cell usually are iridium (anode) and platinum (cathode), which are costly thus increase the input of the system. On the other hand, the acidity of the system is high (equal to about 1M sulfuric acid solution), which requires costly noble metals as catalysts for the endurance of the production[58]. Thus, the stack price of PEMEC is higher than other H_2O electrolysis systems[55].

2.1.2.3 Solid Oxide Electrolysis Cell (SOEC)

SOEC uses solid ion-conducting ceramics as the electrolyte, as shown in Figure 12. Typically it needs high temperature, which reduces the activation energy barrier and increases the reaction rate with electric energy required at 900°C of about 0.95 V[60]. On the other hand, the overpotential and ohmic voltage also declines at high temperature[60]. Compared to other H_2O electrolysis methods, the materials required for this process are relatively cheap due to the elevated temperature[60].

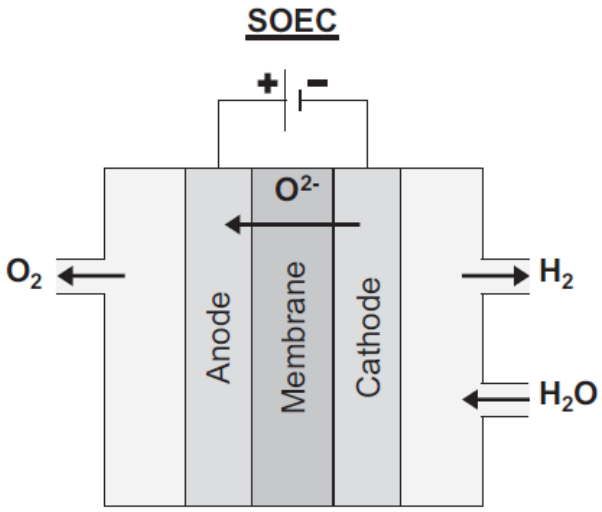

Figure 12 Cell configuration for SOEC[55].

SOEC has the potential to replace the current H_2O electrolysis systems with its lower operating cell voltage (1.29 V) which correspondingly indicates a higher voltage efficiency[58]. However, the maturity of this approach is still lacking since the stability of electrode material and solid electrolyte, and insulation of the system remains unstable. Furthermore, safety issues of producing H_2 at such high temperature also raises concerns[60].

2.1.3 Summary of water electrolysis

Due to the different technology readiness level (TRL) and production scale, the cost for each process is quite different. The AEC has currently the lowest cost (Table 1). However, studies have pointed out that PEMEC and SOEC have the potential to decrease their costs faster than AEC, therefore could be even cheaper than AEC in the future, hence the H_2O electrolyzers could operate at better performance meanwhile cheaper price[61]. As for lifetime, AEC can operate longer than

other methods (Table 1). Hence, the replacement and maintenance cost of it will also be cheaper than other processes.

Here, data for the above-mentioned H_2O electrolysis systems are listed in Table 1. For this study, we chose PEMEC H_2O electrolysis system as the H_2 production route. Studies showing that the stack cost for PEMEC would dramatically drop in the coming decade, which means PEMEC is economically comparable to AEC H_2O electrolysis system while operates at much higher current density (as shown in Table 1)[62].

Table 1 Summary of H_2O electrolysis cells[56]. Reprinted with permission from Ref. [56].

	AEC	PEMEC	SOEC
Electrolyte	Aq. Potassium hydroxide (20-40 wt% KOH)	Polymer membrane (e.g., Nafion)	Yttria stabilized Zirconia (YSZ)
Cathode	Ni, Ni-Mo alloys	Pt, Pt-Pd	Ni/YSZ
Anode	Ni, Ni-Mo alloys	RuO_2, IrO_2	LSM.YSZ
Current density (A/cm^2)	0.2-0.4	0.6-2.0	0.3-2.0
Cell voltage(V)	1.8-2.4	1.8-2.2	0.7-1.5
Voltage efficiency (%)	62-82	67-82	<110
Operating temperature (°C)	60-80	50-80	650-1000
Stack lifetime (h)	60,000-90,000	20,000-90,000	<10,000
Maturity	Mature	Commercial	Demonstration
Capital cost (€/kW)	1000-1200	1860-2320	>2000

2.2 Review of ammonia electrosynthesis

2.2.1 Introduction

Unlike traditional thermal driven chemical reactions, electrochemical reactions use electric power to overcome the reaction activation barrier. This potentially allows the system to reach higher reaction efficiency while using less energy with greater ability for modular configurations[63].

2.2.2 Review of reported studies

Numerous studies have been conducted for NH_3 electrosynthesis from various perspectives. Here, the reactions are categorized based on their synthesis reactions, feedstock, and temperature. In Figure 13, a performance map of NH_3 electrosynthesis experiments is summarized. From the graph, elevated temperature experiments demonstrate better results with higher energy efficiency (around 40%) and current density (around 250 mA/cm^2) compared to room temperature experiments. From this performance, we concluded several major NH_3 electrosynthesis routes in Table 2 and figure 14: NH_3 electrosynthesis directly from proton source (H_2 or H_2O), a combination of H_2O electrolysis and the H-B process, and a hybrid of chemical and electrochemical reactions.

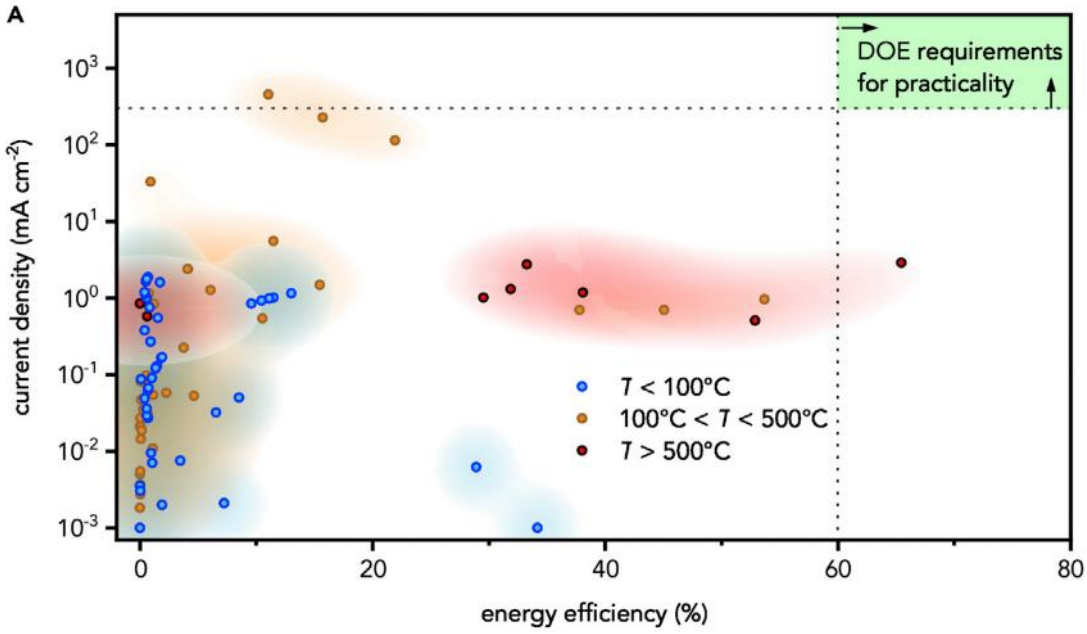

Figure 13 Performance map for NH_3 electrosynthesis[51]. Reprinted with permission from Ref. [51].

Table 2 Summary of NH_3 synthesis routes.

NH_3 electrosynthesis reaction	Reaction voltage	Abbreviation
$2N_2 + 6H_2O \xrightarrow{yields} 4NH_3 + 3O_2$	$E° = 1.17\,V, 25°C$ $E = 1.20\,V, 500°C$	$Scenario\ A\ (RT)$ $Scenario\ A\ (HT)$
$N_2 + 3H_2 \xrightarrow{yields} 2NH_3$	$E° = 0.06\,V, 25°C$ $E = 0.12\,V, 500°C$	$Scenario\ B\ (RT)$ $Scenario\ B\ (HT)$
$N_2 + 3H_2 \xrightarrow{H-B} 2NH_3$	N/A	$Scenario\ C$
$6LiOH \rightarrow 6\mathrm{Li} + 3H_2O + \frac{3}{2}O_2$ $6Li + N_2 \rightarrow 2Li_3N$ $Li_3N + 6H_2O \rightarrow 6LiOH + 2NH_3$	$E° = 2.8\,V, 427°C$ N/A N/A	$Scenario\ D$

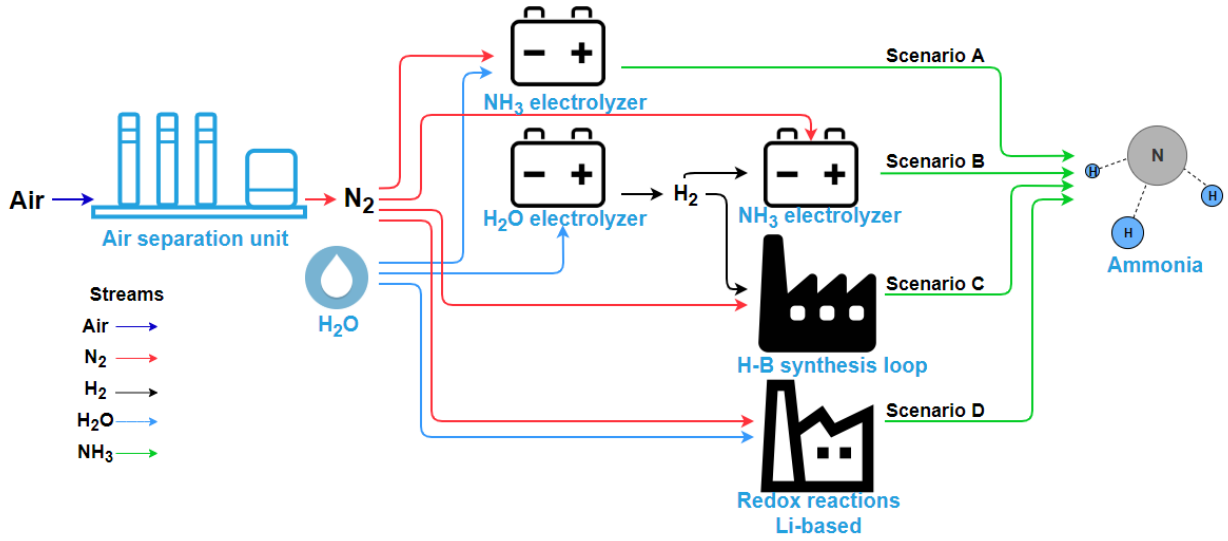

Figure 14 Demonstration of selected NH_3 electrosynthesis routes.

Figure 14 demonstrates the selected NH_3 electrosynthesis routes. Here, the synthesis routes are named with scenario A, B, C, and D for clear distinction. Scenario A represents the

electrosynthesis using N_2 and H_2O as the feedstock, RT stands for room temperature while HT stands for high temperature. Scenario B is using H_2 instead of H_2O as the proton sources, while H_2 is produced from H_2O electrolysis. Scenario C is the combination of H_2O electrolysis and traditional NH_3 synthesis loop (the H-B process), and the Scenario D is electrosynthesis using Li as the intermediate agent.

2.2.2.1 NH_3 electrosynthesis using N_2 and H_2O

NH_3 can be electro synthesized using a one-step N_2 and H_2O reaction where H_2O directly serves as proton source[44]. As shown in Figure 15, this reaction can be categorized based on the temperature. It is concluded that the reactions proceed at either room temperature (around 25°C) or high temperature (around 500°C)[44]. The reactions can happen at temperatures higher than 500°C, though N_2 starts to react with metals beyond 500°C, so here, we chose 500°C as our high-temperature limit condition[11]. 1M KOH solution is considered as electrolyte for room temperature operation whereas molten hydroxide are considered for high-temperature experiments[48,64].

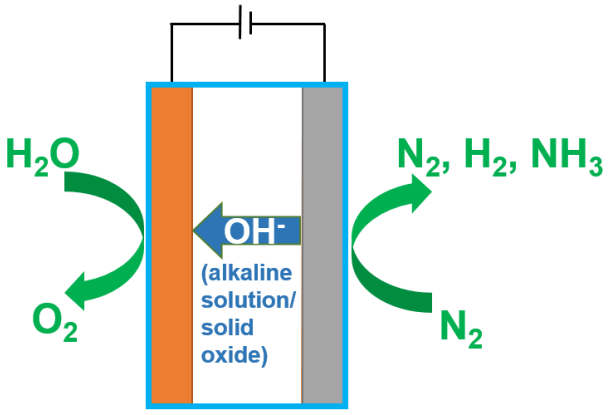

Figure 15 Cell configuration of Scenario A.

The reaction is given by:

$$2N_2 + 6H_2O \xrightarrow{yields} 4NH_3 + 3O_2 (E° = 1.17\,V, 25°C;\ E = 1.20\,V, 500°C) \quad (6)$$

In this reaction, water molecules are oxidized to O^{2-} and H^+ at the anode side, H^+ passes through membrane to the cathode side. At the cathode side, some of the H^+ combines with H^+ to form H_2 gas, while the remainder of the H^+ combines with N_2 to form NH_3. Produced NH_3 dissolves in the KOH solution and flows out of the cell along with the electrolyte[65]. Currently, for this reaction, over 56.55% Faradaic efficiency has been achieved under ambient conditions, with 7.47 μg mg^{-1} h^{-1} NH_3 yield rate observed[66].

The same reaction happens at the high-temperature condition (500°C). In this case, the H^+ is transported through molten hydroxide instead of the base solution. Research in the literature reports that over 35% columbic efficiency and 2 mA/cm^2 can be achieved in a molten hydroxide suspension of nano-Fe_2O_3 [67]. Because of high temperature, produced NH_3 is mixed with unreacted N_2 and side product H_2. Additional thermal energy is required to elevate the reaction temperature, and the literature reveals that the elevated temperature promotes the conductivity of electrolyte[46]. There are two methods to increase the cell temperature: to heat the inlet streams or to heat the electrolyzer. Here, we choose to heat the inlet streams for the simplicity of simulation.

2.2.2.2 NH_3 electrosynthesis using N_2 and H_2, wherein H_2 is produced from H_2O electrolysis

Instead of using H_2O as H^+ sources, H_2 gas can also be used directly as the H^+ source. The overall process becomes a two-step electrosynthesis process at both room (25°C) and high temperature (500°C)[48]. Here, 1M KOH solution and molten hydroxide salt are used to keep the consistency of comparison. The reaction is:

$$N_2 + 3H_2 \xrightarrow{yields} 2NH_3 (E° = 0.06\,V, 25°C;\ E = 0.12\,V, 500°C) \quad (7)$$

As shown in Figure 16, first, we used an alkaline H_2O electrolysis system for H_2 production, and then produced H_2 is transferred to NH_3 electrosynthesis cell. At anode side, H_2 breaks apart to protons and transfers through the electrolyte to the cathode side, where it combines with N_2 and protons to form NH_3, side product H_2 is also produced in this reaction. Over 90% Faradaic efficiency was reported at 25°C using Nafion as electrolyte, with a 3.5 mA/cm^2 current density[68]. For high-temperature experiment, 80% Faradaic efficiency has been reported at 400°C with the assistance of Al cathode and Porous Ni Plate, and it achieved 16 mA/cm^2 current density[68].

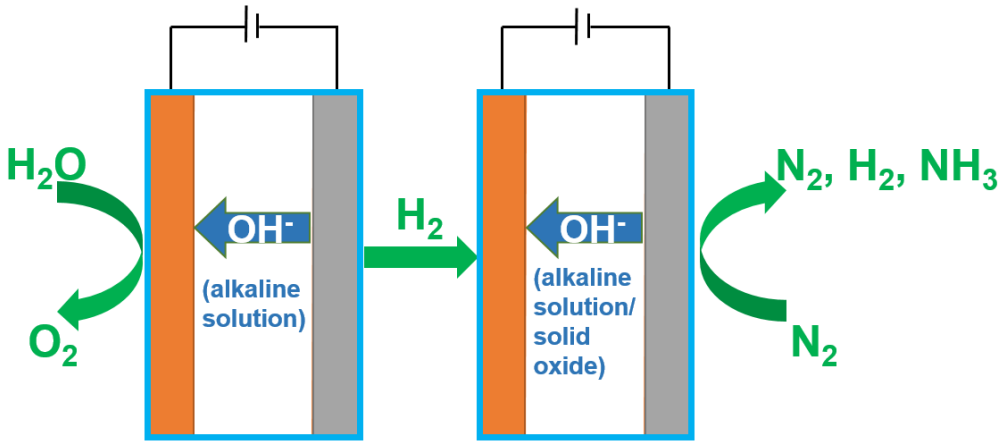

Figure 16 Cell configuration of Scenario B. The left cell is H_2O electrolysis cell for H_2 production while the right one is for NH_3 electrosynthesis.

2.2.2.3 NH_3 synthesis using H-B reactor, where H_2 is produced from H_2O electrolysis

Figure 17 illustrates the concept of coupling the H_2O electrolyzer with a traditional H-B plant[26]. In this case, the feedstock H_2 is produced from H_2O electrolysis cell and reacts with N_2 in the H-B reactor to produce NH_3. This is likely the most technologically mature pathway with technology readiness level (TRL) of between 5 to 6 and 10 for water electrolysis and H-B process, respectively. Today, water electrolyzers are commercially available at scale, from companies such

as Siemens, Hydrogenics, Nel Hydrogen, Teledyne, Proton OnSite; all are commissioning industrial-scale electrolyzers. On the other hand, H-B reactors have been operational in large-scale industrial settings for over a century. Therefore, coupling the H-B reactor with a water electrolyzer could potentially reach the marketplace within the next decade. In 2017, Yara, the world's largest NH_3 producer, announced to build a demonstration plant to produce NH_3 using solar power in Western Australia[69]. In 2018, Hydrogen Utility (H2U), a hydrogen infrastructure company, and ThyssenKrupp announced to build a renewable NH_3 demonstration plant in Southern Australia[70].

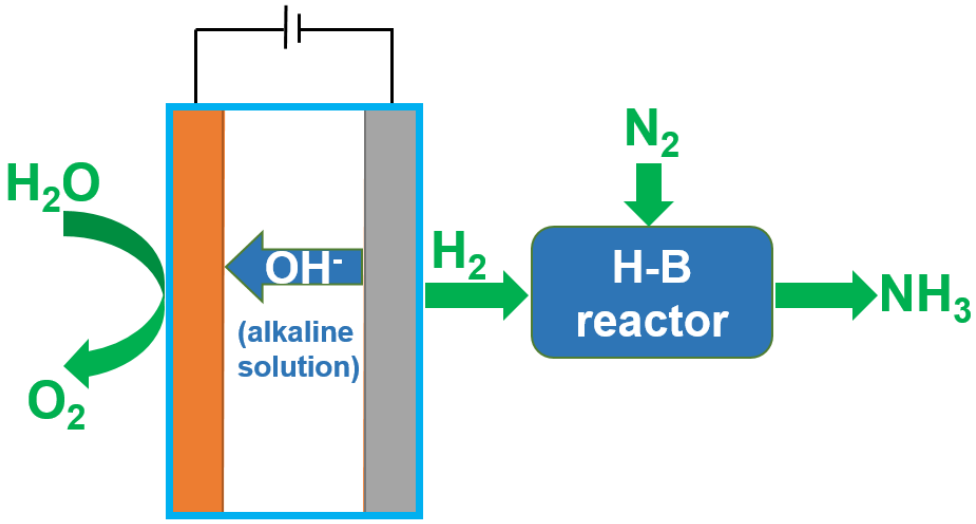

Figure 17 Cell of configuration of Scenario C. The required H_2 is produced from H_2O electrolysis cell.

2.2.2.4 Redox reactions

Apart from the traditional H-B process and electrolyzer-involved routes, there has been growing interest in electro-redox cycles to synthesize NH_3[10,71]. In this context, the use of Li as intermediate synthesis material is a compelling pathway, as illustrated in Figure 18[10].

In this process, pure lithium is produced via lithium hydroxide (LiOH) electrolysis, which is a highly energy-intensive process due to the high voltage (2.8 V) requirements[72]. In the second

step, Li reacts with N_2 to produce trilithium nitride (Li_3N)[72]. In the third step, Li_3N reacts with water to produce NH_3 and LiOH. The produced LiOH can be recycled to the first step to complete the redox cycle. The Li cycling follows next three reactions:

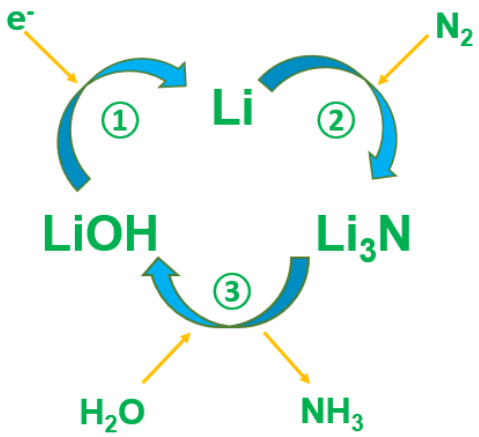

Figure 18 Cell of configuration of Scenario D.

$$6LiOH \rightarrow 6\text{Li} + 3H_2O + \frac{3}{2}O_2 (E° = 2.8\ \text{V}, 427°C) \quad (8)$$

$$6Li + N_2 \rightarrow 2Li_3N \quad (9)$$

$$Li_3N + 6H_2O \rightarrow 6LiOH + 2NH_3 \quad (10)$$

The reaction between Li_3N and H_2O releases large quantities of heat (581.62±1.42 kJ/mol) so extra H_2O supply is required to keep the temperature below LiOH decomposition temperature (924°C), which accordingly increases the NH_3 separation cost[73,74]. Impressive selectivity (i.e., 88% Faradaic efficiency) and reaction rate (500 mA/cm^2 current density for LiOH electrolysis) have been demonstrated at lab-scale[72]. However, concerns remain with the use of Li for large-scale industrial settings due to cost, scarcity, and safety issues[75].

2.2.3 Current status and challenges

Currently, most of the electrosynthesis processes described above remain at lab-scale experiments (excluded using N_2 and H_2 for NH_3 synthesis through the H-B process). The challenges with respect to scale-up arise from various aspects: the selectivity of catalysts that lead to the competitive reaction towards H_2 or NH_3, poor conductivity of electrolytes that limits the production of NH_3, and the stability of NH_3 electrosynthesis cell remains untested[76]. Six of those synthesis routes were summarized for evaluation: a) NH_3 electrosynthesis using N_2 and H_2O at 25°C (Scenario A RT), b) NH_3 electrosynthesis using N_2 and H_2O at 500°C (Scenario A HT), c) NH_3 electrosynthesis using N_2 and H_2 at 25°C, H_2 is produced from H_2O electrolysis (Scenario B RT), d) NH_3 electrosynthesis using N_2 and H_2 at 500°C (Scenario B HT), H_2 is produced from H_2O electrolysis, e) NH_3 synthesis using N_2 and H_2 through H-B reactor, H_2 is produced from H_2O electrolysis (Scenario C), f) NH_3 synthesis using Li redox reaction as intermediate product (Scenario D), RT stands for room temperature and HT for high temperature.

2.3 Conclusions

In this chapter, first, several current H_2O electrolysis methods were reviewed. The PEMEC was chosen as the H_2 production method based on the performance and stability. Approaches for NH_3 synthesis using electricity as an energy source (Table 2) were also reviewed. NH_3 electrosynthesis has been reported in several approaches, however, the economic feasibility of those processes has not been discussed thoroughly and the most important parameters that control the commercial operation of these processes still lack investigation. Hence, there is a need to evaluate both technical and economic perspectives of these processes. In the following Chapters, a technical and economic comparison is conducted on each abovementioned synthesis approach.

Chapter 3 Models and Simulations of Processes

In Chapter 2, current available NH_3 electrosynthesis routes were reviewed and categorized. In this Chapter, the production process for each process is designed and the expense of production is analyzed. First, the processes for each NH_3 electrosynthesis routes were designed. Then, process simulation software was used to model mass and energy balances for each process. From the simulation, the capital and operating expenses for each process was evaluated.

3.1 Process description

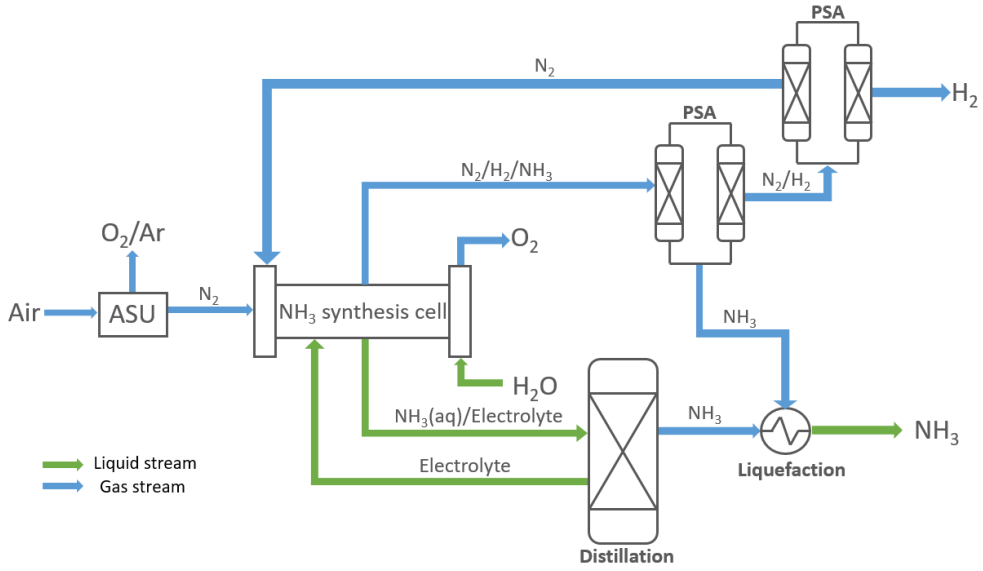

Figure 19 Generalized block flow diagram for the NH_3 electrosynthesis process.

Figure 19 displays the major units for NH_3 electrosynthesis, though the difference of specific units for each process is not shown for the sake of simplicity. Five major units are essential in NH_3 electrosynthesis: 1) air separation unit (ASU), 2) NH_3 synthesis cell (including H_2O electrolyzer for using H_2 as feedstock, LiOH electrolyzer and other related reactors for redox reaction), 3)

Pressure Swing Adsorption (PSA), and/or 4)distillation column, and 5) NH_3 condensation unit. As shown in Figure 19, first, ASU separates N_2 from air and reject O_2 and Ar to the atmosphere. Typically, additional separation units are used to separate Ar from O_2 so both of them can be sold as products[77]. However, this increases the scale and cost for the ASU plant and harms the potential advantages of small-scale or even modular production. Hence, separation of Ar and O_2 was not considered here. Next, separated N_2 is fed to NH_3 synthesis cell along with the proton source (either H_2O or H_2) to synthesize NH_3 at the cathode and O_2 at the anode. In NH_3 electrosynthesis, the hydrogen evolution reaction (HER) is the key competing reaction. In this analysis, the potential revenue that could be generated from H_2 is not considered.

Depending on the operating conditions, NH_3 can be produced in two different phases, i.e., dissolved NH_3 in case of low (room) temperature and gaseous NH_3 for high-temperature operations. For the room-temperature operation, NH_3 can be easily dissolved in the electrolyte because of its high solubility in the electrolyte[78]. Therefore, a distillation column is used to separate NH_3. After distillation, NH_3 in gaseous form proceeds through the condensation unit. Here, we used propane as a cooling agent to liquefy NH_3 for its further storage and transportation. Electrolyte solution exits at the bottom of the distillation tower and recycled back to the NH_3 synthesis cell. Unreacted N_2 and side-product H_2 produced at the cathode are sent to the PSA unit for separation, N_2 is recycled back to the cell to improve the overall efficiency whereas H_2 is not analyzed cause the compression of H_2 is costly.

For the high-temperature operation, NH_3 is produced in gaseous form, so we chose the PSA unit to separate NH_3 from unreacted gases, which has been demonstrated to achieve over 99% efficiency[79]. At the outlet of synthesis cell, unreacted N_2, side-product H_2, and produced NH_3 are together fed to the PSA unit. Unreacted N_2 is recycled back to the cell and H_2 is separated from

NH_3 and produced NH_3 is fed to the condensation unit, meanwhile side product O_2 is compressed and sold.

Other than room temperature and high-temperature operations, the conventional H-B process using H_2 from clean sources and Li cycling process. For the H-B process considered, it typically requires high temperature (to increase the reaction rate) and high pressure (to shift the chemical equilibrium) to synthesize NH_3[11]. Here, we chose a PEM H_2O electrolyzer for the production of H_2, and ASU for N_2, and an H-B reactor for the synthesis of NH_3. The produced NH_3 remains in liquid phase due to the high temperature and high pressure of the process, while unreacted N_2 and H_2 remain in gaseous form and are recycled back to the inlet of reactor for recycling to increase the overall efficiency[11,44]. Therefore, this process does not require an NH_3 separation unit.

For the lithium cycling process, produced NH_3 comes out along with steam (450°C) and is fed to the distillation column, NH_3 is separated and sent to condensation unit meantime H_2O is recycled back to the beginning of lithium cycling process.

3.2 Mass and material balance

In our process modeling, we chose the NH_3 production rate at 100 ton/day (5872 kmole/day)[80,81]. From the material balance, every two moles of produced NH_3 requires one mole of N_2 and six moles of protons, so we need 2936 kmole of N_2 to be produced from the ASU every day, which equals 82.24-ton daily N_2 production rate[82]. Here we note that due to the low single-pass yield, 0.00353%, of NH_3, it would not be economically feasible to separate the NH_3 (see Appendix D). Hence, it was decided to circulate electrolyte with produced NH_3 until it reaches a higher concentration (i.e., 10 wt. %). Figures 20 to 25 summarize the mass flow and power requirements for each process and unit. The calculation for power can be found in Appendix D.

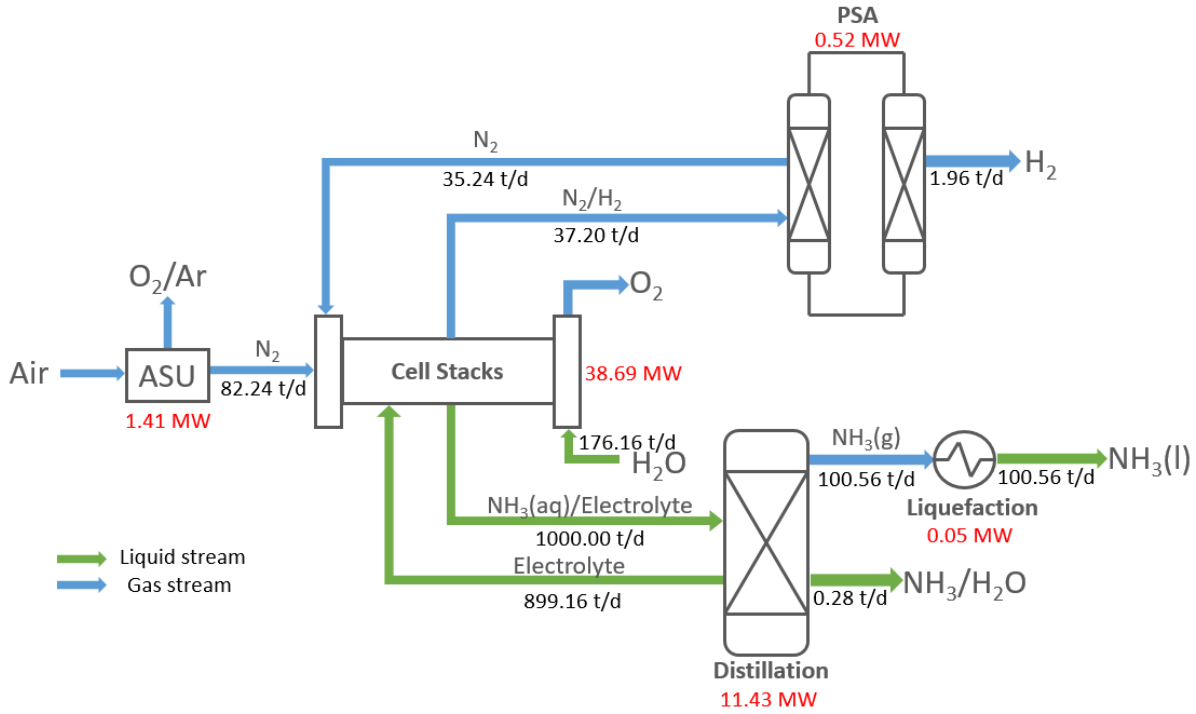

Figure 20 Process flow diagram for Scenario A RT (mass flow rate in ton/day).

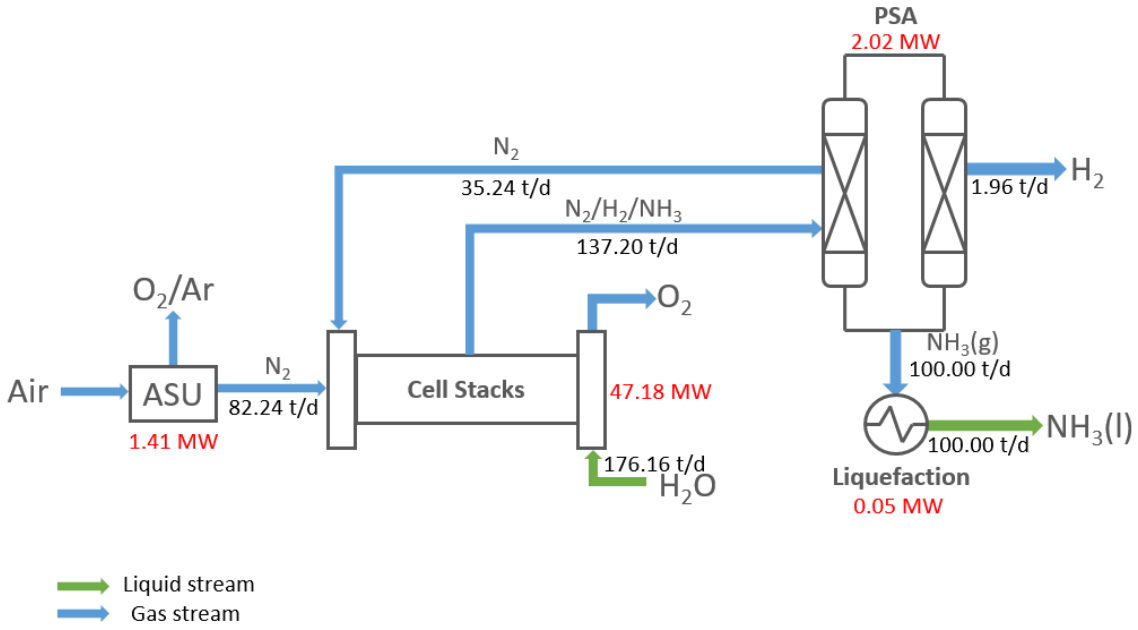

Figure 21 Process flow diagram for Scenario A HT (mass flow rate in ton/day).

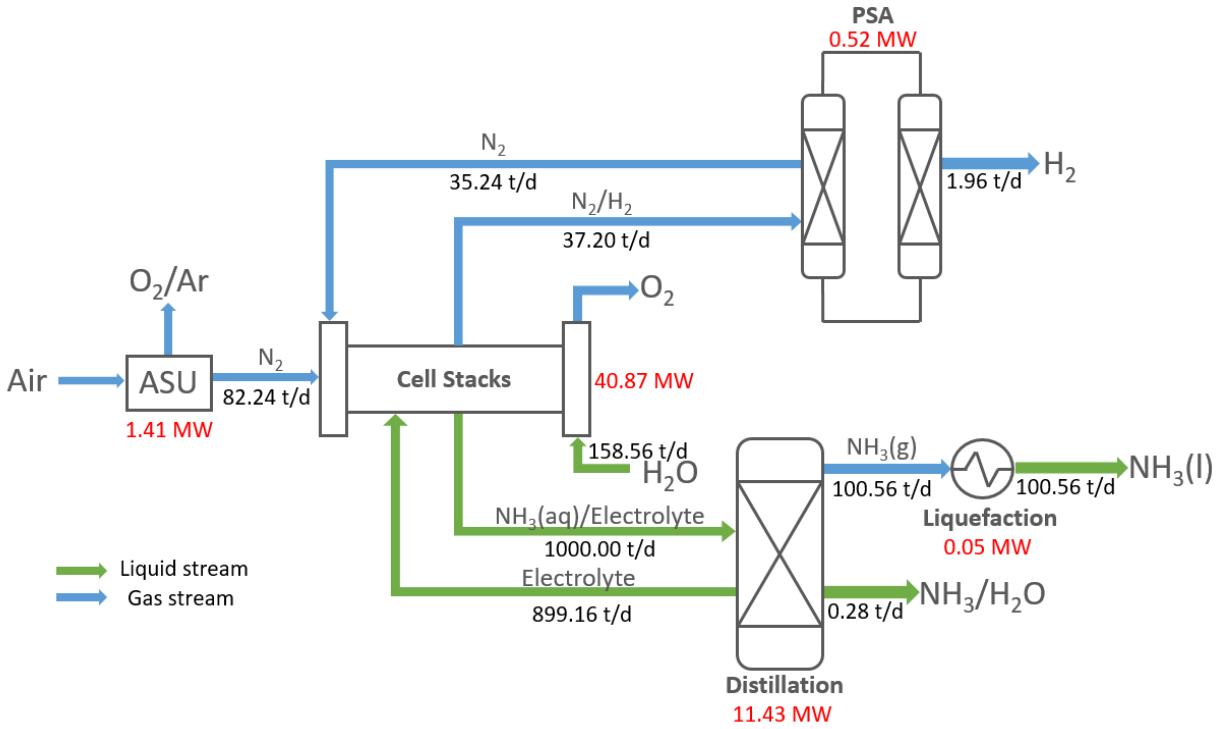

Figure 22 Process flow diagram for Scenario B RT (mass flow rate in ton/day).

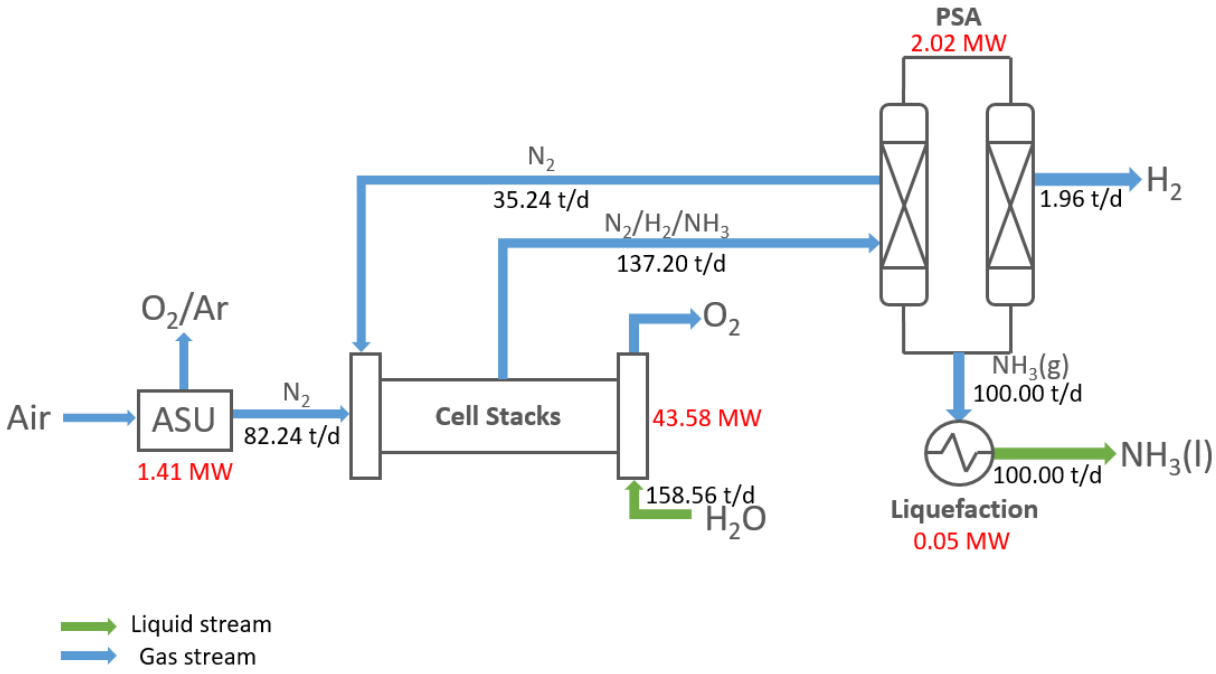

Figure 23 Process flow diagram for Scenario B HT (mass flow rate in ton/day).

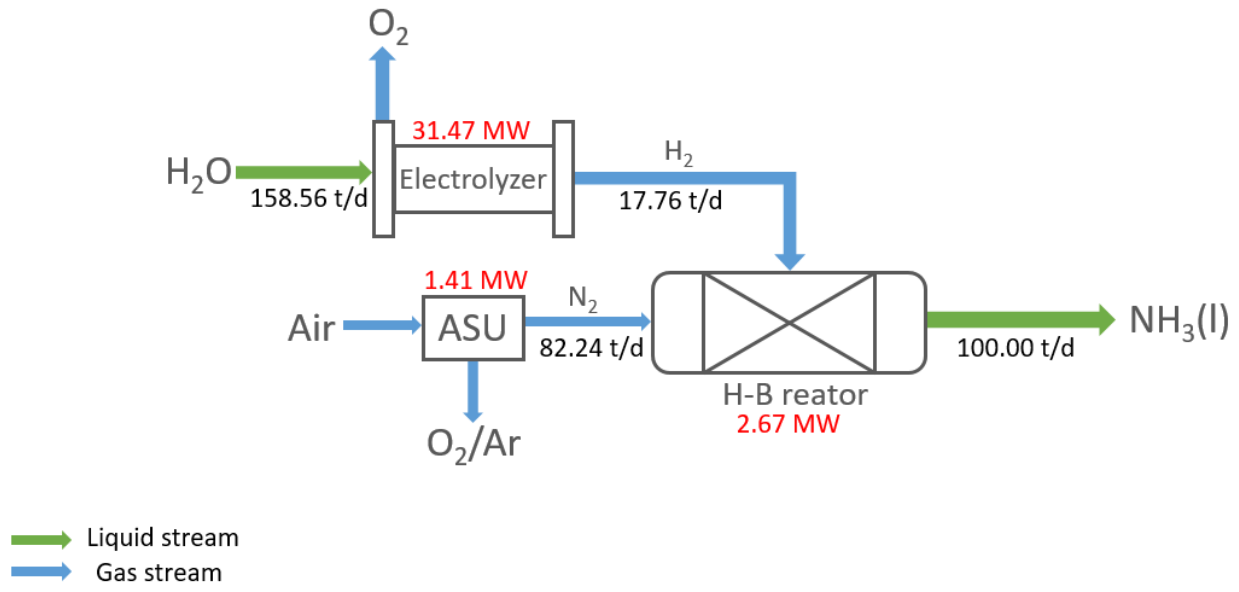

Figure 24 Process flow diagram for Scenario C (mass flow rate in ton/day).

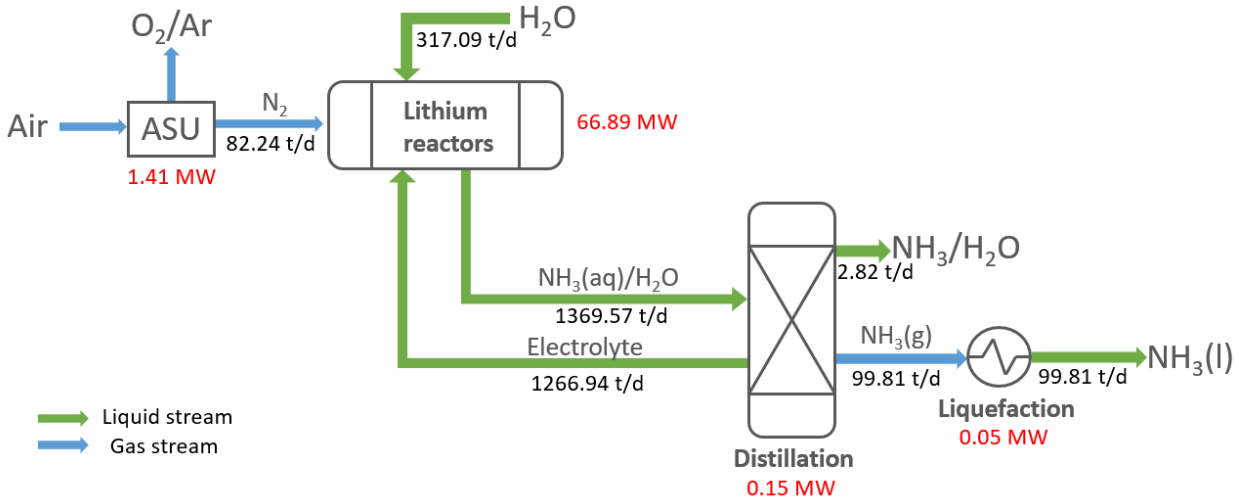

Figure 25 Process flow diagram for Scenario D (mass flow rate in ton/day).

3.3 Simulation and calculation

The Aspen (Aspen HYSYS, 2017) process simulation package was used to simulate the ASU for N_2 feed, to calculate heating energy for high-temperature operation, to separate NH_3 from solution using distillation column, to liquefy NH_3 for further storage and transportation, and to compress side-products O_2. For phase behavior and property calculations, the Peng-Robinson

property package for ASU simulation and Electrolyte NRTL was used for modeling the distillation column to describe the interaction between NH_3 and solution. The expenses are calculated considering equipment cost, installation cost, and other non-field costs.

3.3.1 ASU simulation

Unlike a traditional ASU plant, the ASU simulation conducted here focuses more on the production of N_2 instead of O_2, which decreases the scale and cost compared to conventional ASU plant. In a typical ASU plant, all three major industrial gases, O_2, N_2, and Ar are well separated, which requires significant effort with respect to system design and optimization[83]. Hence, to eliminate the complexity, the process was designed mainly to separate N_2 from O_2 and Ar because N_2 is the synthesis feedstock for NH_3 electrosynthesis, whereas O_2 and Ar separation is not the main object of the operation.

For ASU, the N_2 required is 5872 kmole/day (244.67 kmole/hour) from material balance. Cryogenic distillation for N_2 separation is used[84]. An air filter and molecular sieve are used to block dusts and other particles[85]. Thereafter, the cleaned air consisting of O_2 (21%), N_2 (78%), and Ar (1%) is ready for separation[86]. After cryogenic distillation, the N_2 outlet reaches purity over 99.99%, which fulfills the requirement for electrosynthesis. The process illustration is shown in Figure 26.

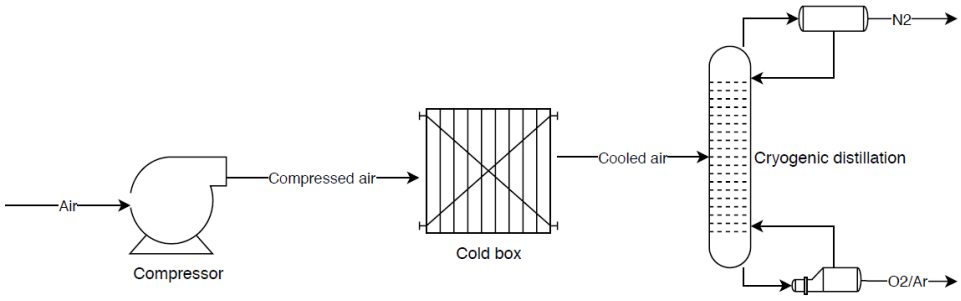

Figure 26 Scheme for Air Separation Unit.

In the simulation, the parameters and costs for the pump, columns, and valves can be simulated and calculated by the Aspen HYSYS process simulation package. However, the heat exchanger ("Cold box" in Figure 26) cannot be simulated by Aspen HYSYS due to the low operating temperature of ASU. The Cold box is a commonly used name for brazed aluminum heat exchanger with carbon steel as supporting structural material[87]. Compared to typical heat exchangers, the cold box can provide a much lower temperature range for multiple streams. Therefore, we gathered the duty (Q), heat transfer efficiency (UA), and log mean temperature difference (LMTD) from the Aspen HYSYS simulation to calculate the required volumes of the cold-boxes, then estimated the costs for the cold boxes from one reported cold box in the literature (see Appendix B). The N_2 cost is calculated over \$100/ton, which is higher than the current market price (see Appendix B). Typically, an ASU is operating at a large-scale to provide high purity level of O_2, N_2, and Ar gas and to decrease their prices. However, that would significantly increase the costs for the ASU unit to balance the N_2 production cost and to separate each product at a high purity level, which contradicts the advantage of modular electrolyzer set-up. Therefore, here we

did not use the N_2 cost from our simulation but from the current market, which accordingly shows that N_2 can not be produced on a smaller production rate using cryogenic distillation.

3.3.2 Cell parameters

The basis for the calculations was based on a production rate of 100 ton of NH_3 daily to compare the economic and environmental aspects of various processes. Typically, chemical production plants can maintain a stable production for 10 to 15 years and with careful maintenance and replacement, the plants can last for more than 35 years[88]. Therefore, a 20-year lifetime was used for the plants evaluated here. Annually, a 2-week downtime for the plants for maintenance and replacement of catalysts is done[89]. Here, all the assumptions for basis case are listed in Table 3.

Table 3 Basic assumptions for NH_3 synthesis model.

Parameter		Basis assumption
Production rate	ton/day	100
Lifetime	year	20
Operating time	day/year	350
Electricity price	$/kWh	0.03
Ammonia price	$/ton	530
Current density	mA/cm^2	300 (RT) 500 (HT)
NH_3 cell cathode overpotential	V	0.5
NH_3 cell anode overpotential	V	0.07V (H_2) 0.3V (H_2O)
Selectivity	%	70
Single-pass conversion	%	50
Electrolyzer cost	$/$m^2$	2000

From the analysis presented above, the production cost for N_2 Around $107/ton, which is higher than the current market N_2 price (less than $40 ton, from a commercialized ASU plant in Cantarell, Mexico which produces 50,000-ton daily N_2 production rate in 1997)[90]. However, here

we are trying to investigate the feasibility of a stand-alone NH_3 electrosynthesis plant, which means the N_2 production cost depends on the actual N_2 requirement, thus we are taking the numbers though it is obviously higher than the market price (detailed calculation can be found in Appendix B).

With the rapid growth of renewable electricity, including hydropower, solar, wind, and nuclear, the electricity price is rapidly dropping over the years. In the SunShot project created by the US Department of Energy (DOE), the target for utility-scale electricity in 2030 is \$0.03/kWh[33]. In certain countries (Dubai, Mexico, Peru, Abu Dhabi, and Saudi Arabia), record low auction prices (\$0.03/kWh) from solar PV has been achieved. In Canada, the grid electricity price is as low as USD \$0.035/kWh (2019 April), which is relatively clean due to a major share from nuclear, and hydropower[91]. To sum up, clean electricity price will continuously decrease and could support the requirement for electrosynthesis. Therefore, the electricity price is chosen at \$0.03/kWh for the base case scenario.

The selling price for NH_3 varies across different geographic locations. The typical price range is from \$400-600/ton for anhydrous ammonia[92]. The reason for various NH_3 price is due to the difference of synthesis materials (from natural gas, coal, or other hydrocarbons), and the influence of the scale and location of the production plant. Therefore, based on the average market price of NH_3 in North America from 2008 to 2018 and with other reported studies, \$530/ton was chosen as the selling price of NH_3[93].

Selectivity (Faradaic efficiency) is an essential experimental parameter in electrochemistry. It measures the ratio of electrons that flow to the products to the electrons that are provided[94]. It defines the efficiency of one electrochemical reaction and is always measured to evaluate the performance of the electrode. In Chapter 2, studies were reviewed on NH_3

electrosynthesis and some results appear adequate under specific conditions, though selectivity is heavily influenced by the catalyst materials (loading, size of the catalysts) on the electrodes, by the electrolytes, and by abundance other interfering factors. In brief, 70% was chosen as base case scenario selectivity based on recently reported studies on NH_3 electrosynthesis under ambient conditions, and 90% as the selectivity for optimistic future prediction from a demonstrated high Faradaic efficiency analogous CO_2 electrolyzer[66].

Another critical performance indicator in electrosynthesis processes is overpotential. It measures the difference between the theoretical required voltage and the voltage that has to be supplied[94]. Various factors cause overpotential including the mass-transfer effects, the charge-transfer effects, and the reaction-associated effects[94]. The reaction overpotential is profoundly impacted by the operational conditions (temperature, pressure, flow rate, etc.), electrode (catalysts, size, and shape, design, etc.), streams (feedstock, purity, etc.), etc. Hence, to simplify the comparison, the overpotential used here arises purely from cathodic overpotential (overpotential due to cathode related effects) and anodic overpotential (overpotential due to anode related effects). For the anode side, we chose two different anode overpotential due to different proton source: 0.2 V anode overpotential for using H_2 as proton source and 0.3 V for using H_2O as proton source, based on reported studies in the literature[56,95].

On the other hand, for reactions which use H_2O as proton sources, also known as HOR (Hydrogen Oxidation Reaction), a 0.07V anode overpotential was selected based on state-of-art experimental results reported in the literature[56]. For the cathode side, where N_2 is reduced to NH_3 (NRR, Nitrogen Reduction Reaction), 0.5 V was taken as the cathode overpotential at base case operational conditions[89].

Electrolyzer price is another essential indicator in this economic analysis. Electrolyzers have been demonstrated by many companies, and typically they are priced with specific working power and capacity which makes it difficult to estimate the real cost. Given data in the literature, we chose \$2000/m^2 as the electrolyzer cost for both room and high temperature at base case conditions[62]. While these are ambitious targets, the cost should drop substantially with the continuous development of electrolyzers and the increase of the production scale[96].

Current density is defined as the current divided by the area of electrode, which indicates the reaction rate of one electrochemical reaction[54]. The performance of an electrochemical reactor is more defined by the current density than the total current[54]. An increased current density results in lower capital cost. Here, 300 mA/cm^2 is chosen as the room-temperature base case current density from current commercial H_2O electrolyzers, while 500 mA/cm^2 is chosen for high-temperature base case conditions[56].

The single-pass conversion refers to the ratio between the N_2 that reacted and the N_2 provided in total. The single-pass conversion efficiency affects separation, mainly PSA units, costs. Here, unreacted N_2 is recycled back to the inlet of the synthesis cell to increase the overall efficiency and to reduce the cost.

There are also some other essential factors worth considering. For example, plant scale is another factor worth considering; a larger production plant would have a tremendous NH_3 production rate and decreased synthesized NH_3 cost, but then it would lose a key advantage of electrosynthesis: modular production. Plantlife is also another critical factor; a longer plant life would weaken the side effect brought by capital expenditure. However, a 20-year chemical industry plant life is a more practical and reliable estimation in current status[97].

3.3.3 Heating equipment

In this part, the electric resistance heater was selected to heat the inlet streams. Furthermore, the use of an electric resistance furnace reduces the complexity in estimating the capital and operating cost for the heating part[98]. The heaters cost were estimated from a similar all-electric hydrogen production plant, with a cost at $77000/MW and 4.1-installation factor[98]. The simulations for heating the N_2, H_2, and H_2O streams and gathered the power requirement were estimated from the Aspen HYSYS simulation package. Typically, there are heat losses from roof and sidewalls in the electric resistance heater, so this was accounted for with a 5% heat loss based on a scrap-based electric arc furnace (see Appendix D)[99].

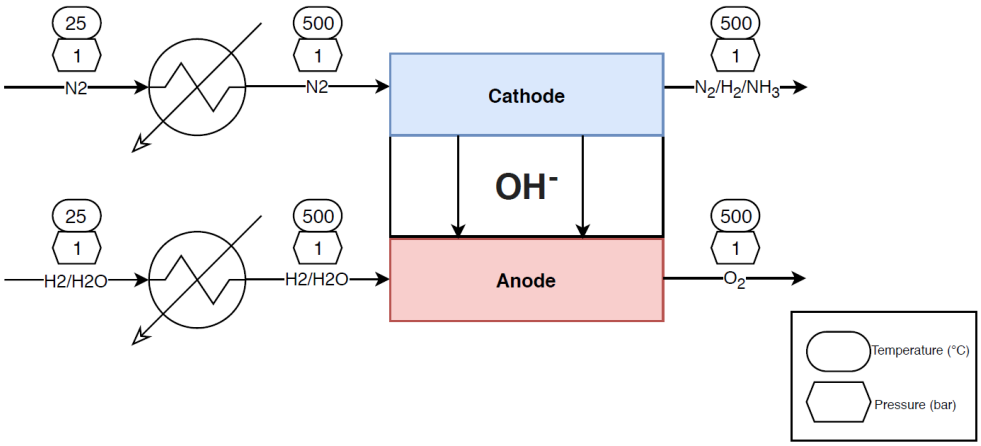

Figure 27 Scheme for the heating process.

3.3.4 NH_3 separation

Two forms of NH_3 need to be separated from outlet stream: dissolved NH_3 (for room temperature operation) and gaseous NH_3 (for high-temperature operation). Here, the Aspen HYSYS package was used to simulate the separation process using the Electrolyte NRTL property package to describe the interaction between NH_3 and KOH solution. The cost of the distillation

process was determined by using the Aspen Economic Analyzer (see Appendix D). The produced NH_3 is required to be separated from NH_3/KOH solution for using N_2 and H_2O at 25°C, as shown in Figure 28, and from NH_3/H_2O solution for Li recycling, displayed in Figure 29.

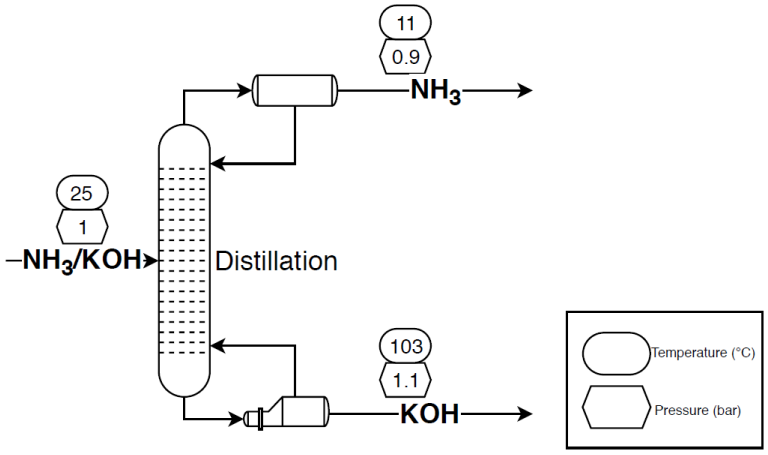

Figure 28 Scheme for distillation column. NH_3 is synthesized from Scenario A.

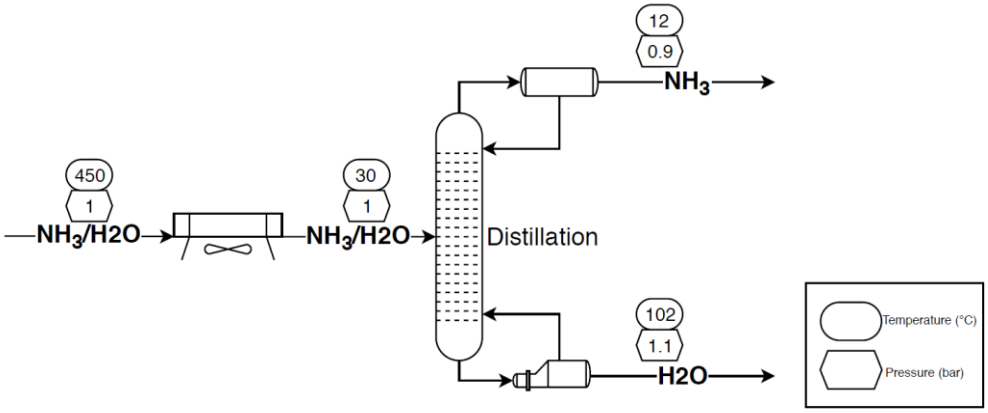

Figure 29 Scheme for distillation column. NH_3 is synthesized via Scenario D.

For the high-temperature operation, PSA was used as the separation process. PSA has been used in separating gases for decades and the principle is simple: the adsorbent preferentially

adsorbs one component from a mixed feed[100]. PSA has been demonstrated with over 99% separation efficiency for NH_3. For the cost of PSA, it is difficult to estimate the actual cost of one PSA plant because it is highly related to the process parameters, including flow rate, pressure, temperature, the component that needs to be separated, and the product purity that need to be achieved. Here, the cost for PSA unit was estimated from a biogas upgrading review ($1,990,000 on a 1000 Nm^3/h basis), and the illustration of a PSA is shown in Figure 30 (see Appendix G for more details).

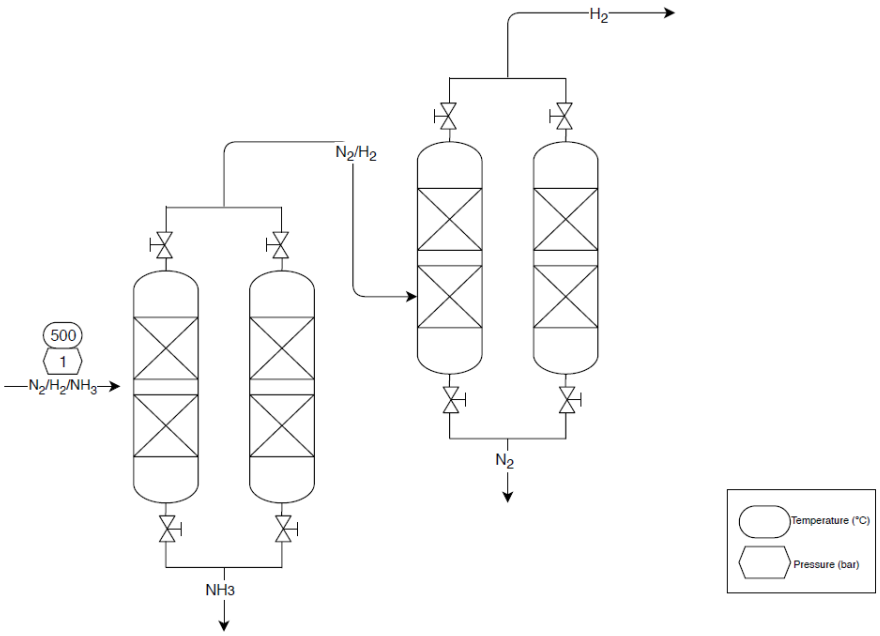

Figure 30 Scheme for PSA unit, the gas mixture is from high-temperature reactions.

3.3.5 Condensation

NH_3 is typically transported in liquid form either via pipelines or transportation truck [101]. In this thesis, the condensation process was also simulated by using Aspen HYSYS.

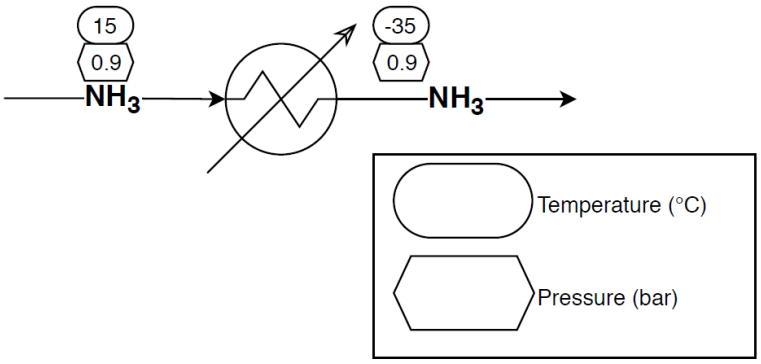

Figure 31 Scheme for condensation unit.

At first, we compared the difference between using the cooling agent and compression, using cooling agent is a more economically preferable choice. The condensation cycle was done using propane as refrigerant, shown in Figure 31. A cooling agent also causes less trouble in maintenance and operating aspects. To sum up, the costs for these condensation units was calculated using Aspen Economic Analyzer (see Appendix D).

3.3.6 O_2 compression unit

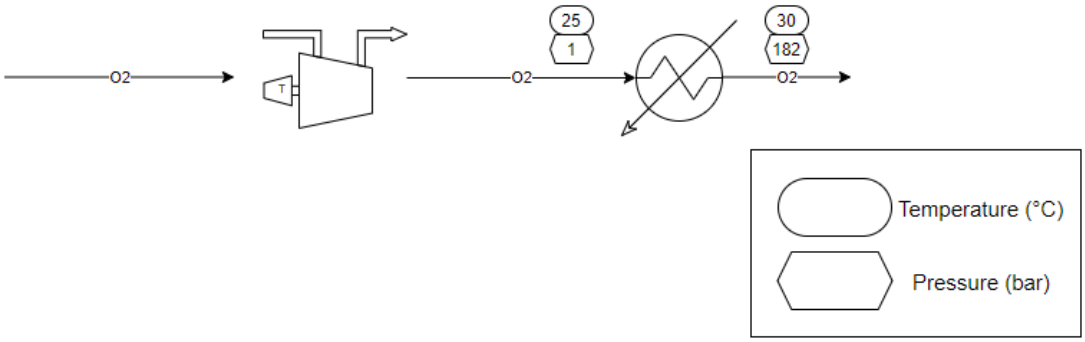

Figure 32 Scheme for O_2 compression unit.

Here, we choose to use the centrifugal compressor to compress O_2 gas for further storage and transportation, as shown in figure 32. Typically, O_2 is compressed through a series of compressors and coolers to reduce the cost for this system, due to the limited compression ratio of compressors (1:3 or 1:4). Relevant expenses are summarized in Table 4.

3.3.7 Results and summary on simulation and calculation

Table 4 Summary from Aspen simulation.

		Capital expenses ($)	Depreciable capital cost ($)	Electricity (kW)	Coolant ($/h)	Heating energy (kJ/h)
Distillation	RT	2,894,110	793,000	52.32	4.48	4.12E+07
	Scenario D	4,276,480	610,800	147.92	24.70	0
Condensation (NH_3)	RT	1,765,710	166,000	52.32	0.94	N/A
	HT	1,775,570	175,700	52.32	0.93	N/A
Heating	Scenario A HT	2,472429	N/A	(7440)	N/A	2.68E+07
	Scenario B HT	648,016	N/A	(1897)	N/A	1.77E+06
O_2 compression	All	10436100	4316400	1473.08	N/A	N/A

3.4 Economic analysis

3.4.1 Overview

In this part, an economic analysis for NH_3 electrosynthesis was conducted. Tax, depreciation, and effect of time are all considered in the calculations. The economic analysis is evaluated from various aspects, including NPV (net present value), LCP (levelized cost of product), Capex (capital expenditure) and Opex (operating expenditure), energy consumption, and sensitivity analysis.

3.4.1.1 Introduction of terminologies

In this analysis, two types of capital costs are considered: depreciable and in-depreciable[102]. To be more specific, for example, in capital expenses, there are two kinds of costs: field cost and

non-field cost. Field cost includes all the costs related to equipment purchase, installation, construction, etc. Non-field cost are the cost for taxes, contingency, contract fees, etc., and it is non-depreciable. Therefore, in the spreadsheets, listed in Appendix F, the value of capital expenses does not match with capital cost because capital cost does not include non-field cost[103]. Net profit means the amount of money that was made in one year after considering depreciation and operating cost, while net earnings is the value of that money after calculating tax. Discounted cash flow is calculated with consideration of the benefit of depreciation[104]. The net present value is given by [105]:

$$NPV = \sum_{t=1}^{n} \frac{CF_t}{(1 + IRR)^t} \tag{11}$$

where *t* is time in years, *n* is the number of years of plant life, *CF* is the cash flow, and *IRR* is the internal rate of return. The cash flow is defined as the net amount of cash and cash-equivalent (depreciable capital cost) being transferred into and out of business, and cash flow (present value) is cash flow with consideration of nominal interest rate[106]:

$$Cash\ flow = (Cash\ from\ operations) - (Capital\ expenditures) \tag{12}$$

Next, the capital expenses and working capital are combined with cash flow that year to obtain a cumulative present value for that year. Eventually, we added up all cumulative present values from each year to get the NPV.

The Aspen Economic Analyzer (Aspen, 2017) was used as the primary cost estimation tool, the project type is grass root and location is set in North America, while the system start date is the first quarter of 2016. The assumptions are listed in Table 5.

Table 5 Basis for economic analysis.

Parameters		assumption
Income tax	%	38.9
Nominal interest rate	%	10
Project type		Grass root
Location		North America
System start date		2016, first quarter

3.4.2 NPV and LCP

The basis for NPV is not difficult to understand: money in the present is worth more than the same amount in the future due to inflation and earnings from alternative investments that could be made during the intervening time. In other words, a dollar earned in the future would not be worth as much as one earned in the present[107]. The definition for levelized cost of product (LCP) is determined from the NPV: the LCP is the cost of products when NPV equals zero[108].

$$NPV = 0 = Product\ revenue\ PV\ (LCP)\ \text{-}\ Operating\ cost\ PV - total\ capital\ cost$$

The detailed calculation for NPV for all processes is described in Appendix E.

Chapter 4 Results and Discussion

In this Chapter, detailed economic analysis is done for various electrosynthesis pathways for NH_3 production. The economic analysis is conducted for three different scenarios: conservative case, base case, optimistic case. The NPV is compared for six different electrochemical synthesis routes under base case and optimistic case scenarios. The various components of the capital and operating costs being explored. The levelized cost of the product (LCP) was calculated and compared with that of the conventional process (i.e., H-B). To reveal the sensitivity of input parameters on the overall economics of the process, a sensitivity analysis is conducted. Furthermore, the effect of electricity price on the economic feasibility of various electrosynthesis routes is evaluated. Based on this analysis, the target performance metrics that need to be achieved at scale are estimated, including Faradaic efficiency, selectivity, energy efficiency, and current density. From the energy consumption, the CO_2 reduction potential for all processes is also compared.

4.1 Results of economic analysis

4.1.1 NPV on base case and optimistic cases

Table 6 summarises different parameters applied in base and optimistic cases. Using those parameters, we compared the NPVs for every process under different conditions. The results are shown in Figure 33. As shown in the figure, in the base case, none of the six processes is profitable, and all NH_3 electrosynthesis processes are showing worse results compare to Scenario C, the hybrid of H_2O electrolysis and NH_3 synthesis loop. Hence the processes need to be compared under optimistic parameters. Among all these processes, Scenario A RT and Scenario B HT would be

the most economically compelling pathway, while Scenario B RT and Scenario D are showing less profitable margins compare to others.

Table 6 Parameters for base and optimistic prediction.

Parameter		Base case	Optimistic case
Electricity price	\$/kWh	0.03	0.02
Ammonia price	\$/ton	530	+15%
Current density	mA/cm^2	300 (RT) 500 (HT)	500 (RT) 700 (HT)
NH_3 cell cathode over potential	V	0.5	0.3
NH_3 cell anode over potential	V	0.07V (H_2) 0.3V (H_2O)	0.07V (H_2) 0.3V (H_2O)
Selectivity	%	70	90
Single-pass conversion	%	50	70
Electrolyzer cost	$\$/m^2$	2000	1000

To further compare the contribution of each cost component in economic analysis, we performed a detailed capital and operating expense analysis in the following section.

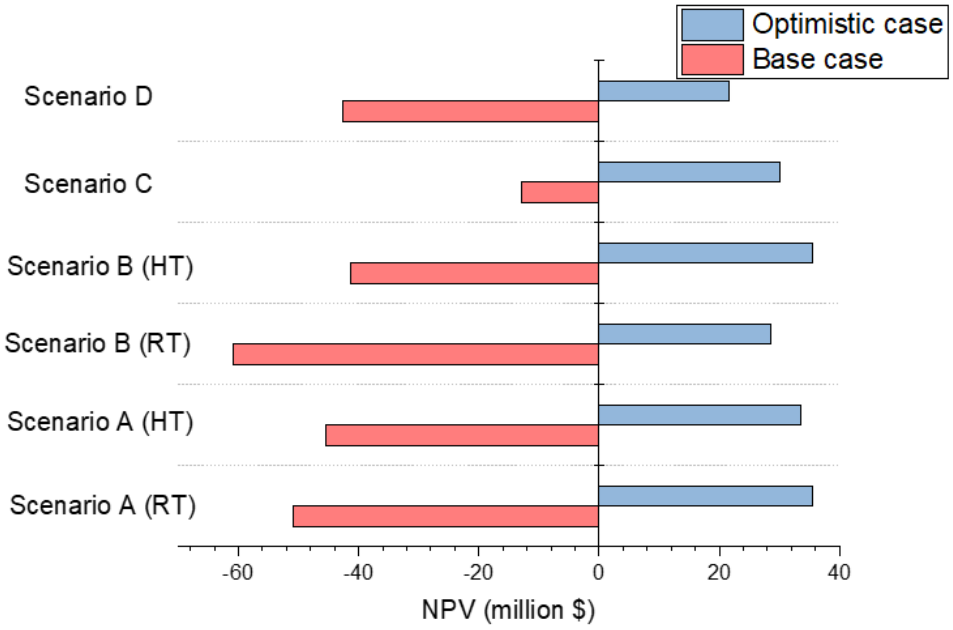

Figure 33 NPV results for all processes, base case, and optimistic case.

4.1.2 Capex and Opex under optimistic case scenario

4.1.2.1 Introduction

In this section, the capital and operating costs for all processes are calculated based on optimistic condition. Here, capital cost includes the cost of including equipment, installation, and other field and non-field costs, while operating cost includes the costs that are required to complete the production but does not include labor costs.

4.1.2.2 Results

Figure 34 shows the contribution of each unit in capital cost calculation. First, the ASU is occupying a significant amount of capital input for all processes. It indicates that if the requirement for N_2 purity is less strict, for example, using air other than using higher purity N_2, then all NH_3 electrosynthesis routes would be apparently more profitable. The O_2 compression unit needs a huge amount of money as well, though the revenue from selling O_2 compensates that. Second, Scenario C has the highest capital investment, which is mainly attributed to the capital cost of the H-B synthesis loop (orange bar). This massive capital cost of the H-B reactor is due to the low single-pass conversion efficiency (i.e., 0-15 vol. %) of NH_3 synthesis. To make it economically feasible, industries typically recycle the unreacted N_2 and H_2 through a series of H-B reactors to increase the overall efficiency (~97%). To compensate for this high capital cost, the H-B process typically runs at large scale industrial settings. The capital cost estimation for the H-B reactor is provided in Appendix D.

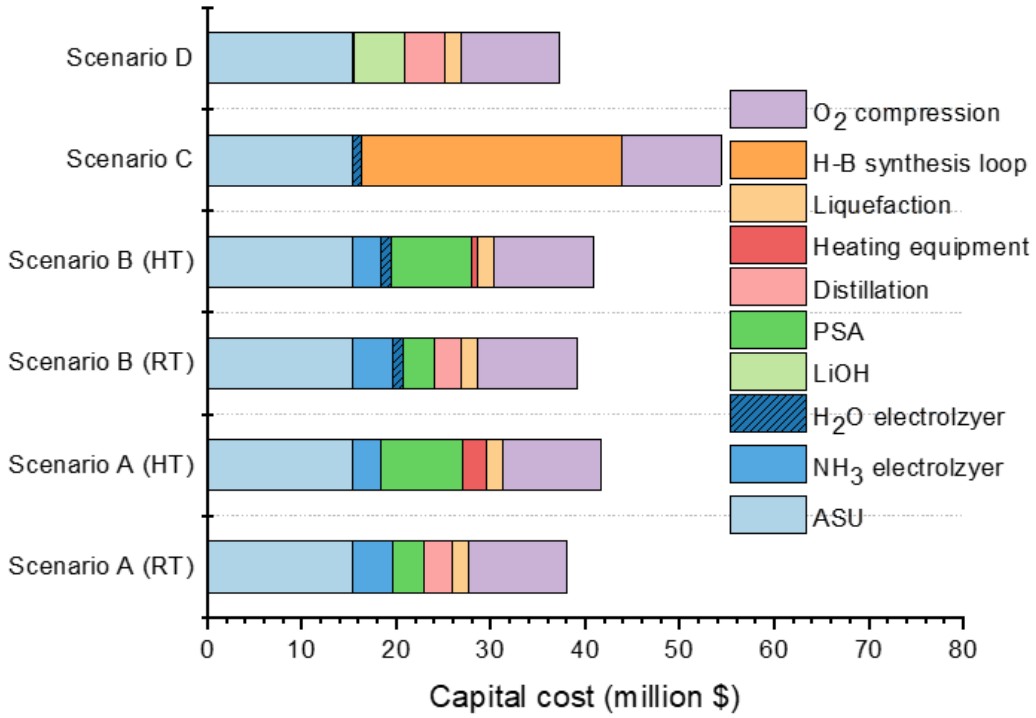

Figure 34 Capital cost of all processes under optimistic conditions.

On the other hand, Scenario A RT and Scenario D are using less capital investment, which is mainly due to less investment in NH_3 separation. For Scenario D, the purchase for LiOH is the third highest capital investment, which implies that the dropping price of LiOH could positively impact the feasibility of this process. Besides, high-temperature cases are less profitable compared to room temperature cases due to the large amount of investment in PSA units, which demonstrates the urgent need for cheaper gas separation process. From figure 34, we can summarise that the major capital investment for electrosynthesis is for supplementary systems, while the electrolyzers are occupying a relatively minor amount.

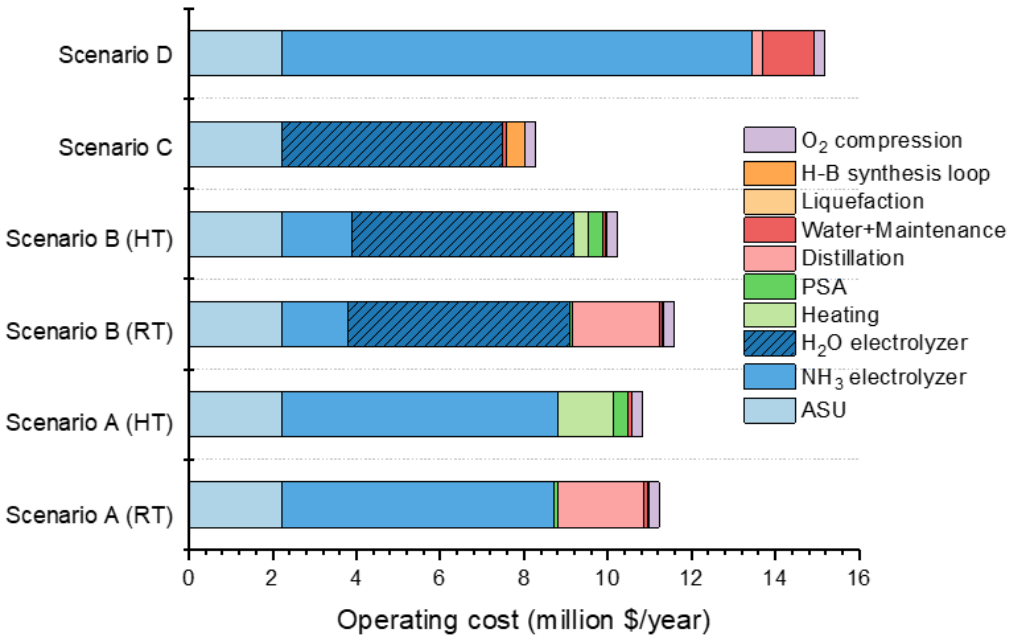

Figure 35 Operating cost of all processes under optimistic conditions.

Then in Figure 35, we compared the operating costs for all processes. As expected, electricity (blue) is the most critical part of operating cost, requiring approximately $5M to $10M every year. Therefore, a cheap electricity source is crucial for electrosynthesis routes. Secondly, ASU is occupying a notable amount of operating cost, which, again, reminds us to decrease the purity requirement for N_2, therefore, decrease the ASU operating cost. The next essential part is the distillation operating cost, distillation column needs substantial operating cost annually, it needs around $3M annually for room temperature experiments, while around $0.2M for Scenario D after heat integration. This cost is mainly attributed to the energy requirement for the reboilers in distillation column. In a typical distillation column, the heat is mainly provided by either low pressure saturated steam or superheated steam. However, using steam causes higher operating cost and more CO_2 emission. Here, the heat (kJ/h) is converted to the power requirement (kW) because

we chose the electric resistance heater to elevate the reactor temperature and brings simplicity in the following calculation.

As illustrated in Figure 35, Scenario D requires the highest operating cost while Scenario C needs the least operating cost, which is mainly due to the difference in electricity requirement. For Scenario D, it requires more electricity compared to other cases (3.1 V at optimistic condition). For Scenario C, it requires electricity for H_2O electrolysis (1.6 V) and for NH_3 synthesis loop (2.67 MW, see Appendix D).

Third, in Scenario D, the maintenance cost is another major part, while that is less noteworthy in other processes. In this thesis, we defined the maintenance cost as the cost for the annual maintenance of the electrolyzers and replacement of catalysts. We assumed 2.5% of electrolyzer cost as maintenance cost for processes excluding Scenario D[89]. In the cost estimation for Scenario D, we assumed an analogous smelter configuration used for alumina refinery[109]. In alumina electrolysis, Al_2O_3 is heated to molten form, and then Al^{3+} ion is reduced to Al element at the cathode, while O^{2-} ion is oxidized at the anode side.

$$Cathode: Al^{3+} + 3e^- \xrightarrow{yields} Al \tag{13}$$

$$Anode: O^{2-} + C \xrightarrow{yields} CO + 2e^- \tag{14}$$

The oxidization of O^{2-} is typically conducted using carbon anode, which makes alumina electrolysis a CO_2 emissive process[110]. To overcome that problem, we chose to use inert anode, which is also cheaper and cleaner than carbon anode[111]. However, the electrolysis reactions are required on a 100 ton/day NH_3 production basis, and the inert anodes are required to be replaced every three years[111]. Hence, the maintenance cost of the Scenario D is clearly higher than in other cases. The inert anodes could be recovered after the electrolysis, but it would increase the

complexity of the process, and out of this study's scope, so we did not consider the recycle of anodes.

4.1.3 LCP and contribution of each part at optimistic case

We compared the contribution of each part in levelized cost in Figure 36. The colors in each bar are showing the contribution of each cost component on a 20-year basis. The left y-axis indicates the levelized cost in \$/ton produced NH_3. From the results, all processes are profitable under optimistic conditions.

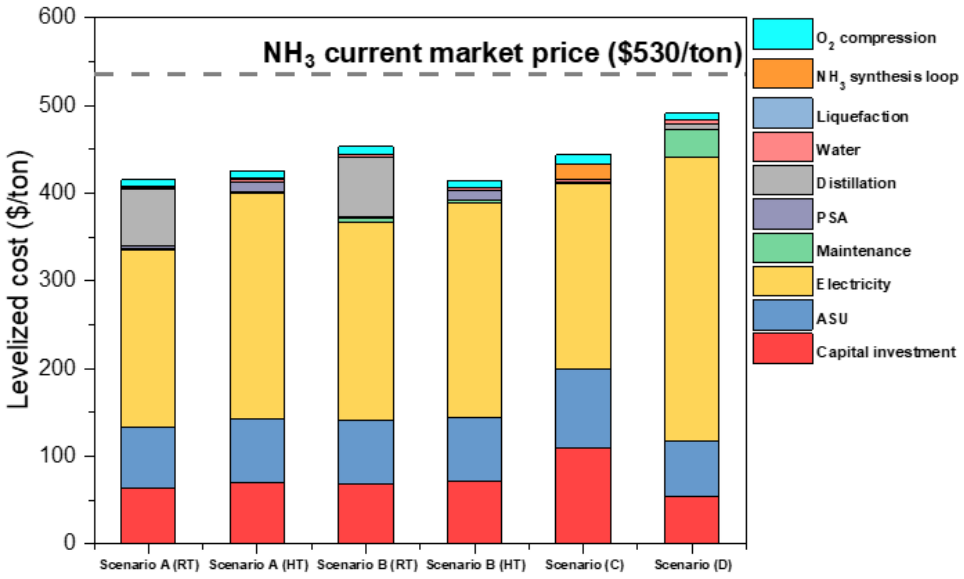

Figure 36 Levelized cost of NH_3 via all processes under optimistic conditions.

Clearly, the electricity (yellow bar) is the most noteworthy cost component, which is due to the nature of electrosynthesis. The second largest part is the capital investment, which acquires nearly one fifth in all scenarios. The third part is the investment for ASUs, which continuously reminds us to find cathodes that are more tolerable on the purity of N_2.

4.1.4 Sensitivity analysis

Up to this part, we showed the economic analysis on overall performance and the results from a bird's view. However, it is not clear which parameter impacts more on the economic feasibility. To better understand the sensitivity of various assumed parameters, sensitivity analysis was performed. Several parameters (capacity factor, single-pass conversion, current density, electrolyzer cost, cathode overpotential, product selectivity, NH_3 selling price, and electricity price) are chosen for analysis that are considered critical. They are summarized in Table 7. For each parameter, the future performance in optimistic, base, and conservative predictions are considered as listed in Table 7.

Table 7 Value ranges of factors for sensitivity analysis.

Sensitivity parameters		Optimistic	Base	Conservative
Electricity price	\$/kWh	0.02	0.03	0.04
NH_3 selling price	\$/ton	+15%	530	-15%
Selectivity	%	90	70	50
NH_3 cell cathode over potential	V	0.3	0.5	0.7
NH_3/H_2O cell price	$\$/m^2$	1000	2000	3000
Current density	mA/cm^2	500(RT) 700(HT)	300(RT) 500(HT)	100(RT) 300(HT)
Single-pass conversion	%	70	50	30
Capacity factor		1.0	0.9	0.8

With the consideration of those parameters, the results are summarized in the following sensitivity graphs, Figures 37 to 42. Both the LCP and NPV graphs for individual process are listed together. The vertical blue dashed line indicates the current market price of NH_3 ($530/ton).

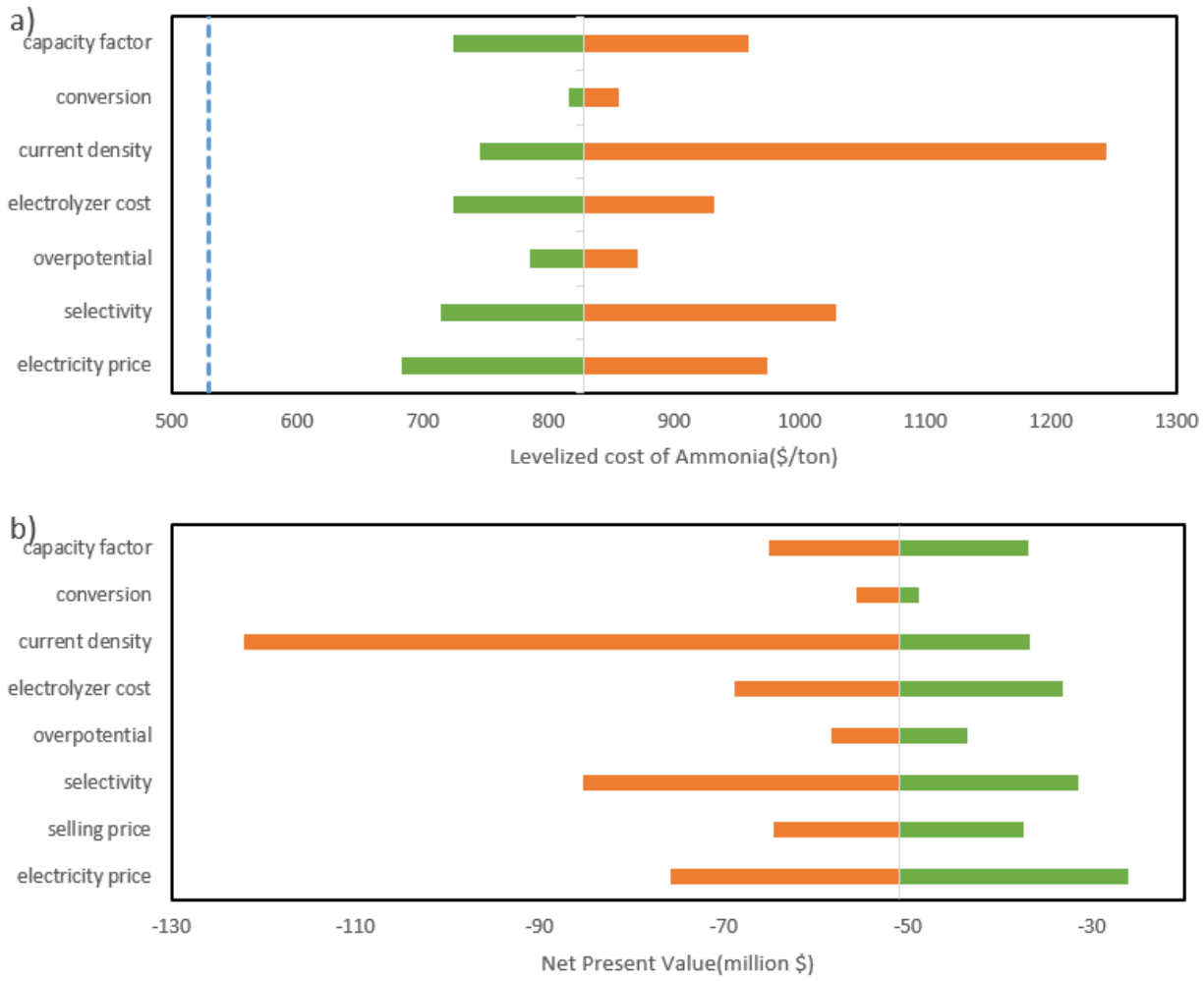

Figure 37 Sensitivity analysis of a) LCP and b) NPV for Scenario A RT. The blue dashed line indicates the current NH_3 market price ($530/ton).

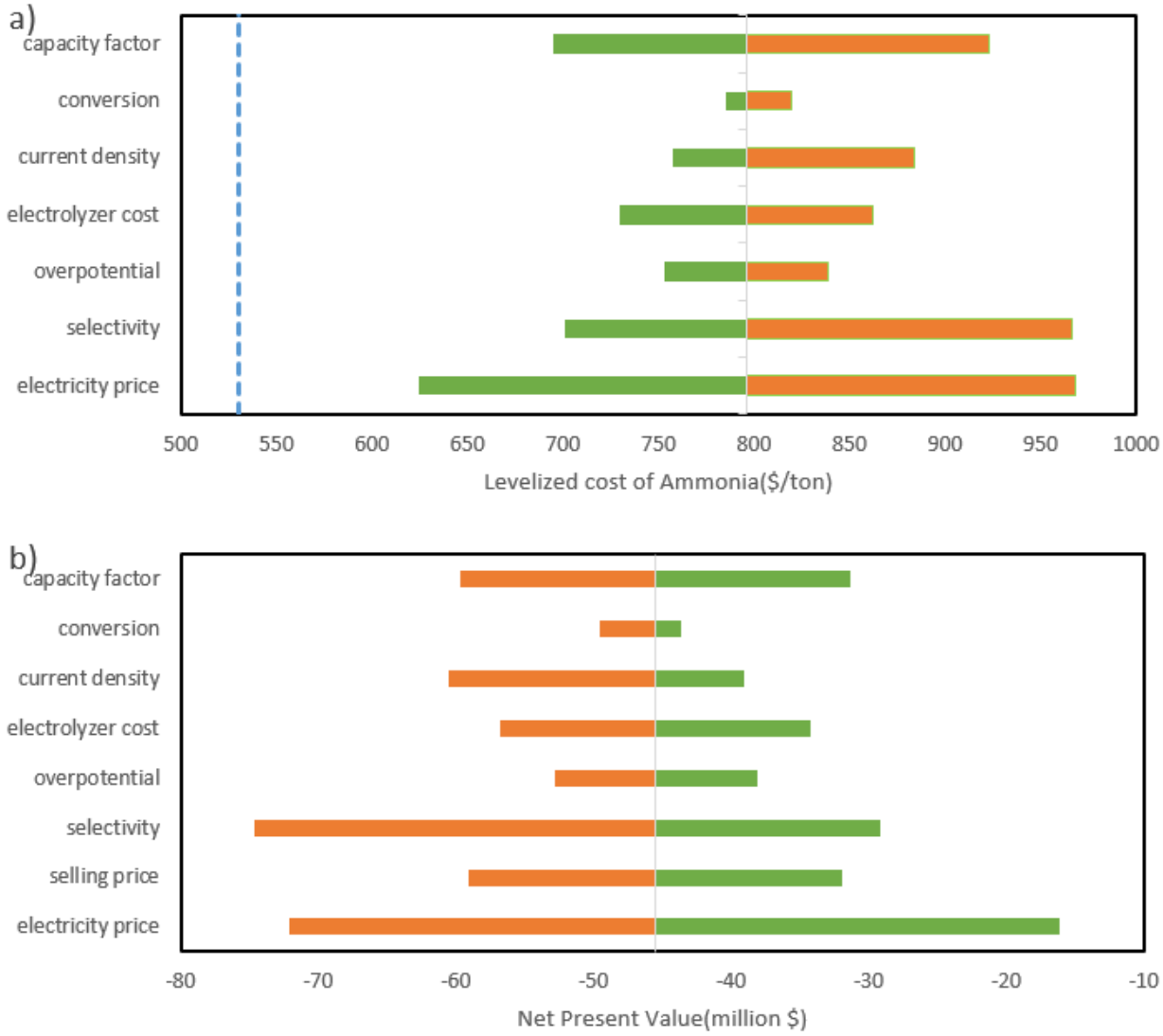

Figure 38 Sensitivity analysis of a) LCP and b) NPV for Scenario A HT. The blue dashed line indicates the current NH_3 market price ($530/ton).

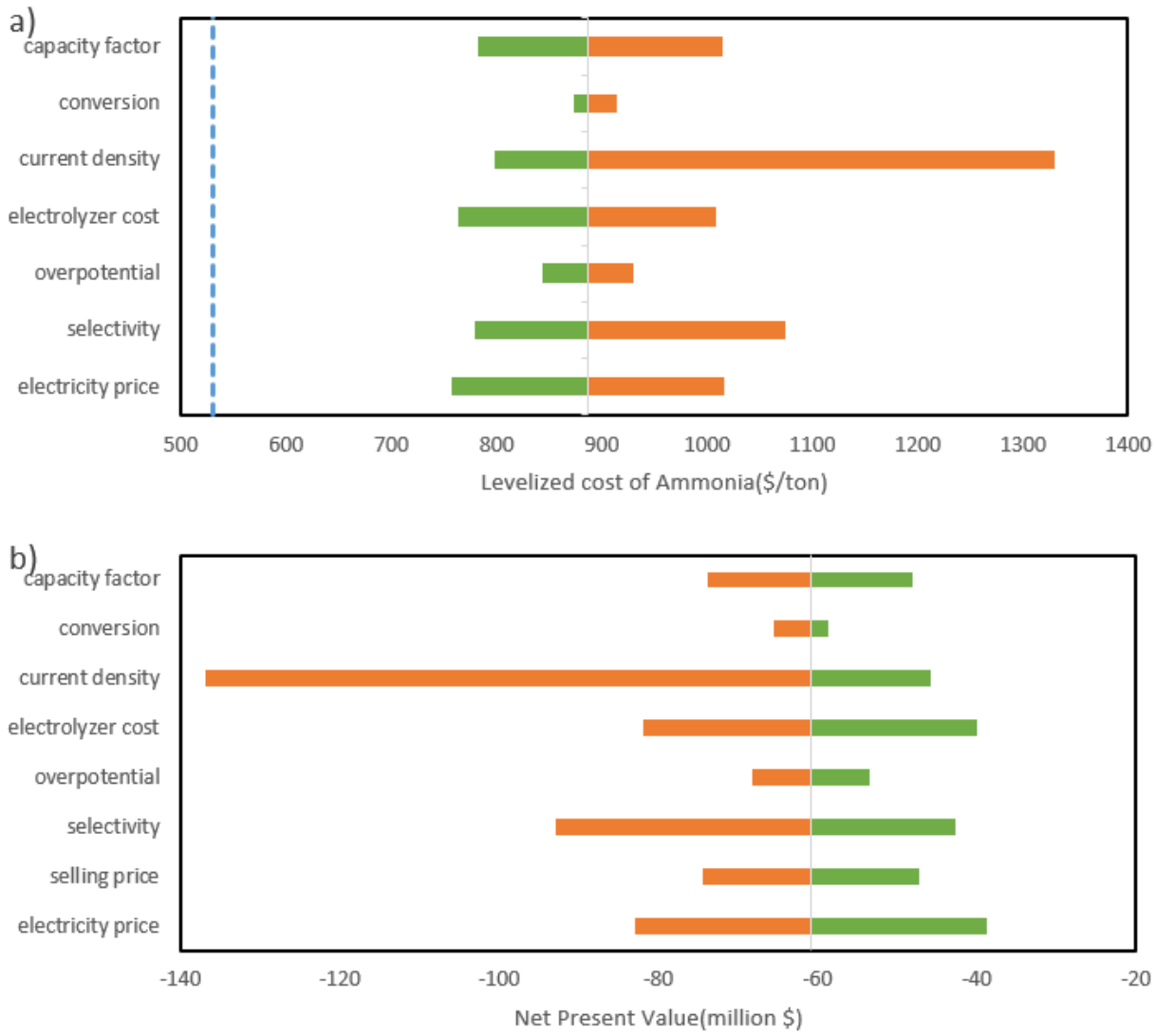

Figure 39 Sensitivity analysis of a) LCP and b) NPV for Scenario B RT. The blue dashed line indicates the current NH_3 market price ($530/ton).

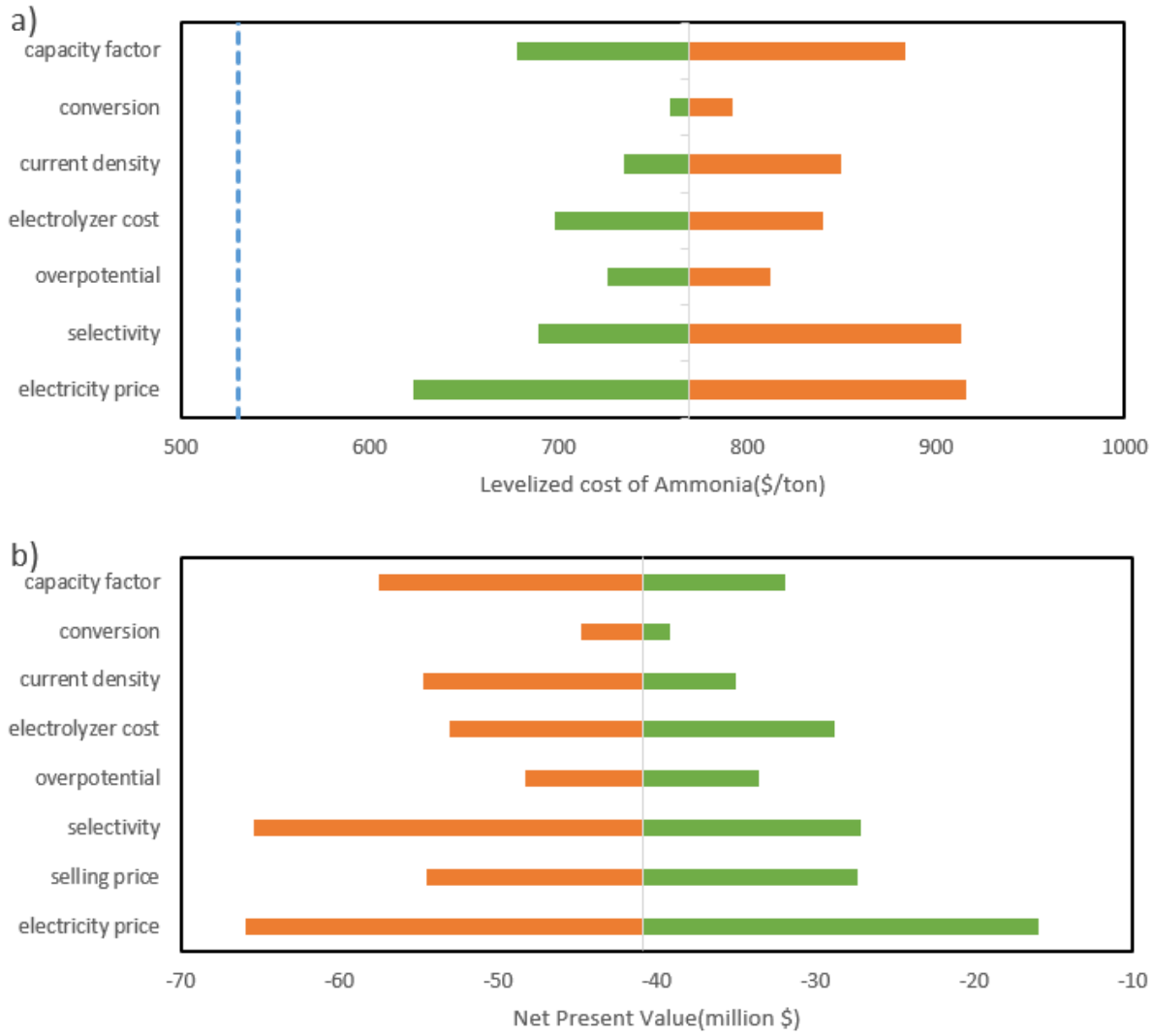

Figure 40 Sensitivity analysis of a) LCP and b) NPV for Scenario B HT. The blue dashed line indicates the current NH_3 market price ($530/ton).

The results reveal that none of the processes is profitable neither in base case, nor in optimistic case scenarios. For all processes, electricity is one of the most sensitive parameters because it influences the operating cost for all parts, which results in a strong dependence on the

electricity price. Even one cents difference would lead to around $20-30 million difference on a 20-year basis. Therefore, the pursue of cheap and stable power source is critical.

As for the parameters related to electrolyzer performance, selectivity and current density are more sensitive. A higher selectivity led to less waste of electricity toward the target product. , which correspondingly led to lower power need and, thus, lower electricity operating expenses. Reduced H_2 production also declined the PSA unit cost for separating NH_3 from N_2 and H_2, which was considered for both room and high temperature cases. Current density is another sensitive parameter for all processes; reduced current density heavily influenced the NPV. For example, Scenario A and B, a decrease in current density from 300 mA/cm^2 to 100 mA/cm^2 resulted in around $30 million NPV decrease.

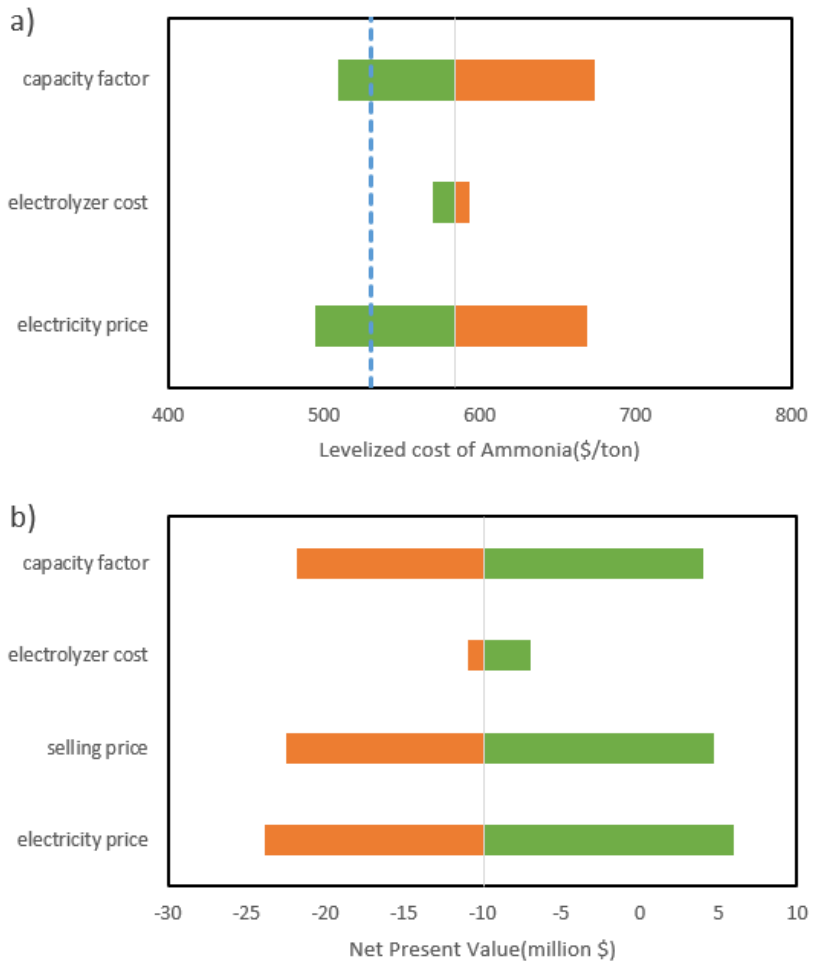

Figure 41 Sensitivity analysis of a) LCP and b) NPV for Scenario C. The blue dashed line indicates the current NH_3 market price ($530/ton).

For Scenario C, shown in Figure 41, there are not as many parameters as in other cases because they are both well-commercialized technologies. Hence not many improvements can be made to them. However, the same conclusion applies: the electricity price is the most sensitive and critical parameter.

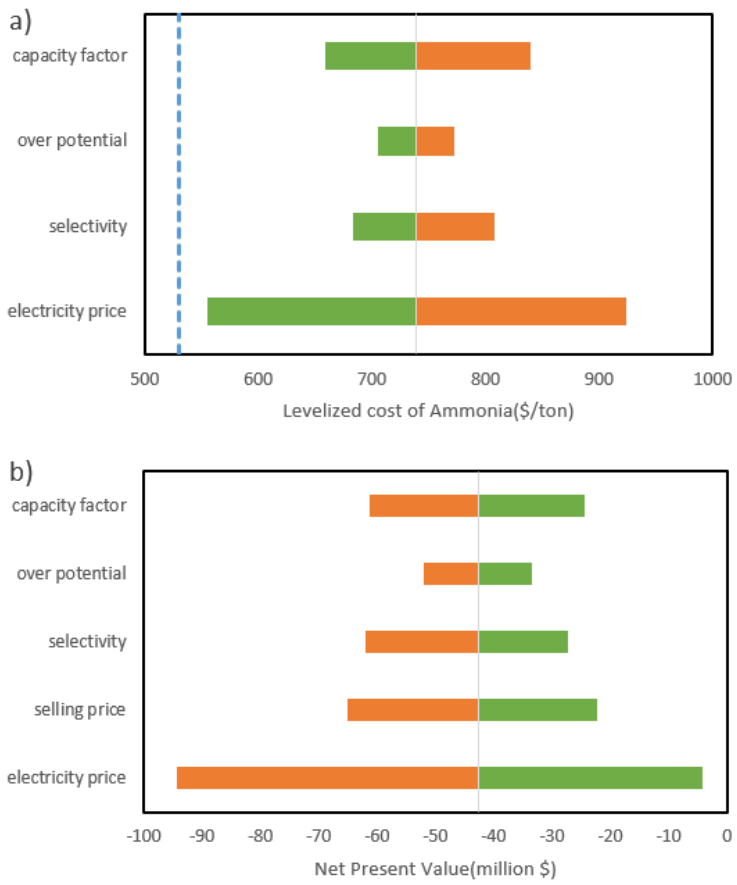

Figure 42 Sensitivity analysis of a) LCP and b) NPV for Scenario D. The blue dashed line indicates the current NH_3 market price ($530/ton).

As for Scenario D, displayed in Figure 42, unlike other cases, the single-pass conversion is already high (100% conversion was reported). The selectivity is also high, 90% for base case, and we chose 80% and 100% for worse and ideal prediction. Besides, it requires high reaction voltage (2.8 V theoretically). Thus, electricity price is, again, the most apparent impactor in sensitivity analysis.

To sum up, electricity price, current density, and selectivity are the more sensitive parameters. Hence, we chose them as the key performance indicators. In addition, we noticed that

overpotential is an essential indicator that is often used by researchers. Hence, we also used overpotential in the following parts.

4.2 Energy efficiency vs. electricity price

4.2.1 Introduction

Here, the energy efficiency (ε) is defined as the ratio of the NH_3 enthalpy ($\Delta H°$) and total input energy. Here, $\Delta H°$ is calculated as 22.5MJ/kg NH_3 (calculated in Appendix C), and the total energy is the summation of reaction energy for NH_3 electrolyzer (E_1), reaction energy for H_2O electrolyzer (E_2), thermal energy requirement (Q_1), and other required energy (Q_2)[63].

$$\varepsilon = \frac{\Delta H}{E_1 + E_2 + Q_1 + Q_2} \times 100\% \quad (15)$$

The required Gibbs free energy is calculated from reaction enthalpies and entropies, and those enthalpies and entropies are gathered and calculated from their physical property data at various temperatures (see Appendix C). The reaction energies for NH_3 electrolyzer is calculated with varied cathode overpotential as well:

$$E_1 = (E_1^\circ + \eta_1) * n * F/FE \quad (16)$$

$$E_2 = (E_2^\circ + \eta_2) * n * F/FE \quad (17)$$

Here, E_1° stand for the reaction voltages for NH_3 cell at different temperature (1.17 V for 25°C and 1.20 V for 500°C, related calculation is in Appendix C), E_2° stands for the reaction voltage for H_2O electrolysis at standard condistion (1.23 V). η_1 stands for the overpotential for NH_3 electrolyzer, while η_2 stands for the overpotential for H_2O electrolyzer (0.37 V since we choose 1.6 V as the reaction voltage). *n* stands for the electrons transferred in the reaction (3 e^- /mole produced NH_3, 2 e^-/mole produced H_2), *F* stands for Faradaic constant (96485 C/mole), and *FE* is the abbreviation for Faradaic Efficiency, which is considered as 90% for NH_3 electrolzyer

and 100% for H_2O electrolyzer. Here, all the data are summarized (from Figure 20-25, Table 4, Appendix B, and Appendix D) in Table 8 and converted to kWh per produced kg of NH_3.

Table 8 Summary of energy consumption. Numbers are shown in kWh/kg produced NH_3.

	ASU	Electrolyzer	Heating	PSA	Distillation	H-B synthesis loop	Condensation	O_2 compression	Q_1	Q_2	Total
Scenario A RT	0.34	9.28	N/A	0.12	2.90	N/A	0.01	0.35	N/A	3.73	13.02
Scenario A HT	0.34	9.44	1.88	0.48	N/A	N/A	0.01	0.35	1.88	1.19	12.51
Scenario B RT	0.34	9.81	N/A	0.12	2.90	N/A	0.01	0.35	N/A	3.73	13.54
Scenario B HT	0.34	9.97	0.49	0.48	N/A	N/A	0.01	0.35	0.49	1.19	11.65
Scenario C	0.34	7.55	N/A	N/A	N/A	0.64	0.01	0.35	N/A	1.33	8.89
Scenario D	0.34	16.05	N/A	N/A	0.04	N/A	0.01	0.35	N/A	0.74	16.79

The thermal energy is mainly used for high-temperature synthesis case; the energy is used to elevate N_2, H_2, and H_2O temperature from 25°C to 500°C. We used the Aspen HYSYS simulation package to calculate the heat load and then convert it to electrical energy because an electric resistance furnace was used for heating. For Scenario C, the required temperature is achieved by compression. For a typical H-B reaction, around 150-200 bar pressure is required to improve the NH_3 conversion, which also elevates the temperature of the stream during compressing. Here, only the compression power is required for this synthesis route, which is calculated from a similar off-shore-wind-power supplied H-B plant[26]. For selectivity, it is fixed 90% under the optimistic prediction case.

For overpotential, it is varied from 0 to 3 V to compare energy efficiency at the same scale. The cathode overpotential for the N_2 reduction reaction is the only one changed because that is where N_2 is reduced to NH_3 while anode side reactions are already demonstrated and optimized from numerous experiments[59]. The required Gibbs free energy for each process is different, which means the upper and lower limit of energy efficiency for each process is also different. The same overpotential range (0-3 V) was assumed to compare each process under the same experiment performance.

For the synthesis routes using H_2 as feedstock, there are two reactions involved: H_2O electrolysis and N_2 reduction reaction. For the first reaction, we considered 1.6 V as the cell voltage for the H_2O electrolyzer, which means a 0.37 V overpotential (theoretical voltage is 1.23 V for H_2O electrolysis)[32]. For N_2 reduction reaction, 0.06 V theoretical voltage is calculated at room temperature and 0.09 V at high temperature (Appendix C).

Next, the sum of theoretical required energy, overpotential, and thermal energy required to heat the cell to target temperature (500°C) is the total energy input for NH_3 synthesis (Appendix D). The electricity price is chosen to be from one to five cents per kilowatt-hour.

4.2.2 Results

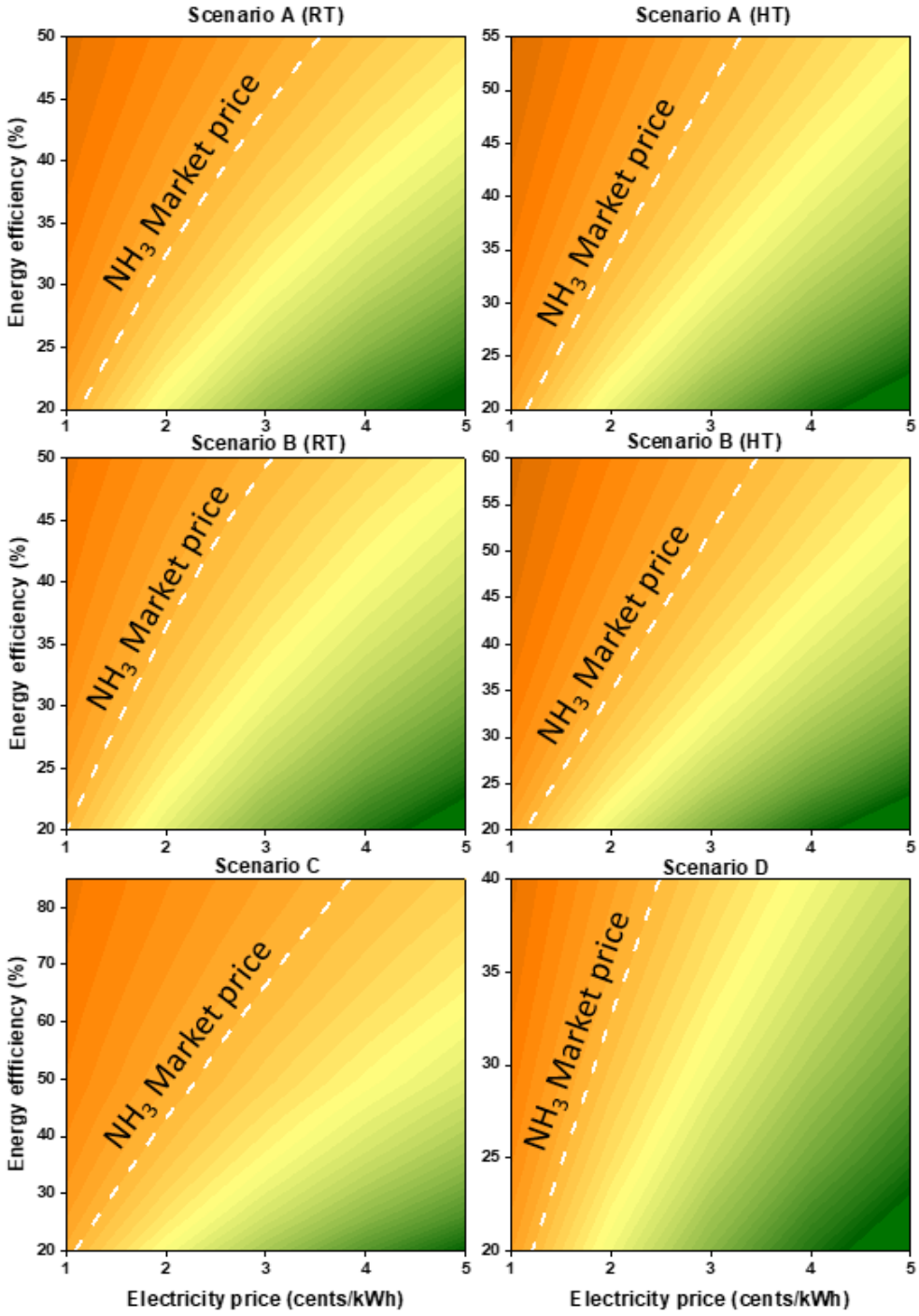

Figure 43 Levelized cost of product (LCP) with various energy efficiency and electricity price. All reactions are considered optimistic conditions. The white lines in the graph indicates current NH_3 market price ($530/ton)

The results from various combination of energy efficiency and electricity price are shown in Figure 43. The white dashed line in the graph indicated the current NH_3 market price ($530/ton). The area to the left of the white dashed line means the combinations (of energy efficiency and electricity price), which are profitable. We calculated the levelized cost of NH_3 based on optimistic future prediction condition (see Table 3).

4.2.3 Discussion

From Figure 43, all processes can be economically profitable at lower electricity price, which further proved that electricity prices is the most critical parameter. Among all processes, Scenario A RT and Scenario C are the most promising approaches because it has the most prominent tolerance on changing electricity price; it can be profitable even the electricity price is 4 cents/kWh. Besides, it also has a higher energy efficiency limit compared to other electrosynthesis routes. If the electricity price is 3 cents/kWh, Scenario A RT needs a 55% energy efficiency (about 0.45 V overpotential on the cathode side) to make it economically viable, which means further optimization would make this process tolerable at even higher electricity prices. For the Scenario A HT, the tolerance on electricity price is slightly lower than room temperature case; it needs approximately 43% energy efficiency (about 0.42 V overpotential) at 3 cents/kWh to make it profitable.

For Scenario B at both room and high-temperature cases, they all need around 40% energy efficiency, which requires 0.64 V and 0.71 V as the cathode overpotential, respectively. Therefore, they are less preferable in energy efficiency wise.

For Scenario D, the electricity price must be lower than 3 cents/kWh, which makes this process less promising than the others do. The main reason is that the lithium recycling process

needs high operating voltage (2.8 V theoretical reaction voltage) and high operating cost (approximately $14 million/year). Besides, the consumable inert anodes add extra load on daily operating expenditure, which further pushed this process toward unprofitable direction.

To sum up, most processes require electricity process to be cheaper than 3 cents/kWh to make them profitable, while scenario A and Scenario C can tolerate up to 4 cents/kWh. However, with reducing electricity prices, all processes can be economically available.

4.3 Over potential vs. Faradaic efficiency

4.3.1 Introduction

In this section, the levelized cost was calculated using another pair of essential parameters: overpotential and Faradaic efficiency. Both of them are essential indicators of electrochemical experiments, so evaluating the performance metrics of them could provide a valid reference in experiment design.

4.3.2 Results

Here, the results are calculated under optimistic conditions (see Table 3) with changing overpotential and Faradaic efficiency. Then with the combinations of overpotential and Faradaic efficiency, we gathered the results of levelized cost and illustrated them in Figure 44.

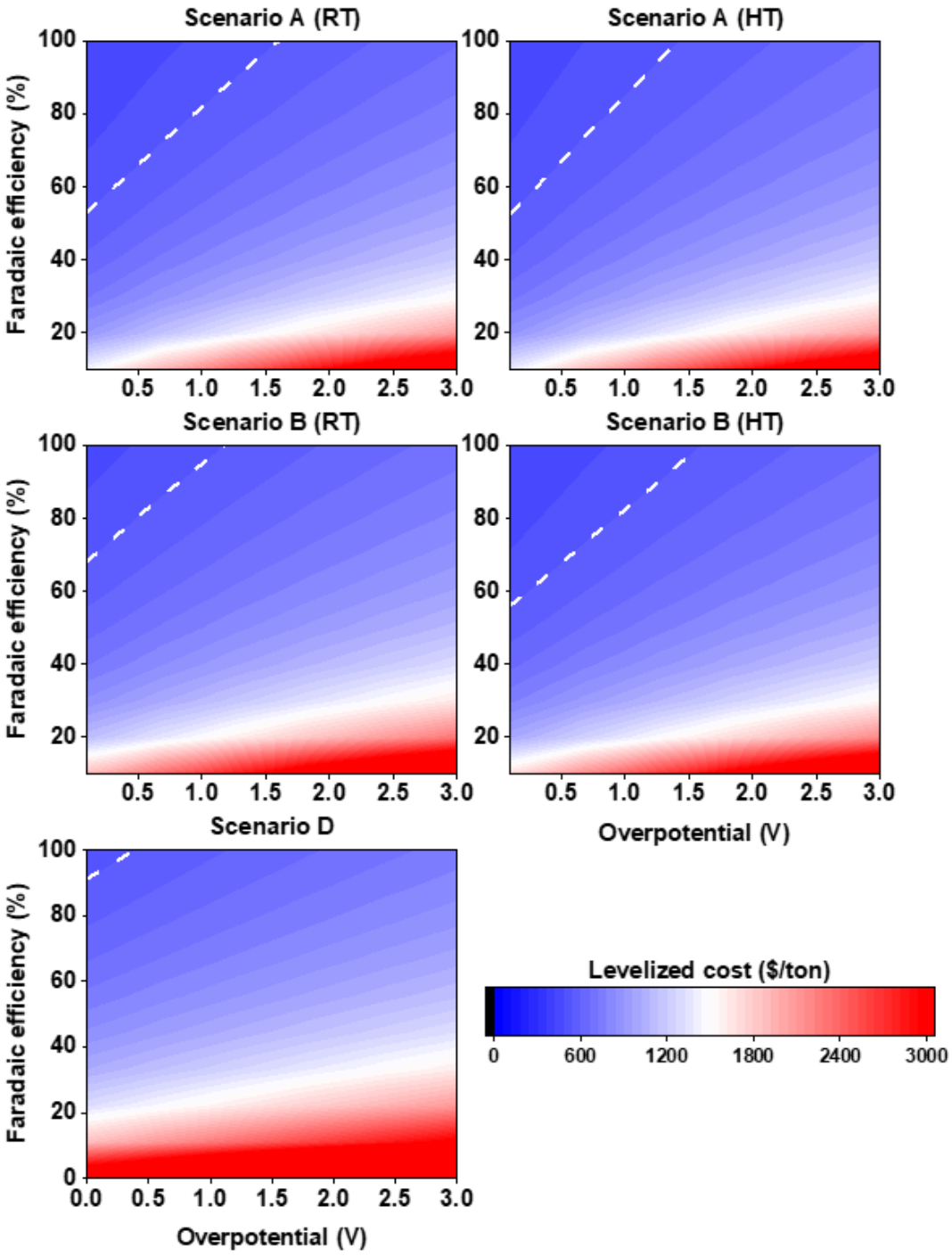

Figure 44 Levelized cost of product (LCP) with various overpotential and selectivity. All reactions are considered optimistic conditions. For scenario B, the overpotentials are considered on the cathode side of NH_3 cell. For scenario D, the overpotential is considered for the LiOH electrolysis. The white lines in the graph indicates current NH_3 market price ($530/ton).

4.3.3 Discussion

From the results in Figure 44, first, Scenario A RT, Scenario A HT, and Scenario B HT can sacrifice more on the cathode overpotential to be economically achievable, all of them can tolerate up to 1.5 V cathode overpotential at around 50% faradaic efficiency. For Scenario B RT, it needs lower cathode overpotential (approx. 1.3 V) to be economically acceptable. Overall, NH_3 electrosynthesis in Scenario A RT and Scenario B HT are slightly better than other processes.

For Scenario D, very limited profitable area is shown even optimistic conditions. From the sections above, we can tell that the only way to produce NH_3 using lithium recycling is a cheaper electricity price (lower than 2 cents/kWh). Hence, lithium recycling would not be most economically favorable.

4.4 Current density

4.4.1 Introduction

Here, we compared the NPVs of Scenario A and B with varying current density to check the influence that current density has on NPVs. The calculation is conducted under optimistic conditions with varying current density. The results are displayed in Figure 45.

4.4.2 Results

Here, we varied the current density from 100 to 1000 mA/cm^2 to investigate the impact it has on NPV.

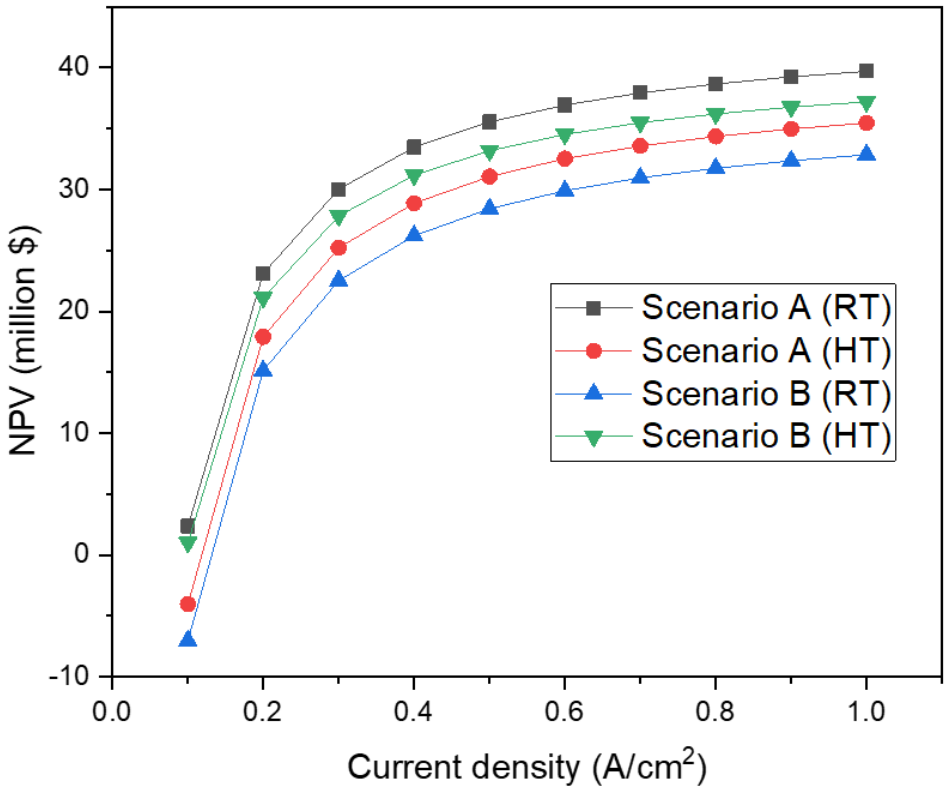

Figure 45 NPV with various current density. All reactions are considered under optimistic conditions.

4.4.3 Discussion

As shown in the results, the same trend is observed in all four processes: after a certain point, the influence from current density is weakened. That phenomenon is well understood: a lower current density would lead electrolyzer cost increased by folds because the total current if fixed (by fixed production rate), while a higher current only decreases the electrolyzer by percentage. Hence, current density affects significantly when the current density is low and has less effect when the current density is getting higher.

4.5 Energy consumption and CO_2 emission

4.5.1 Introduction

In this section, the energy consumption for each process is calculated (as shown in Table 8, section 4.2), and then from those, we calculated the CO_2 emissions for all processes considering different sources of electricity, including natural gas combined cycle (NGCC), solar power, hydropower, wind power, and nuclear power is determined. Here, we took 1500 kg-CO_2/ton NH_3 as the comparison basis from a state-of-art NH_3 plan, which uses natural gas as H_2 source[112,113].

4.5.2 Results and Discussion

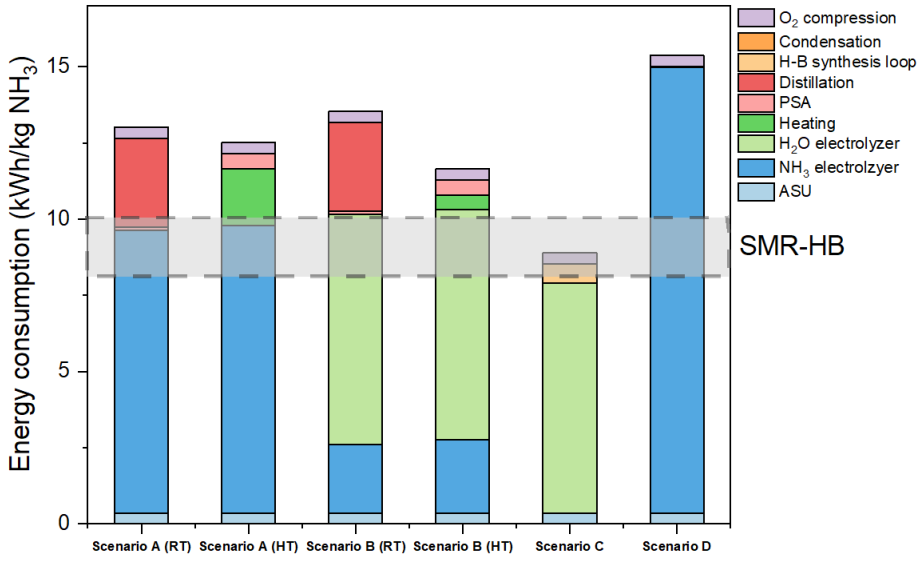

Figure 46 Energy consumption of various processes, colors indicate the energy required for each part (Table 8).

As for energy consumption, only Scenario C is less energy-intensive route. However, the energy we used is mainly from electricity, which does not necessarily emit more CO_2 if the

electricity is produced from a clean source (wind, hydro, nuclear, etc.). Next, we compared the CO_2 emission for each process using energy consumption and CO_2 emission factor.

Table 9 Summary of CO_2 emission factor from various electricity sources[114].

Electricity sources	gram CO_2/kWh
NGCC	499
Solar power	85
Hydropower	26
Wind farm	26
Nuclear plant	29

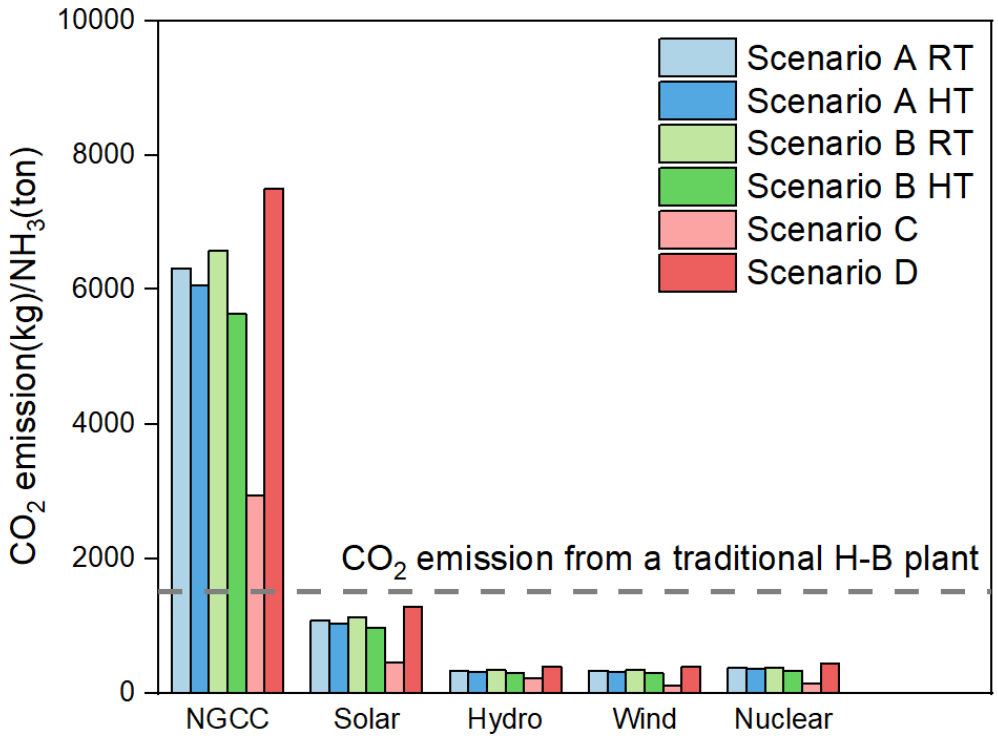

Figure 47 CO_2 emission of different process when electricity is taken from different sources. All reactions are considered optimistic conditions.

From Figure 47, electrosynthesis when using NGCC causes dozens of times more CO_2 emissions compared to traditional H-B process, which means the electrical power needs to be gathered from clean sources, otherwise it would be pointless to replace current H-B process from an environmental aspect. As for the clean sources, all of them are cleaner than current NH_3 production route. Among all the clean electricity sources, we considered nuclear power plant would be the best choice. First, it emits a lower amount of CO_2, which is around the same level of wind power and hydropower but lower than from solar. Second, Solar power, hydropower, and wind power are all influenced by the location and nature. That is, intermittent electricity source cannot fulfill the requirement for a stable supply of electricity, in other words, a lower capacity factor[115]. Therefore, we chose to consider nuclear power as a clean electricity source. Nuclear power could provide cheap and stable electricity with the highest capacity factor, which is even higher than the coal plant and NGCC. In figure 48, we compared the CO_2 emission of the synthesis routes we chose with traditional H-B process when the electricity is taken from nuclear power plants.

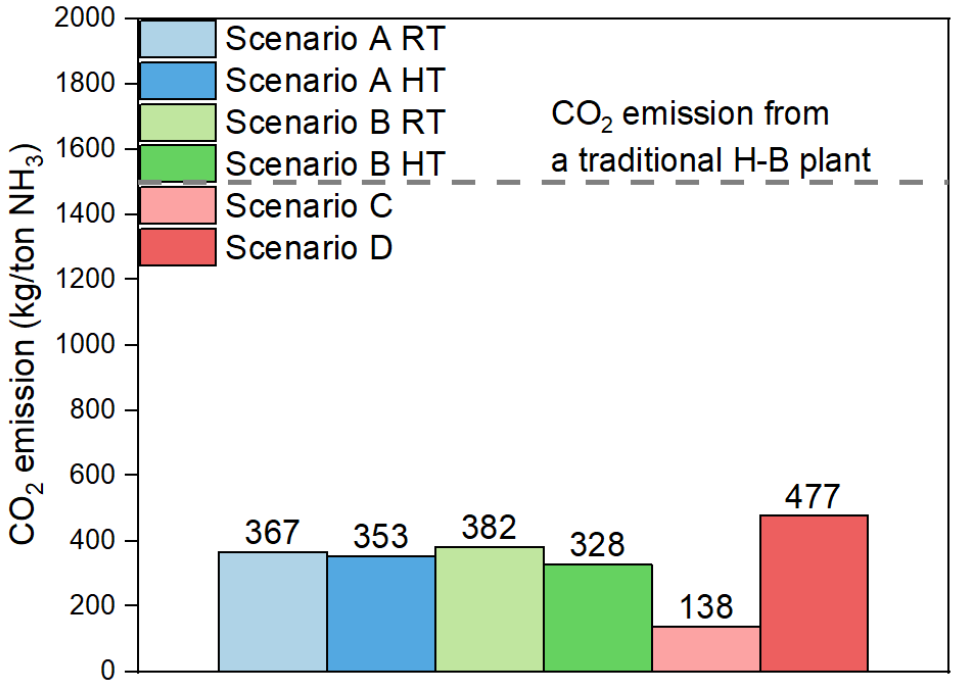

Figure 48 CO_2 emission of different processes when electricity is taken from a nuclear plant. All reactions are considered optimistic conditions.

As shown in Figure 48, all processes could reduce CO_2 emissions by 75-90%. Among them, Scenario C is the least emissive process, of which over 90% CO_2 can be reduced, which makes up for the huge capital investment. In our calculation, we found out that the minimum CO_2 emission need is approx. 190 g/kWh to make electrosynthesis environmentally comparable to traditional H-B plant. Currently, around 100 g/kWh average CO_2 emission is achieved in Canada[116]. Hence, the electrosynthesis of NH_3 has the potential to be environmentally comparable to traditional H-B plants in Canada.

Chapter 5 Conclusions and Recommendations

This thesis presented a broad perspective on the economic aspects of various NH_3 electrosynthesis routes as compared to conventional H-B process. We first reviewed various electrosynthesis routes for NH_3 production. Based on this we developed a general process flow, including feedstock production, NH_3 synthesis, NH_3 separation, and condensation. Economic analysis was performed for each process on a 100-ton/day NH_3 production rate basis. We compared each process from various aspects: capital and operating cost, NPV on a 20-year basis, LCP with contribution from each component, energy consumption if they are all electricity-driven, and sensitivity analysis. From the sensitivity analysis, we figured out that electricity price, selectivity, overpotential, and current density are parameters that are more important. Therefore, we compared those processes with combinations of those parameters.

Key findings

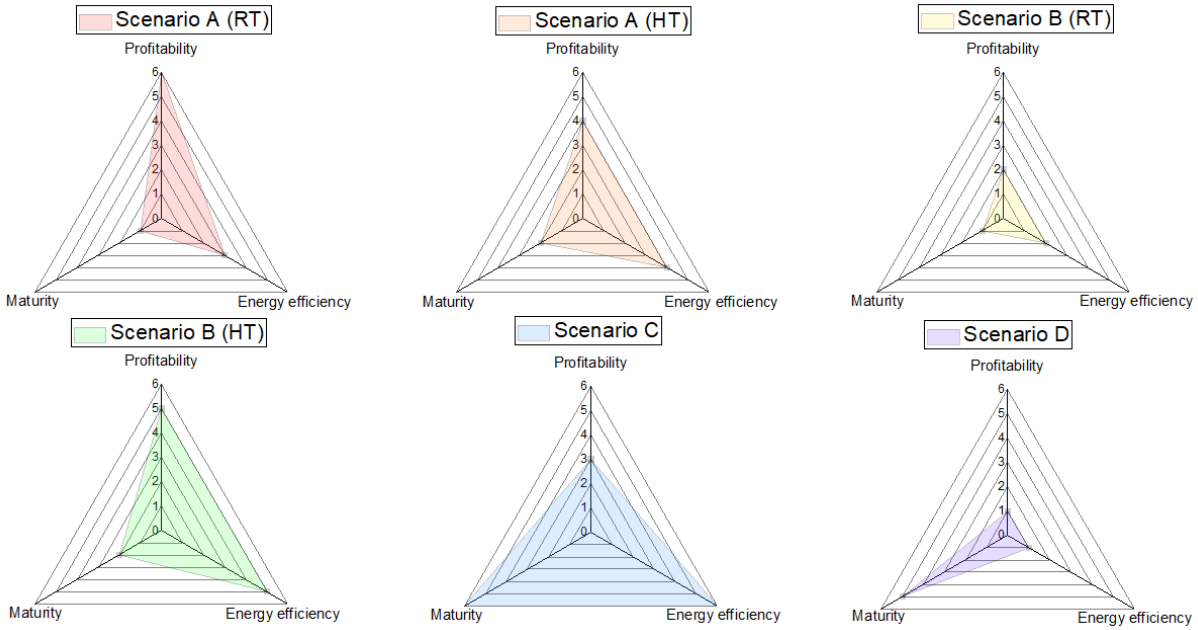

Figure 49 "Golden Triangles" for all selected electrosynthesis routes

- Using N_2 and H_2O to synthesize NH_3 at room temperature would be the most economically feasible approach. The levelized cost of NH_3 could achieve as low as $414/ton at an optimistic case scenario as compared to the cost ($530/ton) via the conventional H-B process.
- As expected, electricity price is one of the essential parameters; a slight change in electricity price would affect the effectiveness and feasibility of the whole process. NH_3 electrosynthesis is highly-electricity dependent (6 e^-/mole NH_3), especially when we are replacing all the thermal equipment with an electric resistance heater. Our calculations reveal that NH_3 electrosynthesis would not be economically competitive with electricity price over ¢3/kWh. Hence, a cheap and stable electricity source would be at the highest priority level.
- Currently, coupling the H-B process with the H_2O electrolyzer is the most mature technology for NH_3 electrosynthesis.
- The electrolyzer cost (approx. $1000/$m^2$) considered here are ambitious as compared to the reported cost estimations in previous studies (over $2400/$m^2$ based on DOE H2A). Therefore, the overall economic analysis will be affected at the current price. Substantial cost reductions would be required to make the electrosynthesis route economically viable.
- Cell parameters, including selectivity and current density have a significant influence on the electrolyzer capital cost. Thus, the major improvement is required in selectivity and current density, though all parameters used in this analysis require continuous improvement. Our results suggest that a current density higher than 400 mA/cm^2, selectivity higher than 60%, energy efficiency higher than 50%, and cathode overpotential lower than 1.5 V to make NH_3 are needed to make electrosynthesis economically competitive as compared to H-B process. Based on the reported results, these performance matrices is certainly an ambitious target that needs to be achieved in order to translate this technology from lab scale to marketplace.

- This analysis suggests that Lithium recycling for NH_3 production has the minimum profit margin as compared to other processes even at most optimistic prediction. Lithium is a highly active material; the production safety would be another major challenge. Besides, the limited supply of lithium would be a bottleneck for the development of large-scale plant in industrial settings.
- All electrosynthesis processes have the potential to reduce CO_2 emission by 75-90% when combined with clean electricity sources, however, the CO_2 emission would be higher than the traditional H-B process if the electricity is taken from conventional combustion plants. We calculated that with less than 190 g/kWh CO_2 emission from electricity source, the electrosynthesis is environmentally comparable to traditional H-B process.

Limitations of this analysis

- In this thesis, we assumed, the electrochemical NH_3 cell and also the H_2O electrolysis cell have lifetimes of 20 years. In practice, the lab-scale demonstrated stability of electrochemical NH_3 synthesis is typically several hours. On the other hand, the stability of H_2O electrolysis cell is ~5-7 years. Stability influence the lifetime and maintenance cost of electrolyzers, which will affect the overall economics of this analysis.
- The NH_3 production rate basis used in the analysis is at 100-ton/day, which is suitable for intermediate-scale industrial production. The levelized cost strongly depends on the production rate, consequently may affect the overall economic feasibility of the process. In this study, this aspect was not addressed.
- Most processes would not be economically feasible until the electricity price is lower than ¢3/kWh.

Key challenges ahead for industrial production via electrosynthesis routes:

- Electrosynthesis of NH_3 is still at its infancy in lab-scale. There is a debate in the literature on the reaction mechanism of NH_3 electrosynthesis. The involvement of computational studies could help in getting a deeper understanding of the reaction mechanism. Besides, computational study could help in designing electrode: Precisely tuned active sites at micro-scale could significantly improve the reaction towards the required direction, which correspondingly helps industrial-level production.
- Currently, the demonstrated performance metrics of lab-scale NH_3 electrosynthesis is below the target values we chose in the economic analysis, though some reports are showing data (i.e. selectivity) that matches our prediction. However, other parameters still remain impractical (current density, overpotential, etc.), which indicates that plenty of efforts are constantly required in this area.
- On the other hand, current synthesis experiments require pure N_2 as feedstock that is not preferable in modular production, if air instead of pure N_2 is used in the experiments, the availability of those processes would be improved.

Suggested Future Work

Overall, NH_3 electrosynthesis is a promising process in future agriculture and energy field if further progress is made. Based on this analysis, we suggest the following studies that could be performed.

- Due to its high volumetric energy density, NH_3 has the potential to function as a clean energy career in future energy infrastructure, which could enable a low carbon “ammonia

economy". However, the roadmap of that remains unclear and requires further deeper investigation. As a result, a more detailed comparative techno-economic and lifecycle analysis can be performed to reveal the potential of "Hydrogen economy" vs "ammonia economy".

- The electrolyzer is the most important unit in the model, yet the modeling of that is mostly relying on the numbers from publication due to the immaturity of NH_3 electrosynthesis. That leads to a huge uncertainty in the analysis results. Thus, a more detailed and reliable analysis regarding the cost structure of NH_3 electrolyzers is highly needed.
- The parameters we chose are from multiple sites, which combines data from all over the world. Therefore, a detailed economic analysis for a certain area, i.e. the Gulf of Maine, could provide deeper insights into the economic analysis of NH_3 electrosynthesis.

References

1. U.S. Geological Survey. *Mineral Commodity Summaries 2019*. Vol 3.; 2019. doi:10.1007/978-3-540-47108-0-4
2. EasyChem. Industrial Uses of Ammonia. https://easychem.com.au/monitoring-and-management/maximising-production/industrial-uses-of-ammonia/. Accessed November 6, 2019.
3. Erisman JW, Sutton MA, Galloway J, Klimont Z, Winiwarter W. How a century of ammonia synthesis changed the world. *Nat Geosci*. 2008;1(10):636-639. doi:10.1038/ngeo325
4. Pearson A. Refrigeration with ammonia. *Int J Refrig*. 2008;31(4):545-551. doi:10.1016/J.IJREFRIG.2007.11.011
5. Kasikowski T, Buczkowski R, Lemanowska E. Cleaner production in the ammonia-soda industry: An ecological and economic study. *J Environ Manage*. 2004;73(4):339-356. doi:10.1016/j.jenvman.2004.08.001
6. Zamfirescu C, Dincer I. Ammonia as a green fuel and hydrogen source for vehicular applications. *Fuel Process Technol*. 2009;90(5):729-737. doi:10.1016/j.fuproc.2009.02.004
7. Lan R, Tao S. Ammonia as a suitable fuel for fuel cells. *Front Energy Res*. 2014;2(AUG):3-6. doi:10.3389/fenrg.2014.00035
8. Valera-Medina A, Xiao H, Owen-Jones M, David WIF, Bowen PJ. Ammonia for power. *Prog Energy Combust Sci*. 2018;69:63-102. doi:10.1016/J.PECS.2018.07.001
9. Ma Q, Peng R, Lin Y, Gao J, Meng G. A high-performance ammonia-fueled solid oxide fuel cell. *J Power Sources*. 2006;161(1):95-98. doi:10.1016/j.jpowsour.2006.04.099
10. Jiao F, Xu B. Electrochemical Ammonia Synthesis and Ammonia Fuel Cells. *Adv Mater*. 2018;1805173:1805173. doi:10.1002/adma.201805173
11. Appl M. *Ammonia: Principles and Industrial Practice*. 1st ed. Wiley-VCH; 1999.
12. Gary D. Christian, Purnendu (Sandy) Dasgupta KS. *Analytical Chemistry*. 7th ed. Wiley; 2014.
13. Ertl G. The nobel prize in chemistry. *Nobel Lect Chem 2006 - 2010*. 2014:37-38. doi:10.1142/9789814635660_0002
14. Philip PM. From Fertile Minds. American Scientist. http://www.americanscientist.org/bookshelf/id.2653,content.true,css.print/bookshelf.aspx. Accessed November 6, 2019.
15. Gerhard Ertl - Biographical. Wikipedia. nobelprize.org. Accessed November 6, 2019.
16. Hongbao M, Passy F, Röntgen WC, et al. Nobel Prizes from 1901. *Nat Sci*. 2006;4(3):86-94. doi:10.7537/marsnsj040306.13
17. Gilbert P, Alexander S, Thornley P, Brammer J. Assessing economically viable carbon reductions for the production of ammonia from biomass gasification. *J Clean Prod*. 2014;64:581-589. doi:10.1016/j.jclepro.2013.09.011
18. Rafiqul I, Weber C, Lehmann B, Voss A. Energy efficiency improvements in ammonia production - Perspectives and uncertainties. *Energy*. 2005;30(13):2487-2504. doi:10.1016/j.energy.2004.12.004
19. Brightling J. Ammonia and the fertiliser industry: The development of ammonia at Billingham. *Johnson Matthey Technol Rev*. 2018;62(1):32-47. doi:10.1595/205651318X696341

20. Brown T. What drives new investments in low-carbon ammonia production? One million tons per day demand. Ammonia Industry. https://patents.google.com/patent/EP0000993A1. Published 2018. Accessed January 20, 2020.
21. *Air Separation Plant. History and Technological Progress in the Course of Time.* Pullach, Germany: Linde AG; 2017.
22. Linde plc - Wikipedia. Wikipedia. https://en.wikipedia.org/wiki/Linde_plc. Accessed November 6, 2019.
23. Office of Energy Efficiency & Renewable Energy. Hydrogen Production: Natural Gas Reforming | Department of Energy. Energy.Gov. doi:10.1016/j.mehy.2009.12.029
24. Williams FE. Flow diagram for the production of Ammonia. Wikimedia Commons. https://commons.wikimedia.org/wiki/File:Haber-Bosch-En.svg. Published 2010. Accessed November 6, 2019.
25. Jennings JR. *Catalytic Ammonia Synthesis: Fundermentals and Practice*. 1st ed. Springer US; 1991. doi:10.1007/978-1-4757-9592-9
26. Morgan ER. Techno-Economic Feasibility Study of Ammonia Plants Powered by Offshore Wind. 2013. http://scholarworks.umass.edu/open_access_dissertations/697.
27. Speight RLJ. *Gasification Processes for Syngas and Hydrogen Production*. 1st ed. Woodhead Publishing; 2014. doi:10.1016/B978-0-85709-802-3.00006-0
28. 11.1 Commercial technologies. National Energy Technology Laboratory. https://netl.doe.gov/research/Coal/energy-systems/gasification/gasifipedia/fertilizer-commercial-technologies. Accessed November 6, 2019.
29. Schiffer ZJ, Manthiram K. Electrification and Decarbonization of the Chemical Industry. *Joule*. 2017;1(1):10-14. doi:10.1016/j.joule.2017.07.008
30. Mai H. Renewable energy prices keep falling: When do they bottom out? UtilityDive. https://www.utilitydive.com/news/renewable-energy-prices-keep-falling-when-do-they-bottom-out/555822/. Published 2019. Accessed January 20, 2020.
31. REN 21. *Renewables 2019 Global Status Report(Paris: REN21 Secretariat)*.; 2019.
32. Carmo M, Fritz DL, Mergel J, Stolten D. A comprehensive review on PEM water electrolysis. *Int J Hydrogen Energy*. 2013;38(12):4901-4934. doi:10.1016/j.ijhydene.2013.01.151
33. Goals of the Solar Energy Technologies Office. U.S. Department of Energy. https://www.energy.gov/eere/solar/goals-solar-energy-technologies-office. Accessed November 6, 2019.
34. Denholm, P., Clark, K., and O'Connell M. *On the Path to SunShot: Emerging Issues and Challenges in Integrating High Levels of Solar into the Electrical Generation and Transmission System*.; 2016. https://www.nrel.gov/docs/fy16osti/65800.pdf.
35. Barnhart CJ, Dale M, Brandt AR, Benson SM. The energetic implications of curtailing versus storing solar- and wind-generated electricity. *Energy Environ Sci*. 2013;6(10):2804-2810. doi:10.1039/C3EE41973H
36. Brouwer AS, van den Broek M, Seebregts A, Faaij A. Impacts of large-scale Intermittent Renewable Energy Sources on electricity systems, and how these can be modeled. *Renew Sustain Energy Rev*. 2014;33:443-466. doi:10.1016/J.RSER.2014.01.076
37. Godula-jopek A. *Hydrogen Production: By Electrolysis*. 1st ed. John Wiley & Sons; 2015.
38. Keith DW, Holmes G, St. Angelo D, Heidel K. A Process for Capturing CO2 from the Atmosphere. *Joule*. 2018;2(8):1573-1594. doi:10.1016/j.joule.2018.05.006

39. *Hydrogen from Large-Scale Electrolysis - Efficienct Solutions for Sustainable Chemicals and Energy Storage*. Dortmund Germany: thyssenkrupp AG; 2019. https://www.thyssenkrupp-uhde-chlorine-engineers.com/en/products/water-electrolysis-hydrogen-production.
40. Carbon Dioxide Electrolyzers and Components For Sale - Dioxide Materials. https://dioxidematerials.com/products/anion-exchange-membrane-water-electrolyzers-components-sale/. Accessed November 6, 2019.
41. Tang C, Qiao S-Z. How to explore ambient electrocatalytic nitrogen reduction reliably and insightfully. *Chem Soc Rev*. 2019. doi:10.1039/c9cs00280d
42. Ruthven DM, Farooq S, Knaebel KS, et al. Solid state ammonia synthesis. *Joule*. 2018;2(1):1-10. doi:10.1126/sciadv.1700336
43. Lapina A. Electrolytes and Electrodes for Electrochemical Synthesis of Ammonia. 2013.
44. Wang L, Xia M, Wang H, et al. Greening Ammonia toward the Solar Ammonia Refinery. *Joule*. 2018;2(6):1055-1074. doi:10.1016/j.joule.2018.04.017
45. Giddey S, Badwal SPS, Kulkarni A. Review of electrochemical ammonia production technologies and materials. *Int J Hydrogen Energy*. 2013;38(34):14576-14594. doi:10.1016/j.ijhydene.2013.09.054
46. Amar IA, Lan R, Petit CTG, Tao S. Solid-state electrochemical synthesis of ammonia: A review. *J Solid State Electrochem*. 2011;15(9):1845-1860. doi:10.1007/s10008-011-1376-x
47. Shipman MA, Symes MD. Recent progress towards the electrosynthesis of ammonia from sustainable resources. *Catal Today*. 2017;286:57-68. doi:10.1016/j.cattod.2016.05.008
48. Garagounis I, Kyriakou V, Stoukides M, Vasileiou E, Vourros A. Progress in the Electrochemical Synthesis of Ammonia. *Catal Today*. 2016;286:2-13. doi:10.1016/j.cattod.2016.06.014
49. Cui X, Tang C, Zhang Q. A Review of Electrocatalytic Reduction of Dinitrogen to Ammonia under Ambient Conditions. *Adv Energy Mater*. 2018;8(22):1-25. doi:10.1002/aenm.201800369
50. Brown T. The capital intensity of small-scale ammonia plants. Ammonia Industry. https://ammoniaindustry.com/the-capital-intensity-of-small-scale-ammonia-plants/. Published 2018. Accessed November 6, 2019.
51. Martín AJ, Shinagawa T, Pérez-Ramírez J. Electrocatalytic Reduction of Nitrogen: From Haber-Bosch to Ammonia Artificial Leaf. *Chem*. 2018:263-283. doi:10.1016/j.chempr.2018.10.010
52. IRENA(2018). *Hydrogen From Renewable Power: Technology Outlook for the Energy Transition*. Abu Dhabi: International Renewable Energy Agency; 2018. www.irena.org.
53. Wikipedia. Electrolysis of water. Wikipedia. https://en.wikipedia.org/wiki/Electrolysis_of_water. Accessed November 6, 2019.
54. Bard AJ, Faulkner LR. *Electrochemical Methods: Fundamentals and Applications*. 2nd ed. Wiley; 2000.
55. Schmidt O, Gambhir A, Staffell I, Hawkes A, Nelson J, Few S. Future cost and performance of water electrolysis: An expert elicitation study. *Int J Hydrogen Energy*. 2017;42(52):30470-30492. doi:10.1016/j.ijhydene.2017.10.045
56. Carmo M, Fritz DL, Mergel J, Stolten D. A comprehensive review on PEM water electrolysis. *Int J Hydrogen Energy*. 2013;38(12):4901-4934.

doi:10.1016/j.ijhydene.2013.01.151
57. Wikipedia. Electrolysis of Water. Wikipedia. https://en.wikipedia.org/wiki/Electrolysis_of_water. Accessed November 6, 2019.
58. Millet P, Grigoriev S. Water Electrolysis Technologies. *Renew Hydrog Technol Prod Purification, Storage, Appl Saf*. 2013;(2013):19-41. doi:10.1016/B978-0-444-56352-1.00002-7
59. Rashid MM, Al Mesfer MK, Naseem H, Danish M. Hydrogen production by water electrolysis: a review of alkaline water electrolysis, PEM water electrolysis and high temperature water electrolysis. *Int J Eng Adv Technol*. 2015;4(3):2249-8958.
60. Wang M, Wang Z, Gong X, Guo Z. The intensification technologies to water electrolysis for hydrogen production - A review. *Renew Sustain Energy Rev*. 2014;29:573-588. doi:10.1016/j.rser.2013.08.090
61. Detz RJ, Reek JNH, Van Der Zwaan BCC. The future of solar fuels: When could they become competitive? *Energy Environ Sci*. 2018;11(7):1653-1669. doi:10.1039/c8ee00111a
62. Schmidt O, Gambhir A, Staffell I, Hawkes A, Nelson J, Few S. Future cost and performance of water electrolysis: An expert elicitation study. *Int J Hydrogen Energy*. 2017;42(52):30470-30492. doi:10.1016/j.ijhydene.2017.10.045
63. Martín AJ, Shinagawa T, Pérez-Ramírez J. Electrocatalytic Reduction of Nitrogen: From Haber-Bosch to Ammonia Artificial Leaf. *Chem*. 2019;5(2):263-283. doi:10.1016/j.chempr.2018.10.010
64. Dinh C, Burdyny T, Kibria G, et al. CO2 electroreduction to ethylene via hydroxide-mediated copper catalysis at an abrupt interface. 2018;787(May):783-787.
65. Ammonia. Wikipedia. http://en.wikipedia.org/wiki/Ammonia. Accessed November 6, 2019.
66. Wang M, Liu S, Qian T, et al. Over 56.55% Faradaic efficiency of ambient ammonia synthesis enabled by positively shifting the reaction potential. *Nat Commun*. 2019;10(1):1-8. doi:10.1038/s41467-018-08120-x
67. Licht S, Cui B, Wang B, Li FF, Lau J, Liu S. Ammonia synthesis by N2 and steam electrolysis in molten hydroxide suspensions of nanoscale Fe2O3. *Science (80-).* 2014;345(6197):637-640. doi:10.1126/science.1254234
68. Kyriakou V, Garagounis I, Vasileiou E, Vourros A, Stoukides M. Progress in the Electrochemical Synthesis of Ammonia. *Catal Today*. 2017;286:2-13. doi:10.1016/j.cattod.2016.06.014
69. Yara. Pilbara. http://www.yara.com.au/about-yara/about-yara-local/yara-pilbara/. Accessed November 6, 2019.
70. Brown T. Renewable ammonia demonstration plant announced in South Australia. AMMONIA INDUSTRY. https://ammoniaindustry.com/renewable-ammonia-demonstration-plant-announced-in-south-australia/. Accessed November 6, 2019.
71. Cui B, Wang B, Lau J, Li F-F, Licht S, Liu S. ChemInform Abstract: Ammonia Synthesis by N 2 and Steam Electrolysis in Molten Hydroxide Suspensions of Nanoscale Fe 2 O 3 . *ChemInform*. 2014;45(43):no-no. doi:10.1002/chin.201443014
72. McEnaney JM, Singh AR, Schwalbe JA, et al. Ammonia synthesis from N2 and H2O using a lithium cycling electrification strategy at atmospheric pressure. *Energy Environ Sci*. 2017;10(7):1621-1630. doi:10.1039/c7ee01126a
73. O'Hare PAG, Johnson GK. Lithium nitride (Li3N): standard enthalpy of formation by

solution calorimetry. *J Chem Thermodyn*. 1975;7(1):13-20. doi:10.1016/0021-9614(75)90075-0
74. Lithium Hydroxide. American Elements. https://www.americanelements.com/lithium-hydroxide-1310-65-2. Accessed January 15, 2020.
75. Wang Q, Jiang L, Yu Y, Sun J. Progress of enhancing the safety of lithium ion battery from the electrolyte aspect. *Nano Energy*. 2019;55(October 2018):93-114. doi:10.1016/j.nanoen.2018.10.035
76. Deng J, Iñiguez JA, Liu C. Electrocatalytic Nitrogen Reduction at Low Temperature. *Joule*. 2018;2(5):846-856. doi:10.1016/j.joule.2018.04.014
77. Smith AR, Klosek J. A review of air separation technologies and their integration with energy conversion processes. *Fuel Process Technol*. 2001;(70):115-134.
78. Ammonia. The Merck Index Online. https://www.rsc.org/Merck-Index/monograph/m1758/ammonia?q=authorize. Accessed November 6, 2019.
79. Jegede F. *Ammonia Process by Pressure Swing Adsorption*. Houston; 2010.
80. Ammonia. NIST Chemistry WebBook, SRD 69. https://webbook.nist.gov/cgi/cbook.cgi?Name=ammonia&Units=SI. Accessed November 6, 2019.
81. Jouny M, Luc W, Jiao F. General Techno-Economic Analysis of CO2 Electrolysis Systems. *Ind Eng Chem Res*. 2018;57(6):2165-2177. doi:10.1021/acs.iecr.7b03514
82. Nitrogen. NIST Chemistry WebBook, SRD 69. https://webbook.nist.gov/cgi/cbook.cgi?Name=Nitrogen&Units=SI. Accessed November 6, 2019.
83. Sher shah Amarkhail. Diploma project. *Air Sep Diploma Proj*. 2009. doi:10.1021/ma9000176
84. Khalel Z a. M, Rabah A a., Barakat TAM. A New Cryogenic Air Separation Process with Flash Separator. *ISRN Thermodyn*. 2013;2013(January):1-4. doi:10.1155/2013/253437
85. Min Wang Q, Shen D, Bülow M, et al. Metallo-organic molecular sieve for gas separation and purification. *Microporous Mesoporous Mater*. 2002;55(2):217-230. doi:10.1016/S1387-1811(02)00405-5
86. Air - Composition and Molecular Weight. The Engineering ToolBox. https://www.engineeringtoolbox.com/air-composition-d_212.html. Accessed November 6, 2019.
87. ALPEMA. *The Standards of the Brazed Aluminium Plate-Fin Heat Exchanger*. 2nd ed. Brazed Aluminium Plate-Fin Heat Exchanger Manufacturers' Association(ALPEMA); 2000.
88. Hillebrand R. *Technical White Paper Life Cycle Policy for the Chemical, Petrochemical and Pharmaceutical Industries*.
89. Jouny M, Luc W, Jiao F. General Techno-Economic Analysis of CO2Electrolysis Systems. *Ind Eng Chem Res*. 2018;57(6):2165-2177. doi:10.1021/acs.iecr.7b03514
90. PRICE SUMMARY FOR COMPRESSED GASSES AND REALTED SERVICE. Oklahoma State University. https://purchasing.okstate.edu/sites/default/files/documents/oshop/Compressed Gas Bid Price Summary.pdf. Accessed January 15, 2020.
91. Global aluminium smelters' production costs on decline. National Association of Manufacturers of Refractory Products, Materials and Related Services.

http://www.anfre.com/global-refractories-facing-the-next-production-revolution/. Accessed November 6, 2019.
92. Schnitkey G. Fertilizer Prices Higher for 2019 Crop farmdoc daily. farmdoc daily. https://farmdocdaily.illinois.edu/2018/09/fertilizer-prices-higher-for-2019-crop.html. Published 2018. Accessed November 6, 2019.
93. Michalsky R, Parman BJ, Amanor-Boadu V, Pfromm PH. Solar thermochemical production of ammonia from water, air and sunlight: Thermodynamic and economic analyses. *Energy*. 2012;42(1):251-260. doi:10.1016/j.energy.2012.03.062
94. Bard AJ, Faulkner LR. *Electrochemical Methods: Fundamentals and Applications*. 2nd ed. Wiley; 2000. doi:10.1016/B978-0-12-381373-2.00056-9
95. Davydova ES, Mukerjee S, Jaouen F, Dekel DR. Electrocatalysts for Hydrogen Oxidation Reaction in Alkaline Electrolytes. *ACS Catal*. 2018;8(7):6665-6690. doi:10.1021/acscatal.8b00689
96. Thomas D. *Cost Reduction Potential For Electrolyser Technology*. Berlin; 2018.
97. Kerry F. *Industrial Gas Handbook: Gas Separation and Purification*. 1st ed. Taylor & Francis Group; 2006. doi:10.1201/9781420008265
98. Harvego EA, Brien JEO, Mckellar MG. *System Evaluations and Life-Cycle Cost Analyses for High-Temperature Electrolysis Hydrogen Production Facilities*.; 2012. doi:10.2172/1047199
99. Madias J. *Electric Furnace Steelmaking*. Vol 3. Elsevier Ltd; 2014. doi:10.1016/B978-0-08-096988-6.00013-4
100. Douglas M. Ruthven , S. Farooq KSK. *Pressure Swing Adsorption*. Wiley-VCH; 1; 1993.
101. Bartels JR. A feasibility study of implementing an Ammonia Economy. 2008.
102. Hajipour S. Economic Evaluation using Aspen HYSYS. Process Ecology. http://processecology.com/articles/economic-evaluation-using-aspen-hysys. Accessed January 20, 2020.
103. Brown T. *Engineering Economics and Economic Design for Process Engineers*. 1st ed. CRC Press; 2016. doi:10.1201/b15877
104. Chen J. Discounted Cash Flow - DCF. Investopedia. https://www.investopedia.com/terms/d/dcf.asp. Published 2019. Accessed January 15, 2020.
105. KENTON W. Net Present Value (NPV). https://www.investopedia.com/terms/n/npv.asp. Published 2019. Accessed January 20, 2020.
106. KENTON W. Nominal Interest Rate. Investopedia. https://www.investopedia.com/terms/n/nominalinterestrate.asp. Accessed November 6, 2019.
107. CHEN J. Inflation Definition. Investopedia. https://www.investopedia.com/terms/i/inflation.asp. Accessed November 6, 2019.
108. Spurgeon JM, Kumar B. A comparative technoeconomic analysis of pathways for commercial electrochemical CO2 reduction to liquid products. *Energy Environ Sci*. 2018;11(6):1536-1551. doi:10.1039/c8ee00097b
109. Bacchetti A, Bonetti S, Perona M, Saccani N. *Investment and Management Decisions in Aluminium Melting: A Total Cost of Ownership Model and Practical Applications*. Vol 10.; 2018. doi:10.3390/su10093342
110. Ndjebayi JN. Aluminum Production Costs: A Comparative Case Study of Production

Strategy. 2017.
111. Keniry J. The economics of inert anodes and wettable cathodes for aluminum reduction cells. *Jom*. 2001;53(5):43-47. doi:10.1007/s11837-001-0209-2
112. Pfromm PH. Towards sustainable agriculture: Fossil-free ammonia. *J Renew Sustain Energy*. 2017;9(3):034702. doi:10.1063/1.4985090
113. Brown T. Ammonia production causes 1% of total global GHG emissions. AMMONIA INDUSTRY. https://ammoniaindustry.com/ammonia-production-causes-1-percent-of-total-global-ghg-emissions/. Accessed November 6, 2019.
114. Report WNA. Comparison of Lifecycle Greenhouse Gas Emissions of Various Electricity Generation Sources. *World Nucl Assoc*. 2011:10. doi:10.1002/esp
115. U.S. Energy Information Administration. *Electric Power Monthly with Data for June 2019*.; 2019. http://www.eia.gov/electricity/monthly/pdf/epm.pdf.
116. Sawyer D, Melton N. *Taking Stock of Canada's Electricity Mix and Greenhouse Gas Emissions to 2030*.; 2017.
117. Al-Aidaroos S, Bass N, Downey B, Ziegler J. *Offshore LNG Production*.; 2009. http://repository.upenn.edu/cbe_sdr/11.
118. Koretsky MD. *Engineering and Chemical Thermodynamics*. 2nd ed. Wiley; 2; 2013.
119. Nitrogen. NIST Chemistry WebBook, SRD 69. https://webbook.nist.gov/cgi/cbook.cgi?Name=nitrogen&Units=SI&cTG=on. Accessed November 6, 2019.
120. McCrory CCL, Jung S, Ferrer IM, Chatman SM, Peters JC, Jaramillo TF. Benchmarking Hydrogen Evolving Reaction and Oxygen Evolving Reaction Electrocatalysts for Solar Water Splitting Devices. *J Am Chem Soc*. 2015;137(13):4347-4357. doi:10.1021/ja510442p
121. Hydrogen Density of States. NIST Chemistry WebBook, SRD 69. https://webbook.nist.gov/cgi/cbook.cgi?ID=C1333740&Mask=4. Accessed January 20, 2020.
122. Balance of Plant Systems, Equipment & Services _ GE Power. GE power. https://www.ge.com/power/services/balance-of-plant. Accessed November 6, 2019.
123. Towler G, Sinnott R. *Chemical Engineering Design: Principles, Practice and Economics of Plant and Process Design*. 2nd ed. Butterworth-Heinemann; 2; 2013.
124. Federal Depreciation Rates. A/N Group, Inc. http://www.smbiz.com/sbrl012.html#ex. Accessed November 6, 2019.
125. Bauer F, Hulteberg C, Persson T, Tamm D. *Biogas Upgrading – Review of Commercial Technologies.*; 2013.

Appendix A Air separation streams

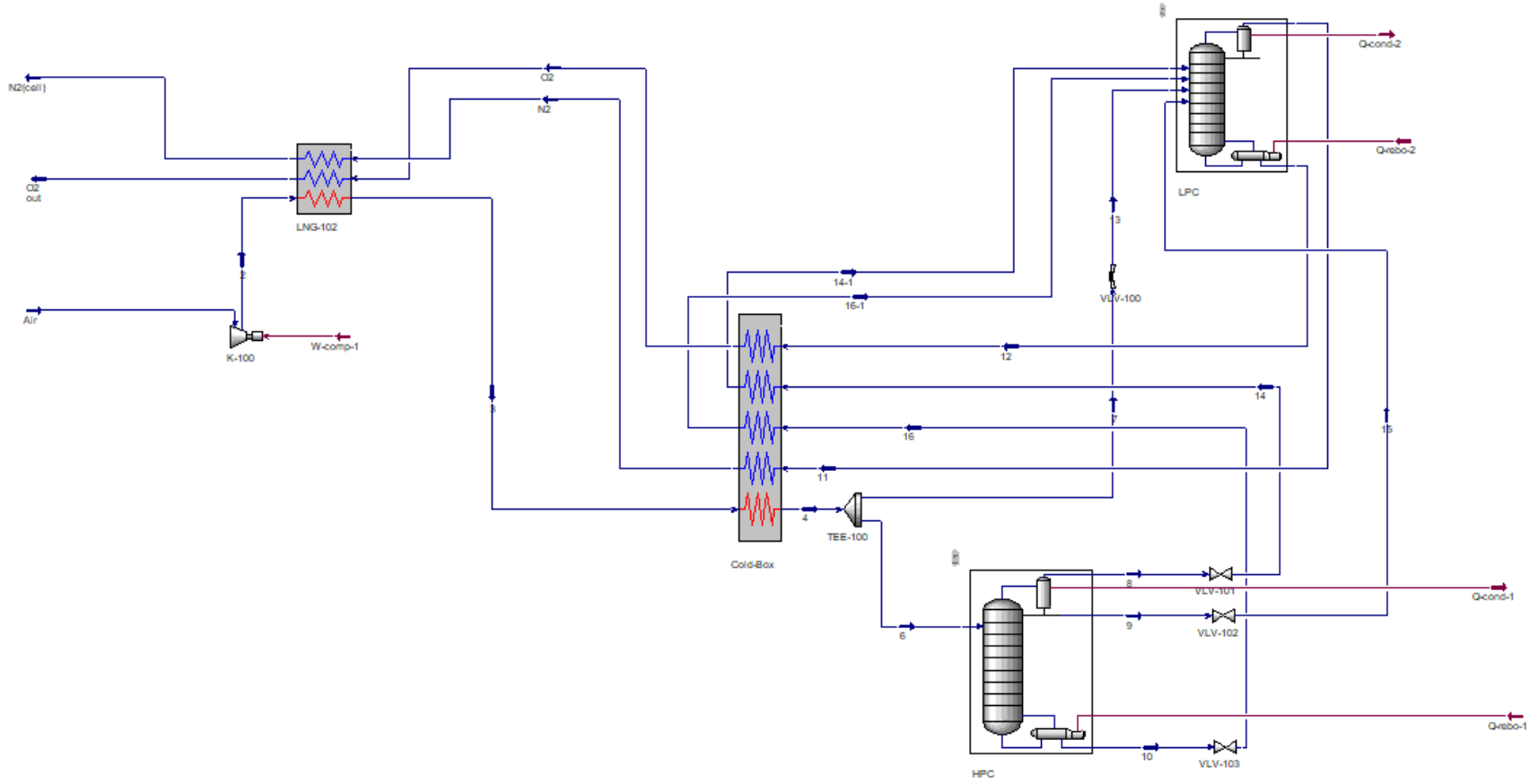

Figure A1. Flowsheet of Air Separation Unit.

Table A1. Properties of streams in Air Separation Unit.

		Air	2	6	7	8	9	10	11	12	13
Vapour Fraction		1.00	1.00	1.00	1.00	1.00	0.00	0.00	1.00	0.00	1.00
Temperature	*C*	30.00	292.18	-170.00	-170.00	-177.93	-177.93	-164.32	-195.80	-185.09	-176.39
Pressure	*kPa*	101.32	607.95	607.95	607.95	486.36	486.36	526.89	101.33	243.18	233.05
Molar Flow	*kgmole/h*	545.00	545.00	272.50	272.50	105.63	137.20	29.67	124.79	420.21	272.50
Mass Flow	*kg/h*	1.58E+04	1.58E+04	7.89E+03	7.89E+03	3.00E+03	3.95E+03	9.49E+02	3.50E+03	1.23E+04	7.89E+03
Liquid Volume Flow	*m3/h*	18.15	18.15	9.07	9.07	3.62	4.62	0.84	4.34	13.81	9.07
Heat Flow	*kJ/h*	7.49E+04	4.35E+06	1.59E+06	1.59E+06	6.38E+05	1.53E+06	3.45E+05	7.95E+05	4.92E+06	1.59E+06
Molar Enthalpy	*kJ/kgmole*	137.45	7977.91	5836.95	5836.95	6040.59	11121.02	11616.61	6367.69	11696.88	5836.95
Mass Enthalpy	*kJ/kg*	4.74	275.39	-201.49	-201.49	-212.93	-386.41	-363.20	-227.31	-399.84	-201.49
Molar Entropy	*kJ/kgmole-C*	152.34	156.02	105.12	105.12	102.94	51.22	47.34	109.25	46.90	112.39
Mass Entropy	*kJ/kg-C*	5.26	5.39	3.63	3.63	3.63	1.78	1.48	3.90	1.60	3.88
Molar Density	*kgmole/m3*	0.04	0.13	0.82	0.82	0.70	26.98	32.47	0.16	29.28	0.31
Mass Density	*kg/m3*	1.17	3.74	23.64	23.64	19.95	776.48	1038.47	4.60	856.62	8.89
Comp Mole Frac (Nitrogen)		0.78	0.78	0.78	0.78	0.93	0.83	0.02	1.00	0.71	0.78
Comp Mole Frac (Oxygen)		0.21	0.21	0.21	0.21	0.07	0.15	0.97	0.00	0.27	0.21
Comp Mole Frac (Argon)		0.01	0.01	0.01	0.01	0.01	0.01	0.01	0.00	0.01	0.01

		14	15	16	N2	4	O2	3	16-01	14-01	O2 out
Vapour Fraction		1.00	0.10	0.09	1.00	1.00	1.00	1.00	1.00	1.00	1.00
Temperature	*C*	-182.84	-187.47	-174.85	-187.55	-170.00	-182.15	10.00	-100.00	-100.00	132.91
Pressure	*kPa*	222.91	212.78	233.05	101.33	607.95	243.18	607.95	233.05	222.91	243.18
Molar Flow	*kgmole/h*	105.63	137.20	29.67	124.79	545.00	420.21	545.00	29.67	105.63	420.21
Mass Flow	*kg/h*	3.00E+03	3.95E+03	9.49E+02	3.50E+03	1.58E+04	1.23E+04	1.58E+04	9.49E+02	3.00E+03	1.23E+04
Liquid Volume Flow	*m3/h*	3.62	4.62	0.84	4.34	18.15	13.81	18.15	0.84	3.62	13.81
Heat Flow	*kJ/h*	6.38E+05	1.53E+06	3.45E+05	7.65E+05	3.18E+06	2.52E+06	2.67E+05	1.07E+05	3.84E+05	1.33E+06
Molar Enthalpy	*kJ/kgmole*	6040.59	11121.02	11616.61	6128.36	5836.95	6002.47	-489.31	3608.97	3636.29	3161.64
Mass Enthalpy	*kJ/kg*	-212.93	-386.41	-363.20	-218.77	-201.49	-205.19	-16.89	-112.84	-128.18	108.08
Molar Entropy	*kJ/kgmole-C*	108.83	51.65	47.71	112.19	105.12	110.66	135.33	123.54	127.76	154.06
Mass Entropy	*kJ/kg-C*	3.84	1.79	1.49	4.00	3.63	3.78	4.67	3.86	4.50	5.27
Molar Density	*kgmole/m3*	0.32	2.87	3.12	0.15	0.82	0.35	0.26	0.16	0.16	0.07
Mass Density	*kg/m3*	8.99	82.65	99.92	4.12	23.64	10.10	7.51	5.24	4.44	2.11
Comp Mole Frac (Nitrogen)		0.93	0.83	0.02	1.00	0.78	0.71	0.78	0.02	0.93	0.71
Comp Mole Frac (Oxygen)		0.07	0.15	0.97	0.00	0.21	0.27	0.21	0.97	0.07	0.27
Comp Mole Frac (Argon)		0.01	0.01	0.01	0.00	0.01	0.01	0.01	0.01	0.01	0.01

		N2(cell)	Reflux @COL 1	To Condenser @COL1	Boilup @COL 1	To Reboiler @COL 1	9 @COL 1	10 @COL 1	6 @COL 1	8 @COL 1	Reflux @COL 2
Vapour Fraction		1.00	0.00	1.00	1.00	0.00	0.00	0.00	1.00	1.00	0.00
Temperature	*C*	25.00	-177.93	-176.12	-164.32	-165.36	-177.93	-164.32	-170.00	-177.93	-195.80
Pressure	*kPa*	101.33	486.36	496.49	526.89	516.76	486.36	526.89	607.95	486.36	101.33
Molar Flow	*kgmole/h*	124.79	527.59	770.42	414.22	443.89	137.20	29.67	272.50	105.63	4778.78
Mass Flow	*kg/h*	3.50E+03	1.52E+04	2.21E+04	1.32E+04	1.42E+04	3.95E+03	9.49E+02	7.89E+03	3.00E+03	1.34E+05
Liquid Volume Flow	*m3/h*	4.34	17.75	25.99	11.80	12.64	4.62	0.84	9.07	3.62	166.01
Heat Flow	*kJ/h*	9.70E+02	5.87E+06	4.60E+06	2.30E+06	5.16E+06	1.53E+06	3.45E+05	1.59E+06	6.38E+05	5.70E+07
Molar Enthalpy	*kJ/kgmole*	-7.77	11121.02	-5975.21	5562.45	11620.97	11121.02	11616.61	5836.95	6040.59	11924.79
Mass Enthalpy	*kJ/kg*	-0.28	-386.41	-208.02	-174.51	-364.49	-386.41	-363.20	-201.49	-212.93	-425.68
Molar Entropy	*kJ/kgmole-C*	148.06	51.22	104.58	103.85	47.99	51.22	47.34	105.12	102.94	37.40
Mass Entropy	*kJ/kg-C*	5.29	1.78	3.64	3.26	1.51	1.78	1.48	3.63	3.63	1.34
Molar Density	*kgmole/m3*	0.04	26.99	0.70	0.65	32.32	26.99	32.47	0.82	0.70	28.74
Mass Density	*kg/m3*	1.15	776.83	20.18	20.74	1030.56	776.83	1038.47	23.64	19.95	805.03
Comp Mole Frac (Nitrogen)		1.00	0.83	0.85	0.05	0.05	0.83	0.02	0.78	0.93	1.00
Comp Mole Frac (Oxygen)		0.00	0.15	0.14	0.94	0.94	0.15	0.97	0.21	0.07	0.00
Comp Mole Frac (Argon)		0.00	0.01	0.01	0.01	0.01	0.01	0.01	0.01	0.01	0.00

		To Condenser @COL2	Boilup @COL2	To Reboiler @COL2	11 @COL2	12 @COL2	13 @COL2	15 @COL2	16-1 @COL2	14-1 @COL2
Vapour Fraction		1.00	1.00	0.00	1.00	0.00	1.00	0.10	1.00	1.00
Temperature	*C*	-194.98	-185.09	-186.91	-195.80	-185.09	-176.39	-187.47	-100.00	-100.00
Pressure	*kPa*	111.46	243.18	233.05	101.33	243.18	233.05	212.78	233.05	222.91
Molar Flow	*kgmole/h*	4903.57	4486.50	4906.71	124.79	420.21	272.50	137.20	29.67	105.63
Mass Flow	*kg/h*	1.37E+05	1.28E+05	1.40E+05	3.50E+03	1.23E+04	7.89E+03	3.95E+03	9.49E+02	3.00E+03
Liquid Volume Flow	*m3/h*	170.35	152.46	166.27	4.34	13.81	9.07	4.62	0.84	3.62
Heat Flow	*kJ/h*	3.11E+07	2.74E+07	5.69E+07	7.95E+05	4.92E+06	1.59E+06	1.53E+06	1.07E+05	3.84E+05
Molar Enthalpy	*kJ/kgmole*	-6350.32	6115.62	11595.00	6367.69	11696.88	5836.95	11121.02	3608.97	3636.29
Mass Enthalpy	*kJ/kg*	-226.69	-214.34	-405.50	-227.31	-399.84	-201.49	-386.41	-112.84	-128.18
Molar Entropy	*kJ/kgmole-C*	108.71	107.97	45.40	109.25	46.90	112.39	51.65	123.54	127.76
Mass Entropy	*kJ/kg-C*	3.88	3.78	1.59	3.90	1.60	3.88	1.79	3.86	4.50
Molar Density	*kgmole/m3*	0.18	0.36	28.29	0.16	29.28	0.31	2.87	0.16	0.16
Mass Density	*kg/m3*	5.03	10.24	809.02	4.60	856.62	8.89	82.65	5.24	4.44
Comp Mole Frac (Nitrogen)		1.00	0.88	0.87	1.00	0.71	0.78	0.83	0.02	0.93
Comp Mole Frac (Oxygen)		0.00	0.11	0.12	0.00	0.27	0.21	0.15	0.97	0.07
Comp Mole Frac (Argon)		0.00	0.01	0.01	0.00	0.01	0.01	0.01	0.01	0.01

Appendix B Cost calculation for ASU

The equipment cost of ASU (Figure A1) is mostly obtained from Aspen Economic Analyzer. As for the cost of cold-box (brazed aluminum heat exchanger) calculation, we gathered related data (Q, LMTD, UA, etc) from Aspen then estimated the cost from a reference cold-box[87,117].

Table B1 Summary of equipment cost for ASU (Figure A1)

Equipment name	Cost ($)
K-100	1887600
HPC	76200
LPC	281000
LNG-102	4024248
Cold box	2473236
Total	15298995.52

Then the operating cost for ASU unit is calculated from electricity and steam requirement:

$$ASU\ operating\ cost = 1414.74\ kW * \frac{24h}{day} * \frac{350days}{year} * \frac{\$0.02}{kWh} + \frac{\$234.89}{hour} * \frac{24hour}{day} * \frac{350days}{year} =$$

$$\$2210752.32/year$$

Appendix C Reaction voltage calculation for NH_3 electrosynthesis

Here, we calculated the enthalpy change of reaction from[118]:

$$\Delta H_{reaction} = \sum v_i(\Delta H_{products}) - \sum v_i(\Delta H_{reactants}) \quad (1)$$

We assumed the experiments at room pressure, so the enthalpies of reactants and products can be calculated from heat capacity at constant pressure (C_p)[118]:

$$\Delta H = \int_{T1}^{T2} C_p dT \quad (2)$$

While heat capacity data for components can be calculated by[118]:

$$\frac{C_P}{R} = A + BT + CT^2 + DT^{-2} + ET^3 \; with \; T \; in \; [K] \quad (3)$$

Table C1. Heat capacity data[118]

	A	B*10^3	C*10^6	D*10^-5	E*10^9
N_2	3.28	0.59		0.04	
H_2	3.25	0.42		0.08	
O_2	3.64	0.51		-0.23	
$H_2O(g)$	3.47	1.45		0.121	
$H_2O(l)$	9.07				
NH_3	3.58	3.02		-0.19	

Then the Gibbs free energy for reactions can be calculated from enthalpy and entropy [118]:

$$G_i \equiv H_i - TS_i \tag{4}$$

While the enthalpy data is in the following table:

Table C2. Entropy data[119]

	ΔS (J/Mole K)
N_2	191.61
H_2	130.68
O_2	205.15
$H_2O(g)$	188.84
$H_2O(l)$	69.95
NH_3	192.77

Thus, based on the following equation, the reaction voltage can be calculated from the following equation[54]:

$$\Delta G = -nFE_{rxn} \tag{5}$$

n=transferred electrons in reactions F=Faradaic constant (96485 C/mole) E_{rxn}=reaction voltage

To sum up:

Table C3 Enthalpies, Gibbs free energies and reaction voltages at various temperature.

	ΔH(J/4 mole NH_3)	ΔG(J/4 mole NH_3)	E_{rxn}(V)
Scenario A RT	1530511.93	1356506.22	-1.17
Scenario A HT	1290818.07	1391112.64	-1.20
Scenario B RT	-92219.72	-103584.38	0.06
Scenario B HT	-103077.67	50090.30	-0.09

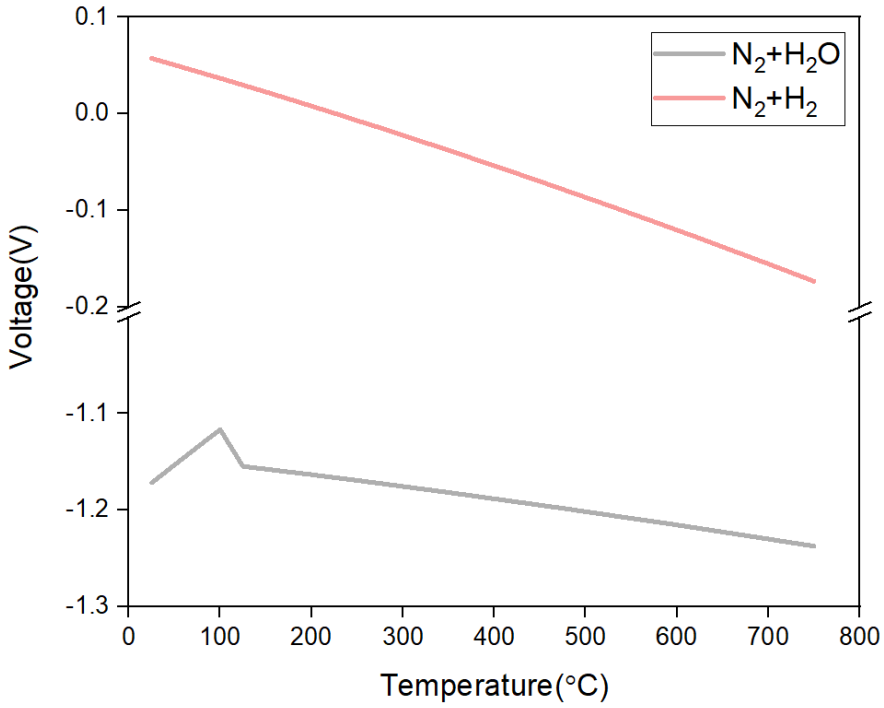

Figure C1. Reaction voltages at different temperature.

The enthalpy for NH_3 reaction can be converted to:

$$\Delta H° = \frac{1530511.93J}{4\,mole}\,NH_3 = \frac{382628J}{mole}NH_3 = \frac{22.47MJ}{kg}NH_3$$

Appendix D Detailed capital and operating cost calculation

In the following calculation sample, we are making a sample calculation for NH_3 electrosynthesis using N_2 and H_2O at room temperature (Scenario A RT). Here, all calculations are under optimistic conditions.

In the experimental design, we are considering a flow cell configuration for NH_3 electrosynthesis. We set the flow rate of electrolyte as 50 mL/min from a similar CO_2 electrolyzer set up[64]. Under optimistic condition, the single-pass weight concentration of NH_3 in KOH is[80]:

$$NH_3, wt.\% = \frac{0.5A}{3e^- * \frac{96485C}{mole}} * \frac{60s}{min} * \frac{17.03g}{mole} \div \frac{50mL}{min} * 100\% = 0.00353\%$$

As calculated, the concentration of dissolved NH_3 would be too low to be separated, so the circulation of electrolytes would be a better choice until it reaches a higher concentration. In this simulation, the NH_3 concentration in exiting electrolyte (1M KOH) is considered at 10 wt. %.

Assuming a 100 ton/day production rate, the current required is:

$$I_{used} = 100000kg * \frac{1000g}{kg} \div \frac{3600s}{hour} \div \frac{24hour}{day} \div \frac{17.03g}{mole} * 3e^- * \frac{96485C}{mole}$$

$$= 19672187.97\ A$$

Then the needed current equals to used current divided by the faradaic efficiency, here we use 90% which is the most optimistic prediction:

$$I_{total} = \frac{19672187.97}{90\%} = 21857986.63A$$

The power requirement for electrolyzer equals to the product of total current, I_{total}, and operating voltage, 1.17 V plus a 0.3 V cathode over potential gathered from NH_3 fuel cell plus a 0.3 V anode overpotential from state-of-art OER[10,120]:

$$P = V * I = 1.77V * 21857986.63A = 38.69\ MW$$

From the total needed current, we calculate the electrolyzer area from current density:

$$Area = \frac{21857986.63A}{0.5A/cm^2} \div \frac{10000cm^2}{m^2} = 4371.60\ m^2$$

A recycle system was considered to bring back unreacted N_2, so the amount of required N_2 is fixed since produced NH_3 (100 ton/day) is fixed. Therefore, we calculate the amount of daily required N_2 from total current:

$$N_{2(reacted)} = 21857986.63A * \frac{1}{6\frac{e^-}{mole\ N_2} * \frac{96485C}{mole}} * \frac{28.01g}{mole} * \frac{86400s}{day} = 82237.23\ kg/day$$

At optimistic condition, the single-pass conversion is set as 70%, so total required N_2 is:

$$N_{2(\ inlet)} = N_{2(reacted)} \div 70\% = 117481.75kg/day$$

Then unreacted N_2 can be calculated:

$$N_{2(unreacted)} = N_{2(inlet)} - N_{2(reacted)} = 35244.53\ kg/day$$

At cathode side, not all electrons flow to the N_2 to produce NH_3, hence the flow rate of H_2 produced by HER side reaction:

$$H_{2(produced)} = 21857986.63A * (1 - 90\%) * \frac{1}{2e^- * \frac{96485C}{mole}} * \frac{2g}{mole} * \frac{86400s}{day}$$

$$= 1957.33\ kg/day$$

Therefore, the water required for anode side to provide protons is:

$$H_2O_{required} = 21857986.63A * 2 * \frac{1}{4e^- * \frac{96485C}{mole}} * \frac{18g}{mole} * \frac{86400s}{day} = 176159.72\ kg/day$$

And the O_2 produced can be calculated from mass balance:

$$O_{2\,produced} = m_{H_2O} \quad - m_{H_2,produced} \quad = 176159.72 - 1957.33 = 174202.39\ kg/day$$

As a result, we calculate the total gas flow[82,121]:

$$Q_{total} = Q_{NH_3} + Q_{N_2} + Q_{H_2} = 0 + 35244.53\ kg/day \div \frac{1.25kg}{m^3} + 1957.33\ kg/day \div \frac{0.09kg}{m^3}$$

$$= 49943.74m^3/day = 2080.99m^3/hour$$

Capital cost analysis:

Here we have shown capital cost analysis for ammonia synthesis from N_2 and H_2O at room temperature (Scenario A RT) under optimistic case. The reference PEM electrolyzer operates at 1.6 V and 2.0 A/cm^2, and the cost for the PEM system is considered as \$1000/m^2. Thus, the total capital cost of the electrolyzer system equals to the product of the total electrolyzer area and cost per area:

$$NH_3\ Electrolyzer\ cost = 4371.60m^2 * \frac{\$1000}{m^2} = \$4371597$$

The balance of plant is a terminology for all the supporting and auxiliary facilities required for a power plant[122]. Here, we consider the balance of plant is 55% of total stack cost, and a 60% cost deduction due to the successful scaling of equipment[26,105]:

$$Balance\ of\ plant = 0.4 * NH_3\ electrolyzer\ cost * \frac{0.55}{0.45} = \$2137225$$

For synthesis using H_2 as feedstock, we consider 1.6 V and 2.0 A/cm^2 for PEM water electrolyzer with a \$1000/m^2 stack cost[56]. Based on material balance (every mole of N_2 needs three moles of H_2 to synthesize NH_3), the amount the required H_2 daily is 8808 kmole. Hence, the total current for H_2O electrolyzer is:

$$I_{total} = 21857986.63A$$

H_2O electrolyzer cost:

$$H_2O\ electrolyzer\ area = \frac{21857986.63\ A}{2.0\ A/cm^2} \div \frac{10000 cm^2}{m^2} = 1092.90\ m^2$$

$$H_2O\ electrolyzer\ cost = \ 1092.90\ m^2 * \frac{\$1000}{m^2} = \$1092899.33$$

Similar balance of plant calculation can be applied here:

$$Balance\ of\ plant = 0.4 * H_2O\ electrolyzer\ cost * \frac{0.55}{0.45} = \$534306.34$$

The separation costs for various synthesis routes are various, for room temperature case and Lithium case, distillation columns are designed and calculated using Aspen HYSYS (see Table S7) while PSA are used to separate gaseous products for high-temperature electrosynthesis with a 0.7 scaling factor[81]:

$$PSA\ Capital\ cost = \$1989043 * \left(\frac{2080.99\frac{m^3}{hour}}{1000\frac{m^3}{hour}}\right)^{0.7} = \$3322256$$

For high-temperature electrosynthesis, electric resistance heater is used to elevate the temperature of inlet streams to 500°C, and we calculate that cost at around $77000/MW with a 4.1 installation factor based on an all-electric driven H_2 production plant, a 5% heat loss due to heat loss from roof and sidewalls is considered[98,99].

For NH_3 electrosynthesis using N_2 and H_2O at 500°C, the electric heater cost is:

$$Electric\ heater\ cost = \frac{\$77000}{MW} * \frac{MW}{1000kW} * \frac{7440kW}{0.95} * 4.1 = \$2472429$$

For H-B reactor, the capital cost was estimated using six-tenth rules and 10% contingency factor, from an offshore wind power ammonia synthesis loop at 300 ton/day production rate[26,123]:

$$\$53420000 = (reactor\ cost) * (\frac{300}{100})^{0.6}$$

From the Goal Seek analysis in Excel, the cost is:

$$reactor\ cost = \$27633196.85$$

For Lithium recycling, based on material balance, 8808 kmole of LiOH is needed (every one mole of NH_3 needs 1.5 moles of LiOH). Currently, LiOH is at around $20-30/kg, so we consider LiOH cost is $25/kg so the total cost is[72]:

$$Cost\ of\ LiOH = \frac{\$25}{ton} * 8808kmole * \frac{24g}{mole} = \$5284800$$

Cost for LiOH electrolysis cell is calculated from an aluminum smelter because the similarity in cell configuration ($10.16/ton produced aluminum, crucible furnaces), and we chose consumable inert anodes instead of carbon anodes to avoid CO_2 emission ($128/ton produced aluminum), and the anodes are replaced every three years[109,111]:

$$Capital\ cost\ of\ LiOH\ cell = 8808kmole * \frac{7g}{mole} * \left(\frac{\$10.16}{ton}\right) = \$626.42$$

$$Anode\ cost\ for\ LiOH\ cell = 8808kmole/day * \frac{7g}{mole} * \left(\frac{\$128}{ton}\right) = \$7891.97/day$$

Operating cost analysis:

Then operating cost was calculated from several aspects:

Electricity cost for the electrolyzer is calculated based on the total power requirement:

$$Electricity\ cost = 38.69MW * \frac{1000kW}{MW} * 24hour * \frac{\$0.02}{kWh} * \frac{350days}{year} = \$6499920/year$$

Then the electricity cost for heating in high-temperature case is:

$$Heating\ cost = \frac{7.44MW}{0.95} * \frac{1000kW}{MW} * \frac{24hour}{day} * \frac{350days}{year} * \frac{\$0.02}{kWh} = \$1315705/year$$

For the replacement and maintenance of electrolyzers annually, we considered it is 2.5% of capital cost:

$$Maintenance\ cost = \$2409845 * 2.5\% = \$60246/year$$

Then the operating cost of the PSA unit, a linear scaling calculation was used (at $0.02/kWh electricity price):

$$PSA\ operating\ cost = 2080.99\frac{m^3}{hour} * 0.25kWh * 24hour * \frac{\$0.02}{kWh} * \frac{350days}{year}$$

$$= \$87402/year$$

The operating cost for distillation column is the sum of electricity, coolant, and heating energy costs, while we convert the heating energy to electricity for the sake of simplicity (Table D2.):

$$W_{heating} = \frac{Q}{t} = \frac{41160000kJ/h}{3600s/h} = 11433.33\ kW$$

Therefore:

$$Distillation\ operating\ cost$$

$$= (W_{heating} + W_{pump}) * \frac{24hour}{day} * \frac{350day}{year} * \$0.02/kWh + \frac{\$4.48}{hour} * \frac{24hour}{day}$$

$$* \frac{350day}{year} = \$2068316/year$$

While for Condensation cost (Table D2.):

$$Condensation\ operating\ cost$$

$$= W_{pump} * \frac{24hour}{day} * \frac{350day}{year} * \$0.02/kWh + \frac{\$0.93}{hour} * \frac{24hour}{day} * \frac{350day}{year}$$

$$= \$16602/year$$

Cost of H_2O is[81]:

$$H_2O\ cost = \frac{176159.72kg}{day} * \frac{\$0.0054}{gal} \div \frac{3.79kg}{gal} * 350days/year = \$87847/year$$

While the operating cost for the H-B reactor is mainly due to the compression power and thermal requirement to heat the materials to target temperature, 150 bar and 450 °C separately. So it can be calculated by linearly scaling down from a similar plant[26]:

$$W = \frac{8.02MW}{3} = 2.67MW$$

$$Reactor\ operating\ cost = 2.67MW * \frac{1000kW}{MW} * \frac{24hour}{day} * \frac{350day}{year} * \$0.02/kWh$$

$$= \$448560/year$$

To sum up:

Table D1 Summary of capital costs ($)

	ASU	Electrolyzer/Reactor +balance of plant	LiOH	PSA	Distillation	Heating equipment	Condensation	H-B reactor	O_2 compression	Total
Scenario A RT	15298996	6508823	0	3322255	2894110	0	1765710	0	10436100	40225994
Scenario A HT	15298996	4649159	0	8576781	0	2472429	1775570	0	10436100	43209035
Scenario B RT	15298996	7973308	0	3322255	2894110	0	1765710	0	10436100	41690479
Scenario B HT	15298996	6113644	0	8576781	0	648016	1775570	0	10436100	42849107
Scenario C	15298996	1464448	0	0	0	0	0	27633197	10436100	54832740
Scenario D	15298996	326436	5284792	0	4276480	0	1765710	0	10436100	37388514

Table D2 Summary of operating costs ($/year)

	ASU	Electricity	Maintenance	PSA	Distillation	Water+N_2	Condensation	H-B reactor	O_2 compression	Total
Scenario A RT	2210752	6499691	60246	87402	2068316	87847	20997	0	247477	11282728
Scenario A HT	2210752	7925560	78064	338794	0	87847	16686	0	247477	10905181
Scenario B RT	2210752	6866905	133880	87402	2068316	79167	16602	0	247477	11710501
Scenario B HT	2210752	7321911	102654	338794	0	79167	16686	0	247477	10317442
Scenario C	2210752	5287749	24590	0	0	79165	0	448560	247477	8298293
Scenario D	2210752	11236754	1084335	0	232357	158125	16602	0	247477	14036799

Appendix E Detailed NPV calculation

Here, again, we take N_2 and H_2O room temperature NH_3 synthesis (Scenario A RT) as an example to illustrate the calculation for economics.

NPV:

Net Present Value (NPV) = sum of all present values (PV) of the cash flows (CF)[105]

$$NPV = \sum_{t=1}^{n} \frac{CF_t}{(1 + IRR)^t} \tag{6}$$

t = year, *n* = plant life, *CF* = cash flow, *IRR* = internal rate of return

Here, the end-of-life NPV is estimated on a 20-year basis, with a 38.9% tax rate and a 10% internal rate of return[81]. The capital expenses are $35560185, and the working capital is taken as 5% of capital expenses, while the depreciable capital cost is $23848761[102]. The million dollars difference between capital expenses and depreciable capital cost is that in Aspen Economic Analyzer, direct field costs (equipment rental, insurance, etc.) and indirect costs (taxes, permits, administrative expenses, etc.) are both calculated, indirect costs are not depreciable nor bring benefit in cash flow (see following calculation). In addition, 20% of life salvage value is considered. Besides, we used a MACRS 10-year depreciation system to recover our capital investment, because it is a powerful tool in estimating similar electric systems[124]

In year 0, the facility is under construction, so the cumulative present value is:

$$Year\ 0\ cumulative\ present\ calue = -\$40225994 - \$2011300 = -\$42237293$$

In year 1, produced NH_3 and O_2 brings income:

$$Product\ income = \frac{\$530}{ton} * 1.15 * \frac{100ton}{day} * \frac{350day}{year} + \frac{0.096\$}{kg} * \frac{174202kg}{day} * 350days/year$$

$$= \$27175359.75/year$$

Then income minus operating cost gives us net profit:

$$year\ one\ Net\ profit = Product\ income - operating\ cost$$

$$= \$21332500 - \$4783037 - \$6499691 = \$15892631.65$$

$$year\ 1\ depreciation = \$23848761 * 10\% = \$2384876$$

$$year\ 1\ net\ earning = (\$15892631.65 + \$2384876) * (1 - 0.389) = \$11167557$$

$$year\ 1\ discounted\ cash\ flow = \$11167557 - \$2384876 = \$8782681$$

$$year\ one\ cash\ flow(present\ value) = \frac{\$8782681}{(1 + 0.1)^1} = \$7984256$$

After 20 years, a cumulative present value is $35.56M for Scenario A at optimistic conditions.

LCP:

$$NPV = 0 = Levelized\ cost\ of\ Product(LCP) - Operating\ Cost\ PV - Capital\ expense \quad (7)$$

LCP is calculated when NPV equals zero, which means the price that NH_3 needs to be sold to make this industry exactly not earning or losing money[108]. This calculation can directly indicate the price that NH_3 need to be sold at; hence, the experimental parameters required. The LCP data was gathered from Excel Goal Seek analysis.

Appendix F 20 years detailed NPV calculation.

Table F1 NPV calculation for NH_3 electrosynthesis using N_2 and H_2O at 25°C.

Total depreciable capital:	23848761	**Income tax**	0.389	**Nominal Interest Rate**	0.100			
Year	***Capital Expenses***	***Working Capital***	***Depreciation***	***Net Profit***	***Net Earning***	***Discounted Cash Flow***	***Cash Flow (Present Value)***	***Cumulative Present Value***
0	-40,225,994	-2,011,300				-42,237,293	-42,237,293	-42,237,293
1			-2,384,876	15,892,632	11,167,557	8,782,681	7,984,256	-34,253,038
2			-4,292,777	15,892,632	12,333,285	8,040,508	6,645,048	-27,607,990
3			-3,434,222	15,892,632	11,808,707	8,374,486	6,291,875	-21,316,115
4			-2,747,377	15,892,632	11,389,045	8,641,668	5,902,376	-15,413,739
5			-2,198,856	15,892,632	11,053,899	8,855,043	5,498,285	-9,915,454
6			-1,757,654	15,892,632	10,784,324	9,026,671	5,095,320	-4,820,134
7			-1,562,094	15,892,632	10,664,837	9,102,743	4,671,147	-148,987
8			-1,562,094	15,892,632	10,664,837	9,102,743	4,246,497	4,097,510
9			-1,564,479	15,892,632	10,666,294	9,101,816	3,860,058	7,957,568
10			-1,562,094	15,892,632	10,664,837	9,102,743	3,509,502	11,467,070
11			-782,239	15,892,632	10,188,346	9,406,107	3,296,783	14,763,853
12				15,892,632	9,710,398	9,710,398	3,094,032	17,857,885
13				15,892,632	9,710,398	9,710,398	2,812,756	20,670,641
14				15,892,632	9,710,398	9,710,398	2,557,051	23,227,692
15				15,892,632	9,710,398	9,710,398	2,324,592	25,552,284
16				15,892,632	9,710,398	9,710,398	2,113,266	27,665,550
17				15,892,632	9,710,398	9,710,398	1,921,150	29,586,700
18				15,892,632	9,710,398	9,710,398	1,746,500	31,333,201
19				15,892,632	9,710,398	9,710,398	1,587,728	32,920,929
20		8,045,199		15,892,632	9,710,398	17,755,597	2,639,256	35,560,185

Total depreciable capital:	28932753	**Income tax**	0.389	**Nominal Interest Rate**	0.100			
Year	***Capital Expenses***	***Working Capital***	***Depreciation***	***Net Profit***	***Net Earning***	***Discounted Cash Flow***	***Cash Flow (Present Value)***	***Cumulative Present Value***
0	-43,209,035	-2,160,452				-45,369,487	-45,369,487	-45,369,487
1			-5,207,896	16,270,178	13,123,103	7,915,208	7,195,643	-38,173,844
2			-4,166,316	16,270,178	12,486,698	8,320,382	6,876,349	-31,297,495
3			-3,333,053	16,270,178	11,977,575	8,644,521	6,494,757	-24,802,738
4			-2,667,600	16,270,178	11,570,983	8,903,383	6,081,130	-18,721,608
5			-2,132,344	16,270,178	11,243,941	9,111,597	5,657,585	-13,064,023
6			-1,895,095	16,270,178	11,098,982	9,203,887	5,195,354	-7,868,669
7			-1,895,095	16,270,178	11,098,982	9,203,887	4,723,049	-3,145,619
8			-1,897,989	16,270,178	11,100,750	9,202,761	4,293,156	1,147,537
9			-1,895,095	16,270,178	11,098,982	9,203,887	3,903,347	5,050,883
10			-948,994	16,270,178	10,520,915	9,571,920	3,690,390	8,741,273
11			0	16,270,178	9,941,079	9,941,079	3,484,288	12,225,560
12				16,270,178	9,941,079	9,941,079	3,167,534	15,393,095
13				16,270,178	9,941,079	9,941,079	2,879,576	18,272,671
14				16,270,178	9,941,079	9,941,079	2,617,797	20,890,468
15				16,270,178	9,941,079	9,941,079	2,379,815	23,270,283
16				16,270,178	9,941,079	9,941,079	2,163,468	25,433,752
17				16,270,178	9,941,079	9,941,079	1,966,789	27,400,541
18				16,270,178	9,941,079	9,941,079	1,787,990	29,188,532
19				16,270,178	9,941,079	9,941,079	1,625,446	30,813,977
20		8,641,807		16,270,178	9,941,079	18,582,886	2,762,228	33,576,205

Total depreciable capital:	25313246	**Income tax**	0.389	**Nominal Interest Rate**	0.100			
Year	***Capital Expenses***	***Working Capital***	***Depreciation***	***Net Profit***	***Net Earning***	***Discounted Cash Flow***	***Cash Flow (Present Value)***	***Cumulative Present Value***
0	-41,690,479	-2,084,524				-43,775,003	-43,775,003	-43,775,003
1			-2,531,325	14,881,016	10,638,940	8,107,616	7,370,560	-36,404,443
2			-4,556,384	14,881,016	11,876,252	7,319,867	6,049,477	-30,354,966
3			-3,645,107	14,881,016	11,319,462	7,674,354	5,765,856	-24,589,110
4			-2,916,086	14,881,016	10,874,029	7,957,944	5,435,383	-19,153,727
5			-2,333,881	14,881,016	10,518,302	8,184,421	5,081,882	-14,071,846
6			-1,865,586	14,881,016	10,232,174	8,366,588	4,722,721	-9,349,125
7			-1,658,018	14,881,016	10,105,350	8,447,332	4,334,817	-5,014,308
8			-1,658,018	14,881,016	10,105,350	8,447,332	3,940,743	-1,073,565
9			-1,660,549	14,881,016	10,106,896	8,446,347	3,582,076	2,508,511
10			-1,658,018	14,881,016	10,105,350	8,447,332	3,256,812	5,765,323
11			-830,274	14,881,016	9,599,599	8,769,324	3,073,595	8,838,918
12				14,881,016	9,092,301	9,092,301	2,897,087	11,736,005
13				14,881,016	9,092,301	9,092,301	2,633,716	14,369,721
14				14,881,016	9,092,301	9,092,301	2,394,287	16,764,008
15				14,881,016	9,092,301	9,092,301	2,176,625	18,940,632
16				14,881,016	9,092,301	9,092,301	1,978,750	20,919,382
17				14,881,016	9,092,301	9,092,301	1,798,863	22,718,245
18				14,881,016	9,092,301	9,092,301	1,635,330	24,353,575
19				14,881,016	9,092,301	9,092,301	1,486,664	25,840,239
20		8,338,096		14,881,016	9,092,301	17,430,397	2,590,917	28,431,157

Total depreciable capital:	28572824	**Income tax**	0.389	**Nominal Interest Rate**	0.100			
Year	***Capital Expenses***	***Working Capital***	***Depreciation***	***Net Profit***	***Net Earning***	***Discounted Cash Flow***	***Cash Flow (Present Value)***	***Cumulative Present Value***
0	-42,849,107	-2,142,455				-44,991,562	-44,991,562	-44,991,562
1			-285,728	15,929,233	9,907,342	9,621,613	8,746,921	-36,244,641
2			-571,456	15,929,233	10,081,921	9,510,465	7,859,888	-28,384,753
3			-857,185	15,929,233	10,256,501	9,399,317	7,061,846	-21,322,907
4			-1,142,913	15,929,233	10,431,081	9,288,168	6,343,944	-14,978,963
5			-1,428,641	15,929,233	10,605,661	9,177,020	5,698,207	-9,280,755
6			-1,714,369	15,929,233	10,780,241	9,065,872	5,117,448	-4,163,307
7			-2,000,098	15,929,233	10,954,821	8,954,724	4,595,189	431,882
8			-2,285,826	15,929,233	11,129,401	8,843,575	4,125,593	4,557,475
9			-2,571,554	15,929,233	11,303,981	8,732,427	3,703,401	8,260,877
10			-2,857,282	15,929,233	11,478,561	8,621,279	3,323,876	11,584,753
11			-3,143,011	15,929,233	11,653,141	8,510,130	2,982,749	14,567,502
12				15,929,233	9,732,762	9,732,762	3,101,158	17,668,660
13				15,929,233	9,732,762	9,732,762	2,819,234	20,487,894
14				15,929,233	9,732,762	9,732,762	2,562,940	23,050,834
15				15,929,233	9,732,762	9,732,762	2,329,946	25,380,780
16				15,929,233	9,732,762	9,732,762	2,118,132	27,498,912
17				15,929,233	9,732,762	9,732,762	1,925,575	29,424,487
18				15,929,233	9,732,762	9,732,762	1,750,523	31,175,010
19				15,929,233	9,732,762	9,732,762	1,591,384	32,766,394
20		8,569,821		15,929,233	9,732,762	18,302,583	2,720,562	35,486,957

Total depreciable capital:	42156328	**Income tax**	0.389	**Nominal Interest Rate**	0.100			
Year	***Capital Expenses***	***Working Capital***	***Depreciation***	***Net Profit***	***Net Earning***	***Discounted Cash Flow***	***Cash Flow (Present Value)***	***Cumulative Present Value***
0	-54,832,740	-2,741,637				-57,574,377	-57,574,377	-57,574,377
1			-4,215,633	18,606,216	13,944,149	9,728,517	8,844,106	-48,730,271
2			-7,588,139	18,606,216	16,004,751	8,416,612	6,955,877	-41,774,393
3			-6,070,511	18,606,216	15,077,480	9,006,969	6,767,069	-35,007,324
4			-4,856,409	18,606,216	14,335,664	9,479,255	6,474,459	-28,532,866
5			-3,886,813	18,606,216	13,743,241	9,856,427	6,120,066	-22,412,800
6			-3,106,921	18,606,216	13,266,727	10,159,805	5,734,945	-16,677,855
7			-2,761,239	18,606,216	13,055,515	10,294,276	5,282,591	-11,395,264
8			-2,761,239	18,606,216	13,055,515	10,294,276	4,802,356	-6,592,908
9			-2,765,455	18,606,216	13,058,091	10,292,636	4,365,082	-2,227,826
10			-2,761,239	18,606,216	13,055,515	10,294,276	3,968,889	1,741,063
11			-1,382,728	18,606,216	12,213,244	10,830,517	3,796,030	5,537,093
12				18,606,216	11,368,398	11,368,398	3,622,322	9,159,415
13				18,606,216	11,368,398	11,368,398	3,293,020	12,452,435
14				18,606,216	11,368,398	11,368,398	2,993,654	15,446,089
15				18,606,216	11,368,398	11,368,398	2,721,504	18,167,593
16				18,606,216	11,368,398	11,368,398	2,474,095	20,641,688
17				18,606,216	11,368,398	11,368,398	2,249,177	22,890,865
18				18,606,216	11,368,398	11,368,398	2,044,706	24,935,571
19				18,606,216	11,368,398	11,368,398	1,858,824	26,794,395
20		10,966,548		18,606,216	11,368,398	22,334,946	3,319,947	30,114,342

Total depreciable capital:	19446711	**Income tax**	0.389	**Nominal Interest Rate**	0.100			
Year	***Capital Expenses***	***Working Capital***	***Depreciation***	***Net Profit***	***Net Earning***	***Discounted Cash Flow***	***Cash Flow (Present Value)***	***Cumulative Present Value***
0	-19,446,711	-972,336				-20,419,047	-20,419,047	-20,419,047
1			-1,944,671	8,899,984	6,626,084	4,681,413	4,255,830	-16,163,217
2			-3,500,408	8,899,984	7,576,639	4,076,231	3,368,786	-12,794,430
3			-2,800,326	8,899,984	7,148,890	4,348,563	3,267,140	-9,527,290
4			-2,240,261	8,899,984	6,806,690	4,566,429	3,118,932	-6,408,358
5			-1,792,987	8,899,984	6,533,405	4,740,418	2,943,427	-3,464,931
6			-1,433,223	8,899,984	6,313,589	4,880,367	2,754,840	-710,092
7			-1,273,760	8,899,984	6,216,157	4,942,398	2,536,231	1,826,140
8			-1,273,760	8,899,984	6,216,157	4,942,398	2,305,665	4,131,805
9			-1,275,704	8,899,984	6,217,345	4,941,641	2,095,738	6,227,543
10			-1,273,760	8,899,984	6,216,157	4,942,398	1,905,508	8,133,051
11			-637,852	8,899,984	5,827,618	5,189,766	1,818,981	9,952,032
12				8,899,984	5,437,890	5,437,890	1,732,679	11,684,712
13				8,899,984	5,437,890	5,437,890	1,575,163	13,259,875
14				8,899,984	5,437,890	5,437,890	1,431,966	14,691,841
15				8,899,984	5,437,890	5,437,890	1,301,788	15,993,629
16				8,899,984	5,437,890	5,437,890	1,183,443	17,177,072
17				8,899,984	5,437,890	5,437,890	1,075,858	18,252,930
18				8,899,984	5,437,890	5,437,890	978,052	19,230,982
19				8,899,984	5,437,890	5,437,890	889,138	20,120,121
20		3,889,342		8,899,984	5,437,890	9,327,232	1,386,434	21,506,554

Appendix G Calculation for PSA cost

In this part, we calculated the cost for the PSA unit from the existing commercial plant. The capital and operating costs for the PSA unit are from scale-up calculation based on gas flow rate, the reference flow rate is considered as 1000 Nm^3/h, and the reference cost number is gathered from the graph below.

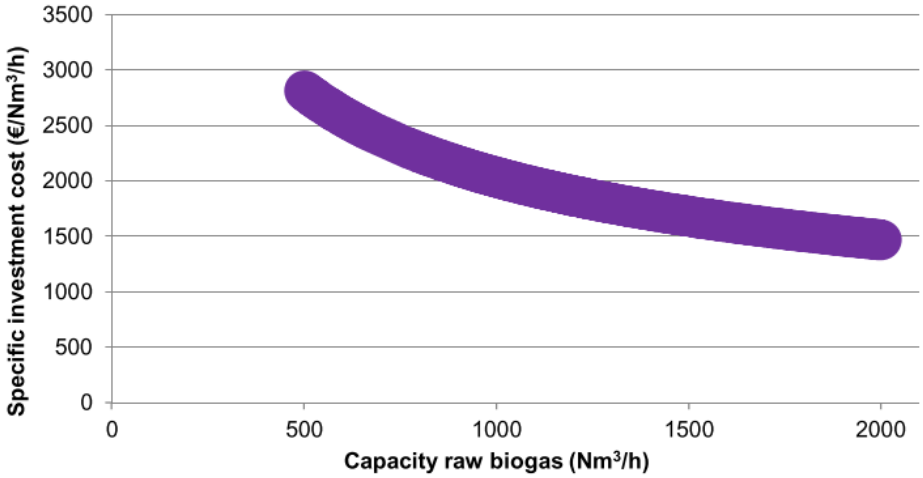

Figure G1 Reference cost for PSA unit[125].

The cost from the above graph is roughly 2000 Eurodollar (€, 2009)) per normal cubic meter on an hourly basis, hence the reference investment for a 1000 Nm^3/h plant would be €2,000,000 (2 million). However, the gas flow we dealt with in our calculations is multiple times higher than that number, so we choose to use €1,500,000 as the reference cost for 1000 Nm^3/h. The results in our calculation are all shown in the U.S. dollar ($), hence the reference cost needs to multiply with the exchange rate. In 2017, the exchange rate is around 0.85, therefore:

$$reference\ cost(\$) = reference\ cost(€) \div 0.85 = 1{,}500{,}000 \div 0.85 = \$\,1764705$$

On the other hand, the same amount of money worth more before due to inflation, so the inflation factor is also needed in this part. Here, we took the inflation factor as 1.1 to correct the error:

$$reference\ cost\ (\$, 2009) = \$1764705 * 1.1 = \$\ 1941176(2017)$$

We chose to round up this reference cost to $1990000 to balance the error in reading figure G1 and also to cross-check with other reported PSA values[81]. Hence, the reference cost for PSA unit is fixed at $1990000 on a 1000 Nm^3/h flow rate basis. The operating cost for the PSA unit is considered from an energy consumption basis. The energy required for this process is mainly used to change the pressure; we took 0.25 kWh/Nm^3 as the energy use basis from a Swedish PSA plant[125]. Thus, the PSA operating cost can be calculated from the flow rate, reference energy consumption, and electricity cost.

Appendix H Copyright Permissions

SPRINGER NATURE LICENSE TERMS AND CONDITIONS

Jan 13, 2020

This Agreement between University of Calgary -- Miao Wang ("You") and Springer Nature ("Springer Nature") consists of your license details and the terms and conditions provided by Springer Nature and Copyright Clearance Center.

License Number	4747160155114
License date	Jan 13, 2020
Licensed Content Publisher	Springer Nature
Licensed Content Publication	Nature Geoscience
Licensed Content Title	How a century of ammonia synthesis changed the world
Licensed Content Author	Jan Willem Erisman et al
Licensed Content Date	Sep 28, 2008
Type of Use	Thesis/Dissertation
Requestor type	academic/university or research institute
Format	print and electronic
Portion	figures/tables/illustrations
Number of figures/tables/illustrations	1
High-res required	no
Will you be translating?	no
Circulation/distribution	1 - 29
Author of this Springer Nature content	no
Title	How a century of ammonia synthesis changed the world
Institution name	University of Calgary
Expected presentation date	Jan 2020
Portions	Figure 1
Requestor Location	University of Calgary 2500 University Dr, NW Calgary, Alberta Calgary, AB T2N 1N4 Canada Attn: University of Calgary
Total	**0.00 USD**
Terms and Conditions	

Springer Nature Customer Service Centre GmbH
Terms and Conditions

This agreement sets out the terms and conditions of the licence (the **Licence**) between you and **Springer Nature Customer Service Centre GmbH** (the **Licensor**). By clicking 'accept' and completing the transaction for the material (**Licensed Material**), you also confirm your acceptance of these terms and conditions.

1. Grant of License

1. 1. The Licensor grants you a personal, non-exclusive, non-transferable, world-wide licence to reproduce the Licensed Material for the purpose specified in your order only. Licences are granted for the specific use requested in the order and for no other use, subject to the conditions below.

1. 2. The Licensor warrants that it has, to the best of its knowledge, the rights to license reuse of the Licensed Material. However, you should ensure that the material you are requesting is original to the Licensor and does not carry the copyright of another entity (as credited in the published version).

ELSEVIER LICENSE
TERMS AND CONDITIONS

Jan 13, 2020

This Agreement between University of Calgary – Miao Wang ("You") and Elsevier ("Elsevier") consists of your license details and the terms and conditions provided by Elsevier and Copyright Clearance Center.

License Number	4747170407194
License date	Jan 13, 2020
Licensed Content Publisher	Elsevier
Licensed Content Publication	Joule
Licensed Content Title	Electrification and Decarbonization of the Chemical Industry
Licensed Content Author	Zachary J. Schiffer,Karthish Manthiram
Licensed Content Date	Sep 6, 2017
Licensed Content Volume	1
Licensed Content Issue	1
Licensed Content Pages	5
Start Page	10
End Page	14
Type of Use	reuse in a thesis/dissertation
Portion	figures/tables/illustrations
Number of figures/tables/illustrations	1
Format	both print and electronic
Are you the author of this Elsevier article?	No
Will you be translating?	No
Title	Electrification and Decarbonization of the Chemical Industry
Institution name	University of Calgary
Expected presentation date	Jan 2020
Portions	Figure 1
Requestor Location	University of Calgary 2500 University Dr, NW Calgary, Alberta Calgary, AB T2N 1N4 Canada Attn: University of Calgary
Publisher Tax ID	GB 494 6272 12
Total	**0.00 USD**
Terms and Conditions	

INTRODUCTION

1. The publisher for this copyrighted material is Elsevier. By clicking "accept" in connection with completing this licensing transaction, you agree that the following terms and conditions apply to this transaction (along with the Billing and Payment terms and conditions established by Copyright Clearance Center, Inc. ("CCC"), at the time that you opened your Rightslink account and that are available at any time at http://myaccount.copyright.com).

GENERAL TERMS

2. Elsevier hereby grants you permission to reproduce the aforementioned material subject to the terms and conditions indicated.
3. Acknowledgement: If any part of the material to be used (for example, figures) has appeared in our publication with credit or acknowledgement to another source, permission must also be sought from that source. If such permission is not obtained then that material may not be included in your publication/copies. Suitable acknowledgement to the source must be made, either as a footnote or in a reference list at the end of your publication, as follows:
"Reprinted from Publication title, Vol /edition number, Author(s), Title of article / title of chapter, Pages No., Copyright (Year), with permission from Elsevier [OR APPLICABLE SOCIETY COPYRIGHT OWNER]." Also Lancet special credit - "Reprinted from The Lancet, Vol. number, Author(s), Title of article, Pages No., Copyright (Year), with permission from Elsevier."
4. Reproduction of this material is confined to the purpose and/or media for which permission is hereby given.
5. Altering/Modifying Material: Not Permitted. However figures and illustrations may be altered/adapted minimally to serve your work. Any other abbreviations, additions, deletions and/or any other alterations shall be made only with prior written authorization of Elsevier Ltd. (Please

ELSEVIER LICENSE TERMS AND CONDITIONS

Jan 13, 2020

This Agreement between University of Calgary – Miao Wang ("You") and Elsevier ("Elsevier") consists of your license details and the terms and conditions provided by Elsevier and Copyright Clearance Center.

License Number	4747180099581
License date	Jan 13, 2020
Licensed Content Publisher	Elsevier
Licensed Content Publication	Chem
Licensed Content Title	Electrocatalytic Reduction of Nitrogen: From Haber-Bosch to Ammonia Artificial Leaf
Licensed Content Author	Antonio José Martín,Tatsuya Shinagawa,Javier Pérez-Ramírez
Licensed Content Date	Feb 14, 2019
Licensed Content Volume	5
Licensed Content Issue	2
Licensed Content Pages	21
Start Page	263
End Page	283
Type of Use	reuse in a thesis/dissertation
Portion	figures/tables/illustrations
Number of figures/tables/illustrations	1
Format	both print and electronic
Are you the author of this Elsevier article?	No
Will you be translating?	No
Title	Electrocatalytic Reduction of Nitrogen: From Haber-Bosch to Ammonia Artificial Leaf
Institution name	University of Calgary
Expected presentation date	Jan 2020
Portions	Figure 2
Requestor Location	University of Calgary 2500 University Dr, NW Calgary, Alberta Calgary, AB T2N 1N4 Canada Attn: University of Calgary
Publisher Tax ID	GB 494 6272 12
Total	**0.00 USD**
Terms and Conditions	

INTRODUCTION

1. The publisher for this copyrighted material is Elsevier. By clicking "accept" in connection with completing this licensing transaction, you agree that the following terms and conditions apply to this transaction (along with the Billing and Payment terms and conditions established by Copyright Clearance Center, Inc. ("CCC"), at the time that you opened your Rightslink account and that are available at any time at http://myaccount.copyright.com).

GENERAL TERMS

2. Elsevier hereby grants you permission to reproduce the aforementioned material subject to the terms and conditions indicated.
3. Acknowledgement: If any part of the material to be used (for example, figures) has appeared in our publication with credit or acknowledgement to another source, permission must also be sought from that source. If such permission is not obtained then that material may not be included in your publication/copies. Suitable acknowledgement to the source must be made, either as a footnote or in a reference list at the end of your publication, as follows:
"Reprinted from Publication title, Vol /edition number, Author(s), Title of article / title of chapter, Pages No., Copyright (Year), with permission from Elsevier [OR APPLICABLE SOCIETY COPYRIGHT OWNER]." Also Lancet special credit - "Reprinted from The Lancet, Vol. number, Author(s), Title of article, Pages No., Copyright (Year), with permission from Elsevier."
4. Reproduction of this material is confined to the purpose and/or media for which permission is hereby given.
5. Altering/Modifying Material: Not Permitted. However figures and illustrations may be altered/adapted minimally to serve your work. Any other abbreviations, additions, deletions and/or any other alterations shall be made only with prior written authorization of Elsevier Ltd. (Please

ELSEVIER LICENSE TERMS AND CONDITIONS

Jan 13, 2020

This Agreement between University of Calgary – Miao Wang ("You") and Elsevier ("Elsevier") consists of your license details and the terms and conditions provided by Elsevier and Copyright Clearance Center.

License Number	4747171419150
License date	Jan 13, 2020
Licensed Content Publisher	Elsevier
Licensed Content Publication	International Journal of Hydrogen Energy
Licensed Content Title	A comprehensive review on PEM water electrolysis
Licensed Content Author	Marcelo Carmo,David L. Fritz,Jürgen Mergel,Detlef Stolten
Licensed Content Date	Apr 22, 2013
Licensed Content Volume	38
Licensed Content Issue	12
Licensed Content Pages	34
Start Page	4901
End Page	4934
Type of Use	reuse in a thesis/dissertation
Portion	figures/tables/illustrations
Number of figures/tables/illustrations	1
Format	both print and electronic
Are you the author of this Elsevier article?	No
Will you be translating?	No
Title	A comprehensive review on PEM water electrolysis
Institution name	University of Calgary
Expected presentation date	Jan 2020
Portions	Table 1
Requestor Location	University of Calgary 2500 University Dr, NW Calgary, Alberta Calgary, AB T2N 1N4 Canada Attn: University of Calgary
Publisher Tax ID	GB 494 6272 12
Total	**0.00 USD**
Terms and Conditions	

INTRODUCTION

1. The publisher for this copyrighted material is Elsevier. By clicking "accept" in connection with completing this licensing transaction, you agree that the following terms and conditions apply to this transaction (along with the Billing and Payment terms and conditions established by Copyright Clearance Center, Inc. ("CCC"), at the time that you opened your Rightslink account and that are available at any time at http://myaccount.copyright.com).

GENERAL TERMS

2. Elsevier hereby grants you permission to reproduce the aforementioned material subject to the terms and conditions indicated.
3. Acknowledgement: If any part of the material to be used (for example, figures) has appeared in our publication with credit or acknowledgement to another source, permission must also be sought from that source. If such permission is not obtained then that material may not be included in your publication/copies. Suitable acknowledgement to the source must be made, either as a footnote or in a reference list at the end of your publication, as follows:
"Reprinted from Publication title, Vol /edition number, Author(s), Title of article / title of chapter, Pages No., Copyright (Year), with permission from Elsevier [OR APPLICABLE SOCIETY COPYRIGHT OWNER]." Also Lancet special credit - "Reprinted from The Lancet, Vol. number, Author(s), Title of article, Pages No., Copyright (Year), with permission from Elsevier."
4. Reproduction of this material is confined to the purpose and/or media for which permission is hereby given.
5. Altering/Modifying Material: Not Permitted. However figures and illustrations may be altered/adapted minimally to serve your work. Any other abbreviations, additions, deletions and/or any other alterations shall be made only with prior written authorization of Elsevier Ltd. (Please